

https://dspace.org/

Coastal foraging of Turbo sarmaticus at Klasies River Main Site: an experimental approach

Holmes, Carl Louis

2024
https://hdl.handle.net/10539/37429

Downloaded from a DSpace repository. https://dspace.org/



UNIVERSITY OF THE
WITWATERSRAND,
JOHANNESBURG

Coastal foraging of *Turbo sarmaticus* at Klasies River Main Site: an experimental approach

by

Carl Louis Holmes

(1447271)

Dissertation

Submitted in fulfilment of the requirements for the degree

Master of Science by research only:

in

Archaeology

In the Faculty of Science, University of the Witwatersrand, Johannesburg, South Africa, in fulfilment of the requirements for the degree of Master of Science.

Supervisor: Prof. Sarah Wurz

Co-supervisors: Dr Jerome Reynard and Dr Jan De Vynck

29 March 2023

Declaration

I declare that this dissertation is my own, unaided work. It is being submitted for the Degree of Master of Science in Archaeology at the University of the Witwatersrand. It has not been submitted for any other degree or examination at any other University.



(Signature of candidate)

29 day of **March** 20 **23** at **Edenvale**

Abstract

An increase in shellfish exploitation and strong seasonal fluctuations in terrestrial foraging at ca. 100 000 years ago along the Cape coast has been noted. It is hypothesised that marine foraging provided a more reliable year-round source of nutrients. As *Turbo sarmaticus* (alikreukel) is one of the major prey species found at Middle Stone Age (MSA) sites along the southern Cape, and Klasies River Main Site (KRM) specifically, this species was targeted in an archaeological and actualistic study. *T. sarmaticus* specimens were collected and processed by two participants to examine the possible methods used by MSA foragers and the meat was extracted using three tool types (bone, lithics, wood). Some specimens were cooked whilst others were processed raw.

An analysis of the lengths of *T. sarmaticus* opercula of the ca. 100 000 years ago Shell Midden One (SMONE) layer from KRM shows that the archaeological opercula are similar in size to the experimental sample. A larger proportion of the archaeological opercula, however, fall within the smaller size range. An age index was developed for *T. sarmaticus* by correlating operculum size to shell size. This suggested that the archaeological specimens were younger when collected, or that they foraged during spring or winter. The opercula from SMONE are markedly smaller than other MSA II opercula from the Cape coast but bigger than LSA opercula. This might be related to more intensive predation, seasonality and sea surface temperature. A taphonomic analysis of both the experimental and archaeological samples was undertaken. The experimental specimens that were processed raw indicated percussion marks typically placed in the 3rd and 4th wedges. A proportion of the archaeological sample shows this pattern as well. This shows that some of the archaeological samples may have been raw extracted. Furthermore, the breakage types are very similar in both samples, however post-depositional breakage only affected the archaeological sample. This study demonstrates that broader insight can be developed through an actualistic study combined with a taphonomic analysis.

Keywords: *Turbo sarmaticus*, alikreukel, opercula, Klasies River Main Site, Middle Stone Age, MIS 5c, Experimental Archaeology, Actualistic study, Taphonomy, Southern Cape, Coastal Foraging.

Acknowledgements

I would like to acknowledge my supervisors, Prof. Sarah Wurz, Dr Jerome Reynard and Dr Jan De Vynck, for all their guidance and support during the process of my research. Their knowledge and expertise was greatly appreciated during the analysis and development of the taphonomic criteria, and for their patience during the entire process. I would not have been able to complete my thesis without their guidance. I would like to specifically thank Prof. Sarah Wurz for the out-of-context MSA stone tools. I would also like to acknowledge Dr Jan De Vynck for his knowledge and assistance during the running of the experimental process . His experience and knowledge about the intertidal zone are truly appreciated. I would like to acknowledge Dr Jan De Vynck's family, for inviting me into their home during my actualistic study, allowing me the space to conduct the processing aspect of my experiment. Dr Jan De Vynck for arranging the *Tragelaphus strepiceros* (Greater Kudu) bones from the local butcher for the bone tool production and collecting the *Olea europaea ssp. africana* (African olive) branches before my arrival. Dr Jan De Vynck for providing me with data from his PhD thesis for comparative study, and for allowing me the time to understand and view the material that was used and collected.

I would like to acknowledge Hlokwa Madithapa for making all travel arrangements required for my trip to Still Bay, especially for assisting and putting up with all the changes that were made due to the COVID–19 lockdowns that restricted my travels to and from the Western Cape. The Department of Environmental Affairs – specifically Zimasa Jika and Lieze Swart for their assistance in receiving my research permit (RES2021–85).

I would like to thank my family for their assistance wherever possible during the process of completing my dissertation. My friends and colleagues for their support and guidance during the two years and their assistance, and their support of my research especially with the never-ending talking about my research and the assistance in gaining access to specific literature.

I would like to graciously thank both Prof. Sarah Wurz (year 1) and Dr Jan De Vynck (year 2) for funding my research and my travels. The funding is greatly appreciated, and I am so very thankful for their assistance. This was through the National Research Foundation

(NRF), GENUS (CoE: Palaeoscience) and the African Centre for Coastal Palaeoscience, Nelson Mandela University.

Table of Contents

Declaration ii

Abstract iii

Acknowledgements iv

List of Figures x

List of Tables xiv

List of Appendix 1 Figures xvi

List of Appendix 1 Tables xvii

Chapter 1: Introduction 1

1.1. Research question 1
1.2. Research Aim and Objectives 1
1.3. Rationale 2
1.4. Hypotheses 3
1.5. Conclusion 3

Chapter 2: Literature Review 4

2.1. Site Context 4
2.2. Coastal Intertidal Zone 7
2.3. Habitat of *Turbo sarmaticus* 8
2.4. MSA foraging of shellfish in the southern Cape 10
2.4.1. Theory 10
2.4.2. Coastal adaptations and shellfish exploitation in the southern Cape 12
2.4.3. Nutritional Value 13
2.5. *Turbo sarmaticus* operculum size and the 'predation hypothesis' 15
2.6. *Turbo sarmaticus* operculum size, growth patterns and the 'climatic and environmental hypothesis' 15
2.7. Seasonality and *Turbo sarmaticus* 17
2.8. Previous work on experimental processing of *Turbo sarmaticus* 18
2.9. *Turbo sarmaticus* opercula and site formation 20
2.10. Conclusion 21

Chapter 3: Experimental Materials and Methods 22

3.1. Introduction 22
3.2. Foraging 22
3.2.1. Participants and Prey 24
3.2.2. Habitat 25
3.2.3. Foraging Tools 26
3.2.4. Foraging Process 33
3.2.5. Processing 34
3.3. Conclusion 38
Chapter 4: Analytical Methods 39
4.1. Introduction 39
4.2. Opercula Size 39
4.2.1. Opercula Length 39
4.2.2. Opercula Width 40
4.2.3. Opercula Thickness and Weight 40
4.3. Opercula Age 41
4.4. Opercula Shape 43
4.5. Opercula Taphonomy Criteria 43
4.5.1. Completeness of Opercula Dome and Flange 44
4.5.2. Breakage Type shown on Opercula 44
4.5.3. Incisions on Opercula 44
4.5.4. Colouration of Opercula 44
4.5.6. Percussion Marks on Opercula 44
4.5.7. Bore marks 46
4.5.8. Etching 46
4.5.9. Encrustation of Opercula 46
4.5.10. Surface Condition 46
4.5.11. Abrasion 46
4.5.12. Preservation of Opercula 46
4.5.13. Perforations on Opercula 47

4.5.14. Periostracum on Operculum 47
4.6. Opercula Placement Model 47
4.7. Conclusion 48
Chapter 5: Results 49
5.1. Introduction 49
5.2. Opercula size 49
5.3. Opercula Shape 54
5.4. Opercula Age 54
5.5. Opercula Taphonomy 55
5.5.1. Incisions of opercula 55
5.5.2. Completeness of Opercula 56
5.5.3. Breakage of Opercula 57
5.5.4. Percussion marks on Opercula 59
5.5.5. Placement of percussion marks 61
5.5.6. Bore marks 63
5.5.7. Opercula Colouration 64
5.5.8. Etching of Opercula 65
5.5.9. Encrustation of opercula 66
5.5.10. Abrasion of Opercula 67
5.5.11. Preservation of Opercula 68
5.6. Conclusion 69
Chapter 6: Discussion 70
6.1. Introduction 70
6.2. Opercula Size and shape 70
6.3. Opercula Age 72
6.4. Opercula Processing 73
6.5. Opercula Taphonomy 75
Chapter 7: Conclusion 77
Future Avenues of Research 77
References 79

Appendices 86
Appendix 1A: Modern-day experimental data 86
Appendix 1A.1. Foraging Data 86
Appendix 1A.1.1. Foraging Notes 86
Appendix 1A.2. Processing Data 87
Appendix 1A.2.1. Processing Notes 87
Appendix 1B: Analytical Data 91
Appendix 1B.1: Experimental Age Index 91
Appendix 1B.2: Opercula Shape 95
Appendix 1B.3: Opercula Age 95
Appendix 1B.4: Opercula Processing 96
Opercula Completeness 96
Breakage Type 96
Colouration of T. sarmaticus opercula 96
Percussion Marks on T. sarmaticus opercula 97
Percussion Marks details 97
Bore Marks on Opercula 97
Appendix 1B.5: Opercula Taphonomy 98
Etching on Opercula 98
Encrustation on Opercula 98
Encrustation percentage 98
Abrasion on Opercula 98
Appendix 1C: Ocean Condition Rating 99
Appendix 1D: Foraging Permits 100
Appendix 1D.1: Research Permit (RES2021–85) 100
Appendix 1D.2: Additional Fishing Permit (1052834) 104

List of Figures

Figure 2. 1: 3D image plan of KRM Cave 1, Witness Baulk deposits (Wurz *et al*. 2018: Fig. 3, 105)..... 6

Figure 2. 2: KRM Cave 1 Witness Baulk south wall profile (Brenner *et al.* 2022: Figure 2, 7)..... 6

Figure 2. 3: Spirals on *T. sarmaticus* operculum (adapted from Galimberti *et al*. 2017: Fig.1, 63).....16

Figure 2. 4: Cooking of *T. sarmaticus* on the coals (De Vynck 2017: Fig. A 3.15a, Appendix 3).....19

Figure 2. 5: Raw extraction of the meat from *T. sarmaticus* shell with a bone tool (De Vynck 2017: Fig. A3.12, Appendix 3).....20

Figure 3. 1: Jongensfontein, where the experimental foraging took place, in relation to the southern Cape coastal archaeological sites Klasies River main site (KRM), Blombos Cave (BBC) and Pinnacle Point (PP) (Google Earth Pro 2021a).....23

Figure 3. 2: Foraging locations for Still Bay foraging experiment, A: Test foraging day at Jongensfontein East, 1: Lithics foraging at Jongensfontein West, 2: Wooden tool and Bone tool foraging at Brandersfontein Farm (Google Earth Pro 2021b). 23

Figure 3. 3: A, the dorsal side of a *T. sarmaticus* shell, B, the ventral side of the *T. sarmaticus* shell with operculum in place. C, of an intact *P. perna* shell. D, of the ventral side of the *S. longicosta* shell. E, of the ventral side of the *C. oculus* shell. F, of the ventral side of the *C. miniata* shell. 24

Figure 3. 4: A, dome (dorsal) surface of the *T. sarmaticus* opercula. B, the flange (ventral) surface of the *T. sarmaticus* opercula.....25

Figure 3. 5: Out of context Middle Stone Age lithics from the Klasies River main site spill heap after use, showing breakage on the lithics as a result of the experiment. 26

Figure 3. 6: A, the measuring of the *Olea europaea ssp. africana* branches to 0.45 m. B, the hand saw used to cut the branches before the production of the tools, and C, the cut *Olea europaea ssp. africana* branches for both participants. 28

Figure 3. 7: Wooden tool production by P2 using the quartzite veins on the Table Mountain Sandstone rocky headlands.....28

Figure 3. 8: Worksite after the tool production, in the image the quartzite veins are protruding from the Table Mountain Sandstone exposed rocky headlands. 29

Figure 3. 9: Worksite after the tool production, in the image the Table Mountain Sandstone exposed rocky headland surface shows the site used to refine and sharpen the tool where no quartzite veins are present. 29

Figure 3. 10: Wooden tools made by P2 out of *Olea europaea ssp. africana* branches. 30

Figure 3. 11: 1, *T. strepiceros* humerus (baked). 2, *T. strepiceros* femur (raw). 3, *T. strepiceros* radius and ulna (baked). 4, *T. strepiceros* femur (raw). 31

Figure 3. 12: Cobblestones used for the hammer and anvil technique to crack open the long bone. A is the Cobblestone used by P1, and B is the Cobblestone used by P2.....32

Figure 3. 13: A, the area where P2 produced the bone tools. B, the remains left behind postproduction (bone marrow, skin, bone fragments).....32

Figure 3. 14: A, bone tools made by P2 out of *T. strepiceros* long bones. B, bone tools made by P1 out of *T. strepiceros* long bones. 33

Figure 3. 15: A, the tool produced by P2 from the baked long bone. B, the bone fragments produced by P2 from the raw long bone. 33

Figure 3. 16: Fire for cooking *T. sarmaticus*.....35

Figure 3. 17: A, the shell length measurement technique by P1. B, the shell width measurement technique by P1. 37

Figure 3. 18: Labelled diagram of the internal portion of the *T. sarmaticus*.....37

Figure 3. 19: A, how the cooked *T. sarmaticus* individuals bubble when done. B, the cooking of the *T. sarmaticus* shells in batches of 15. 38

Figure 4. 1: A, how the length and width are measured on the ventral (flange) of the *T. sarmaticus* operculum. B, how the length and width are measured on the dorsal (dome) of the *T. sarmaticus* operculum.....40

Figure 4. 2: P1 measuring the length of the *T. sarmaticus* shell in the actualistic study..43

Figure 4. 3: A, an experimental *T. sarmaticus* opercula showing percussion notch marks (PM) on the dome surface with a break. B, bone percussion marks caused by hammer and anvil techniques (from Blumenschine *et al.* 1996: Figure 2, 498). C, an archaeological *T. sarmaticus* opercula showing percussion pit marks (PM) on the dorsal surface. 45

Figure 4. 4: Wedge Placement Model (Sherwood *et al.* 2016). A, the dorsal side wedge model 1–8. B, the ventral side wedge model 1–8. 47

Figure 4. 5: Spiral Placement Model. A, the dorsal spiral placement model A–D. B, the ventral spiral placement model A–D. 48

Figure 5. 1: *T. sarmaticus* opercula length of raw and cooked from all three tool types from the experimental sample and the archaeological sample. 51

Figure 5. 2: *T. sarmaticus* opercula width of raw and cooked from all three tool types from the experimental sample and the archaeological sample. 52

Figure 5. 3: A, weight of the *T. sarmaticus* opercula. B, thickness of the *T. sarmaticus* opercula of raw and cooked from all three tool types from the experimental sample and the archaeological sample. 53

Figure 5. 4: Age distribution for the *T. sarmaticus* based on the opercula measurements of the experimental and archaeological sample (see Table 4. 3). 55

Figure 5. 5: A, complete dome (ventral surface) on *T. sarmaticus* opercula for combining the experimental sample and the archaeological sample. B, complete flange (dorsal surface) on *T. sarmaticus* opercula for combining the experimental sample and the archaeological sample. 56

Figure 5. 6: Breakage types seen on the SMONE samples: A, transverse break, B, eroded break, C, irregular break, D, Intact.....58

Figure 5. 7: Breakage type on the archaeological and experimental *T. sarmaticus* opercula. 59

Figure 5. 8: A, percussion marks on the ventral surface of the *T. sarmaticus* opercula, B, percussion mark details on the *T. sarmaticus* operculum.....60

Figure 5. 9: Wedge Placement Model (Sherwood et al. 2016). A, the dorsal side wedge model 1–8. B, the ventral side wedge model 1–8. 62

Figure 5. 10: Spiral Placement Model. A, the dorsal spiral placement model A–D. B, the ventral spiral placement model A–D. 62

Figure 5. 11: Bore Marks were seen on the ventral surface of the *T. sarmaticus* operculum. 63

Figure 5. 12: A, bore mark seen on the experimental opercula. B, bore mark seen on the SMONE opercula. 64

Figure 5. 13: Colouration on *T. sarmaticus* opercula. 65

Figure 5. 14: Evidence of etching on the ventral surface of the *T. sarmaticus* operculum. 65

Figure 5. 15: A, encrustation on the dome of the *T. sarmaticus* opercula. B, coverage of the encrusting on the *T. sarmaticus* opercula. 66

Figure 5. 16: Abrasions on the flange of the *T. sarmaticus* operculum. 68

Figure 5. 17: Preservation of the experimental and archaeological *T. sarmaticus* opercula. 68

Figure 6. 1: *T. sarmaticus* operculum #41 from the SMONE layer at KRM, showing a charcoal line on the flange. 75

List of Tables

Table 2. 1: Intertidal Zones of Southern Africa and their placement within the intertidal and shallow subtidal zone (adapted from Langejans *et al*. 2012: Table 4, 84; Branch *et al.* 2022)..... 8

Table 2. 2: Common species found within the different Intertidal Zones (adapted from Langejans *et al.* 2012). 13

Table 3. 1: Ocean Condition rating scale, calibrated to the Beaufort scale, showing the optimal and suboptimal conditions for shellfish foraging. 34

Table 4. 1: Summary of statistics for the experimental *T. sarmaticus* shell and opercula length. 41

Table 4. 2: Relative age for *T. sarmaticus* shell length (from Yssel 1989: Table 11, 77). .42

Table 4. 3: *T. sarmaticus* age index based on operculum length and inferred shell length (adapted from Yssel 1989: Table 11, 57). 42

Table 5. 1: A, Summary statistics for *T. sarmaticus* opercula with a combination of both P1 and P2, and the combination of all three tool types. B, Summary statistics for *T. sarmaticus* opercula from layer SMONE. 50

Table 5. 2: *T. sarmaticus* operculum shape for the experimental and archaeological sample. 54

Table 5. 3: *T. sarmaticus* opercula length and age index with experimental and SMONE n values. 54

Table 5. 4: Experimental *T. sarmaticus* opercula incision measurements, with tool type and participant. 55

Table 5. 5: Instrument vs breakage type for the experimental sample with P1 and P2 combined. 57

Table 5. 6: Percussion marks on Experimental and SMONE *T. sarmaticus* opercula. 59

Table 5. 7: Percussion mark details on Experimental and SMONE *T. sarmaticus* opercula. 60

Table 5. 8: *T. sarmaticus* opercula percussion mark placement statistics. 61

Table 5. 9: *T. sarmaticus* operculum percussion marks localised statistics (Figure 5. 9 and Figure 5. 10). 61

Table 5. 10: *T. sarmaticus* opercula encrustation placement statistics 67

Table 5. 11: *T. sarmaticus* opercula encrustation localised numbers (Figure 4. 4 and Figure 4. 5). 67

Table 6. 1: Comparison of opercula length measurement (mm) statistics from various MSA II and LSA opercula from KRM and the experimental sample from this study. 71

List of Appendix 1 Figures

Appendix 1A Figure 1: A, cobblestone used by P2 for Hammer and Anvil technique. B, lithic (J-LR 2) used by P1 that broke while raw processing the *T. sarmaticus*.....88

Appendix 1A Figure 2: A, the foot of the *T. sarmaticus*. B, the muscle near the head sealing the operculum in place (Cold Water 2016). 88

Appendix 1A Figure 3: A, the workspace during raw processing using lithics. B, the operculum that fragmented and remained glued to the *T. sarmaticus* foot.....89

Appendix 1A Figure 4: The complete extraction of the *T. sarmaticus* meat from the shell due to cooked extraction.....89

Appendix 1A Figure 5: A, the foot-up technique used for the lithic raw processing. B, the new foot–down approach used for wooden and bone tool raw processing. 90

Appendix 1B Figure 1: Graph of the *T. sarmaticus* opercula shape for the experimental and archaeological samples. 95

Appendix 1C Figure 1: Ocean Condition rating scale, showing the optimal and suboptimal conditions for shellfish foraging (pers. comm De Vynck). 99

List of Appendix 1 Tables

Appendix 1A Table 1: Experimental Opercula processing time for P1 and P2.....87

Appendix 1A Table 2: Experimental Opercula cooking time for P1 and P2.....87

Appendix 1B Table 1: Experimental *T. sarmaticus* shell length age and opercula length age.....91

Appendix 1B Table 2: *T. sarmaticus* opercula shape for both experimental and archaeological samples.....95

Appendix 1B Table 3: Age of *T. sarmaticus* for both experimental and archaeological samples.....95

Appendix 1B Table 4: Dome completeness for experimental and archaeological *T. sarmaticus* opercula.....96

Appendix 1B Table 5: Flange completeness for experimental and archaeological *T. sarmaticus* operculum.....96

Appendix 1B Table 6: Type of breakage seen in the experimental and archaeological *T. sarmaticus* opercula.....96

Appendix 1B Table 7: Colouration seen on the experimental and archaeological *T. sarmaticus* operculum.....96

Appendix 1B Table 8: Percussion marks seen on *T. sarmaticus* opercula.....97

Appendix 1B Table 9: Percussion mark details for the experimental and archaeological *T. sarmaticus* opercula.....97

Appendix 1B Table 10: Bored marks on *T. sarmaticus* opercula.....97

Appendix 1B Table 11: Etching seen on the dome of the experimental and archaeological *T. sarmaticus* opercula.....98

Appendix 1B Table 12: Encrustation of *T. sarmaticus* opercula.....98

Appendix 1B Table 13: Percentage of *T. sarmaticus* opercula encrusted.....98

Appendix 1B Table 14: Abrasion on archaeological *T. sarmaticus* opercula.....98

Chapter 1: Introduction

Turbo sarmaticus (alikreukel) is a species of aquatic *Gastropoda*, that is found along the Cape coastline of Southern Africa (Branch *et al.* 2022). This species of shellfish plays a vital role in understanding the foraging behaviour and coastal adaptation of Middle Stone Age (MSA) groups (e.g., Langejans *et al.* 2012). This study further investigates the role of *T. sarmaticus* in subsistence behaviour through an actualistic study. An actualistic study involves modern-day experimentation and interpretation in order to gain a deeper understanding of the archaeological material (Outram 2008; Toth and Schick 2009). As Outram (2008: 2) notes – "hypotheses can be tested with authentic materials and in a range of environmental conditions that aim to reflect more accurately 'real life' or 'actualistic' scenarios. Such experiments investigate activities that might have happened in the past using the methods and materials that would actually have been available." *T. sarmaticus* and other shellfish specimens were collected during winter along the southern Cape coast, at Jongensfontein and they were processed in various ways. The size of the opercula is an important variable discussed in MSA coastal foraging studies and therefore experimental opercula were measured in addition to the archaeological opercula from ca. 100 000 years ago (ka) layer from Klasies River Main Site (KRM). A taphonomic investigation was undertaken to understand other processes that might have affected the surface conditions of the opercula.

1.1. Research question

1. What information on subsistence behaviour and taphonomy can be inferred from an actualistic study of *T. sarmaticus*?
2. Is the taphonomy of *T. sarmaticus* opercula from layer SMONE at KRM informative of MSA subsistence behaviour?
3. What are the possible site formation processes during this period at the site?

1.2. Research Aim and Objectives

This dissertation aims to undertake an actualistic study through the foraging and processing of *T. sarmaticus* and to compare the foraged opercula with those from SMONE at KRM dating to ca.100 ka (MIS 5c).

Objectives:

1. To forage and process *T. sarmaticus* from the southern Cape coast (Jongensfontein).
2. To determine the taphonomic characteristics resulting from foraging and processing.
3. To analyse and examine the taphonomic conditions of the experimental and archaeological opercula.
4. To infer subsistence behaviour and possible site formation processes in the layer SMONE at KRM.

1.3. Rationale

It is hypothesised that coastal foraging became more prominent around 100ka on the southern Cape coast (Will *et al.* 2019) and that this was associated with evolutionary advantages. Although the notion of shellfish gathering was initially seen as an inherently low-return activity (Meehan 1982), there is now an increased emphasis on the contribution of marine foraged proteins in carbohydrate-rich, plant-based diets (De Vynck *et al.* 2016: 102). Importantly, it is seen that intertidal foraging of shellfish provides a stable and relatively low depletion resource for human foragers. This would have provided a more reliable year-round resource base over the seasonally fluctuating terrestrial-based resources (De Vynck *et al.* 2020). Shellfish exploitation of the recently excavated layers at KRM has been described (Brenner *et al*. 2022; Wurz *et al*. 2022), and it has been shown that *T. sarmaticus* is one of the major prey species (Brenner *et al*. 2022). Notwithstanding its importance little is known about the foraging, processing and site formation processes that affect the opercula of this taxon. De Vynck (2017) undertook an actualistic study where the foraging of *T. sarmaticus* was done in a modern context with indigenous coastal foragers. An actualistic study combined with an archaeological analysis of MSA *T. sarmaticus* has not been undertaken yet, and this in-depth investigation will aid in a deeper understanding of the site formation processes and the shellfish foraging behaviour within this period.

1.4. Hypotheses

Hypothesis 1 – An actualistic study of *Turbo sarmaticus* provides new information on Middle Stone Age coastal foraging.

Hypothesis 2 – The taphonomic analysis of the *T. sarmaticus* opercula provides information on the processing.

Hypothesis 3 – The taphonomic condition of the *T. sarmaticus* opercula, indicates that post-depositional processes affect the opercula in layer SMONE.

1.5. Conclusion

This chapter introduces the areas of research that is investigated in the dissertations, and the rationale behind this particular study. Bringing forward the questions that will be answered in this research through the actualistic study and experimentation. In the next chapter the literature from previous studies is reviewed.

Chapter 2: Literature Review

2.1. Site Context

Klasies River main site (KRM) is situated along the Tsitsikamma coast of the eastern Cape Province, South Africa. *Turbo sarmaticus* (alikreukel) is commonly found in archaeological sites along the southern Cape coastline, including at KRM (Langejans *et al.* 2012: 86). KRM has been recognised since the 1960s for its archaeological findings and importance. In March 2015 the site attained National Heritage Site status (Wurz *et al*. 2018: 103). KRM consists of four closely located caves and shelters (Caves 1, 1A, 1B and 2) (Brenner & Wurz 2019), with the samples analysed here originating from Cave 1, Witness Baulk (Wurz *et al*. 2018: 103).

KRM was first excavated in the period between 1967 – 1968 by Ronald Singer and John Wymer (Singer & Wymer 1982). From 1984 to 1995, KRM was excavated by Hilary Deacon with the Witness Baulk (Figure 2. 1), being excavated between 1991 and 1995 (Deacon 1995; Wurz *et al*. 2018). The excavations were thereafter led by Sarah Wurz since 2015, continuing with the excavation of the Witness Baulk.

The MSA II layers at KRM contain the SASU (Shell and Sand Upper) and the SASL (Shell and Sand Lower) sub-members that fall within the SAS (Shell and Sand) member containing MSA II/Mossel Bay stone artefacts (Wurz *et al*. 2018). The MSA II deposits also consists of large mammal remains, shellfish remains and a large rubble matrix (Wurz *et al.* 2018).

The Wurz excavation started in the SASL sub-member of the Witness Baulk with the excavation of the HHH base and thereafter the SMONE (Shell Midden One) layer (Wurz *et al*. 2018), the layer investigated in this study. Singer and Wymer excavated the equivalent of the SASL member in layer 17 (Singer & Wymer 1982; Deacon 1995).

The palaeoenvironmental conditions at KRM during the MSA II lower can be understood by investigating the link between fauna and the environment. Reynard & Wurz (2020) investigate the role that ungulate diversity at KRM play in understanding the environmental conditions during the MSA. Reynard & Wurz (2020) undertook a study to interpret the richness of ungulates in the deposit and the frequency of grazers. The results indicated a peak during the MSA I, with a substantial drop in the MSA II and a slight

increase again in the MSA III. This shows that changes in vegetation and the environment have an effect on the diversity of ungulates. It is suggested that the increase in ungulates, indicates a grassland environment. Therefore, during the MSA II, the environment around KRM was less grassland and more likely consisting of closed bushy vegetation (Reynard & Wurz 2020). It has been suggested that the faunal density is higher in the MSA II lower layers at KRM, in SMONE, during a period that is associated with MIS 5c. The shellfish density during that same period at KRM is also relatively high, suggesting some link between occupation intensity and coastal settlement (Reynard 2022).

The layer investigated in this research is Shell Midden One (SMONE), which is situated in the Witness Baulk and is a ca. 12 m of baulk sediment in the central part of cave 1 (Figure 2. 1) (Deacon & Geleijnse 1988). Layer SMONE dates to ca. 100ka (Brenner & Wurz 2019). Figure 2. 2 shows the southern profile of the Witness Baulk. Layer SMONE is a sloped wedge deposit with a thickness of 5 cm in the western part, thickening towards the east to 15 cm. The layer consists of shellfish in a soil and rubble matrix with small charcoal pieces and small patches of leached ash preserved (Brenner & Wurz 2019; Morrissey *et al.* 2022).

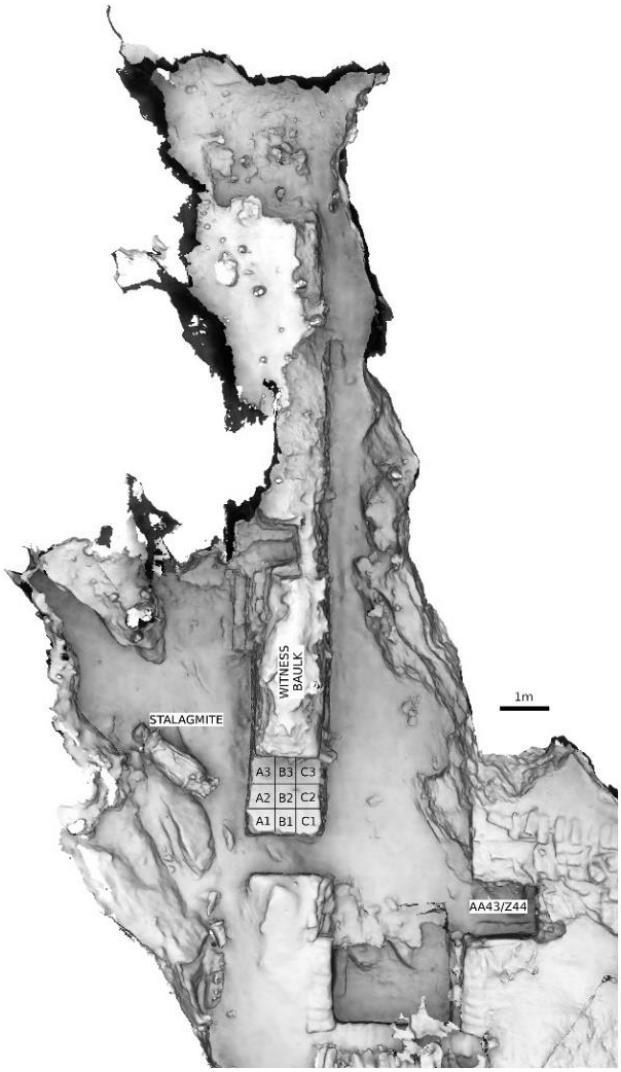


Figure 2. 1: 3D image plan of KRM Cave 1, Witness Baulk deposits (Wurz *et al*. 2018: Fig. 3, 105).

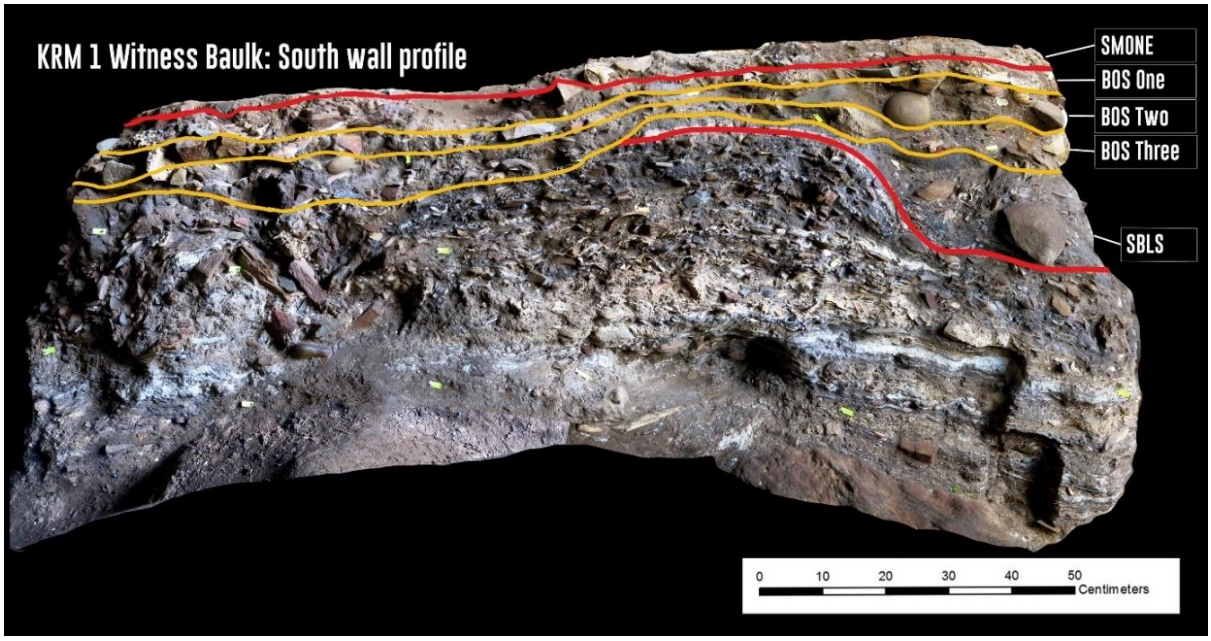


Figure 2. 2: KRM Cave 1 Witness Baulk south wall profile (Brenner *et al.* 2022: Figure 2, 7).

2.2. Coastal Intertidal Zone

The South African coast experiences a semi-diurnal tidal system (the tides occur twice a day). This means that in a one-day cycle there will be two high tides and two low tides (Langejans *et al*. 2012), with the extent and peak of the tides depending on the lunar and solar cycles.

The intertidal zone is the area where the water meets the shore between the high and low tide (Kvale 2006). International tidal zonation classification was determined by Stephenson & Stephenson (1949) and Stephenson (1939), but here the Langejans *et al.* (2012, Table 2.1) convention is followed. The intertidal zone of the southern Cape rocky shores is subdivided into six distinct zones (Table 2. 1). The Littorina Zone (Splash zone) is the highest zone remaining out of the water except during high spring tide (Stephenson 1939; Langejans *et al*. 2012; Branch *et al.* 2022). Just below the Littorina zone or splash zone, the upper Balanoid Zone occurs. This is the zone between the mean sea level (between low tide and high tide) and the sea level during high neap tide. Below this is the Lower Balanoid Zone which is the zone between the mean sea level (between low tide and high tide) and the sea level during low neap tide (Kvale 2006). The lowest intertidal zone is the Cochlear Zone. This is only exposed during low neap tide and low spring tide (Kvale 2006). The Sublittoral/Infra-tidal fringe is directly adjacent to the Cochlear zone and is mostly submerged, except for Spring equinox cycles (a period of a full moon that can be seen during the day and at night) (Da Silva 2004), and during high-pressure cell phenomena (Fu & Pihos 1994; Mather *et al*. 2009; Chandler & Merry 2010). The Subtidal/Infratidal Zone is the zone which is always submerged (Stephenson 1939; Kilburn & Rippey 1982; Langejans *et al*. 2012). However, along the southern Cape coast there are 14-days out of the 28-day lunar cycle where the intertidal zone offers high return rates, and apart from nutritional diversity requirements, terrestrial resources are important to sustain good cost to benefit ratios over one month (Langejans *et al.* 2012).

Along the southern Cape intertidal zone, species distribution is rigidly zoned within these areas (Langejans *et al*. 2012). In the context of this study five different species were collected. *T. sarmaticus* is found within the Lower Balanoid zone to the Subtidal/Infratidal zone (Yssel 1989; Pulfrich & Branch 2002). However, they are known to migrate between the Balanoid and Cochlear zones (see De Vynck *et al.* 2020). *Perna perna* (brown mussel) can be found between the Upper Balanoid and the Subtidal/Infratidal zone, *Cymbula*

oculus (goats eye limpet) is found between the upper and Lower Balanoid, *Cymbula miniata* (pinkray limpet) is found in the Lower Balanoid, and *Scutellastra longicosta* (long-spined limpet) is found in the Lower Balanoid (Kilburn & Rippey 1982; Branch *et al*. 2010: 168; Langejans *et al*. 2012: Table 5, 85).

In this study, as mentioned above, I refer to the South African coastal intertidal zones set out by Langejans *et al*. (2012) (Table 2. 1).

Table 2. 1: Intertidal Zones of Southern Africa and their placement within the intertidal and shallow subtidal zone (adapted from Langejans *et al*. 2012: Table 4, 84; Branch *et al.* 2022).

Intertidal Zone	Placement	Tide Levels
Littorina Zone	Highest Zone	High Spring Tide
Upper Balanoid Zone		High Neap Tide
Lower Balanoid Zone		Low Neap Tide
Cochlear Zone		
Sublittoral/ Infratidal Fringe		Low Spring tide
Subtidal/ Infratidal Zone	Lowest Zone	

2.3. Habitat of *Turbo sarmaticus*

T. sarmaticus occurs in both warm and cool water (catholic species) (Langejans *et al*. 2017), and along the southern Cape along the rocky coastlines between the Lower Balanoid and the Cochlear zones to between 8 – 12 m depth in the Subtidal zone (Langejans *et al*. 2012; De Vynck 2017), with a max of 30 m depth (Yssel 1989; Pulfrich & Branch 2002). As this giant turban snail is abundant, accessible by hand, has a high calorific yield, is easily replenished from the shallow Subtidal/Infratidal zone by

migration, their occurrence and foraging are associated with the "pantry hypothesis" (De Vynck *et al*. 2020: 11). The Agulhas Current, originating from the sub-tropical Indian ocean flows south-westerly along the eastern coast of southern Africa and carries warm, nutrient-poor waters from the Equator to the Southern Ocean (Kyriacou 2017). The Agulhas Current results in high species diversity for shellfish, but with a low within-species abundance. The Benguela Current, originates in the Antarctic region of the Atlantic Ocean, flowing in a north-westerly direction along the west coast of southern Africa (Kyriacou 2017). The Benguela current carries cold nutrient-rich waters from the Antarctic to the subtropics (Garzoli & Gordon 1996; Hutchings *et al.* 2009), with the current resulting in a low diversity in shellfish species, but with high abundance within the individual species (Garzoli & Gordon 1996; Hutchings *et al.* 2009).

On the south and southeast Cape coasts the Agulhas and Benguela confluence results in species diversity and within-species abundance. This is due to the seasonal upwelling of cold water from the Benguela Current, which provides the southern Cape coastline with nutrient-rich waters (Bustamante & Branch 1996; Hutchings *et al*. 2009; Branch *et al.* 2022). KRM is situated in the marine province known as the Algoa province. The Algoa province is influenced by the warm Agulhas current and the unpredictable upwelling of cold water of the Benguela current caused by northward winds (Langejans *et al*. 2017: 62). This is a suitable habitat for a catholic species like *T. sarmaticus* (Langejans *et al*. 2017).

Along the southern Cape coast, the geological formation of aeolianites along the coast, (Helm *et al.* 2018) provides a suitable habitat for *T. sarmaticus* due to the lithified beach sand and is a softer substratum (De Vynck *et al*. 2020). The aeolianites in modern studies show that there is easier access for foragers to *T. sarmaticus* in this context (De Vynck *et al*. 2020). This is because most of the aeolianite shores consist of wide, flat, wave-cut platforms with shallow pools, and are often scattered with large slabs of loose aeolianite (Nami *et al.* 2016). This causes the Intertidal zones to be less defined as the Cochlear to Balanoid zones are wide, with a narrow or no upper Littorina zone because of the presence of aeolianite cliffs (De Vynck *et al*. 2020). Table Mountain Group Sandstones (TMS) are found in the three sub-categories: exposed rocky headlands, wave–cut platforms and boulders (De Vynck *et al*. 2020). TMS has a higher diversity of species targeted by humans. However, the abundance of *T. sarmaticus* is lower than in aeolianite

reefs (De Vynck *et al*. 2020). The remaining marine habitat types are sandy/beach and estuarine. However, these do not harbour *T. sarmaticus* (De Vynck *et al*. 2020).

Along the southern Cape coastline between Cape Town and Gqeberha (formerly Port Elizabeth), there is a large record of sea-level change that is associated with the formation of coastal dunes during the Plio-Pleistocene (Carr *et al.* 2019). These coastal dunes later formed a carbonate-cemented aeolianite due to the shifts in temperature and other possible variables which are still under investigation (Carr *et al.* 2019; Morrissey *et al.* 2022). The surrounding coastal shelf is associated with Table Mountain Sandstone (Brenner & Wurz 2019).

During glacial cycles, the now–submerged Palaeo–Agulhas Plain (PAP), directly south of the southern Cape coast, was partially to fully exposed. Cawthra *et al*. (2020) concluded that the PAP intertidal zone was mostly comprised of aeolianite reefs which possibly increased the calorific productivity for humans. De Vynck *et al*. (2016) showed that the existing aeolianite reefs revealed the highest productivity of all marine habitat types.

An actualistic study by De Vynck was conducted to understand the depletion of *T. sarmaticus* in the intertidal zone, accessible to human foragers in the Still Bay area, 300 km west of Klasies River (De Vynck *et al.* 2020: 3). The study showed that over a period of 10 months there was no significant depletion of this species due to their ability to migrate from adjacent areas to the intertidal zone. Migration was tested and it was found that replenishment of the intertidal zone did not come from long-shore migration but from the subtidal zone. This means that there is a perpendicular migration to the coast as they migrate from the Subtidal 'pantry' (De Vynck *et al*. 2020), behind the tides up to the Balanoid zone. Ninety-five percent of *T. sarmaticus* live in the subtidal zone, but the species strives to live in the Cochlear zone (De Vynck *et al*. 2020). These results were interpreted to indicate a high resilience to persistent foraging of this species during lower pre-historic population densities (De Vynck *et al*. 2020: 10).

2.4. MSA foraging of shellfish in the southern Cape

2.4.1. Theory

For this research, Optimal Foraging Theory (OFT) is used as a broad theoretical background to contextualise foraging patterns. OFT is discussed by Langejans *et al.*

(2012) in the context of shellfish return rates (see also MacArthur & Pianka (1966) and Hawkes *et al*. (1982) for a broader understanding of the theory). OFT for Middle Stone Age (MSA) shellfish collecting relates to foraging strategies and technological developments that involves the handling costs of specific resources, leading to predictions according to the model (Langejans *et al.* 2012: 81). In short, OFT investigates caloric cost to benefit ratios. Langejans *et al.* (2012: 81–82), discuss planning needed for optimal shellfish collecting by MSA foragers. When foraging trips coincided with low tides allowing for a higher return rate due to the most productive intertidal zone being exposed. OFT is used to hypothesise a "pre-historic state" associated with relatively little planning, where shellfish species from higher zones are overrepresented; and for an "evolved state" species from lower zones are well represented (Langejans *et al.* 2012: 81–82). Blombos Cave, Pinnacle Point and KRM show Cochlear zone foraging in some Marine Isotope Stage 5 periods which indicates an evolved understanding of the coastal environment (Langejans *et al*. 2012), as *T. sarmaticus* (alikreukel) are foraged from the lower zones, the Lower Balanoid and the Cochlear zones (Langejans *et al*. 2012).

OFT in relation to shellfish exploitation further involves return rates, handling, and search costs. The profitability of a species that is exploited depends on two variables: The first variable is the return rate, the absolute energetic value of the shellfish. This can be modelled by ranking the species according to their raw meat weight (kilo-calorific values) (Kyriacou *et al*. 2014; Kyriacou 2017). The return rate is the rate at which calories are returned by food, per hour including all caloric costs involved in procurement, processing, and transport (the optimal cost-to-benefit ratio) (Kyriacou *et al.* 2014). Return rate helps with understanding if there was an in-depth understanding of the coastal environment by the foragers (Langejans *et al*. 2012). The second variable is the handling cost (cost to benefit ratio) (MacArthur & Pianka 1966; Langejans *et al.* 2012: 82). Handling cost is a composite variable, dependant on the species' defence mechanisms to avoid predation and on the capabilities of predators concentrated on the habitat along the shore. It is also dependant on the species' abundance and caloric gain (Langejans *et al*. 2012). These species are assumed to have a higher handling cost (MacArthur & Pianka 1966; Langejans *et al.* 2012: 82). Search cost looks at the amount of time the forager spends looking for suitable prey, meaning that if a species is rare, it will only be encountered sporadically and will be uncommon in excavated assemblages, even if it is favoured by foragers (Langejans *et al*. 2012). This means if a species inhabits the

lower intertidal zones of the shoreline, they are difficult to obtain because they are predominantly submerged. The correlation between search cost and handling cost looks at the moment at which the forager decides whether the prey is ignored, and the search continues looking for higher-ranked prey. This is according to OFT and the Diet Breadth Model (MacArthur & Pianka 1966). For example, encounter rates with high-ranked prey species are less likely, whereas more low-ranked prey species are likely to be exploited. This is due to the higher-ranking species according to yield being more difficult to forage. However, this situation does not always apply to the collection of shellfish especially *T. sarmaticus* due to their abundance and are considered a high-ranked species (Langejans *et al*. 2012). Species are not encountered randomly along the shore but occur in specific zones (Langejans *et al.* 2012: 82).

2.4.2. Coastal adaptations and shellfish exploitation in the southern Cape

A definition of coastal adaption according to Will *et al*. (2019: 2) is the behaviour associated with hunter-gatherers where the regular use of coastal resources and the formation of settlement along the shoreline is established. The onset of coastal adaption is first suggested at 164 ka at Pinnacle Point (Will *et al*. 2016, 2019). However, coastal adaptation is fully established along the southern Cape coast between 110 and 100 ka with all the major coastal sites showing coastal foraging on a regular basis within the Cochlear zone and fewer Balanoid species added (Will *et al*. 2016, 2019), and this occurs also between 130 – 115ka along the western Cape coast (Kyriacou *et al.* 2015). Coastal adaption according to the definition above is very different to maritime adaptation. Maritime adaptation is a much more recent adaptation occurring during the Neolithic (Lidour *et al*. 2021: 1). It is the development and diversifying of fishing techniques including the exploitation of marine animal materials that would be harder to forage for (e.g., shark teeth, string ray barbs) for the purpose of both tools and personal adornments, as well as the advancement of seafaring, and colonization of offshore islands due to the increase in the number of people along the coast (Will *et al.* 2016, 2019; Lidour *et al.* 2021).

The Cape south coast has distinct, biotic (tidal) zones characterised by distinctive fauna, some of which are sought by human foragers (see Table 2. 2). The lowest tides generally expose the larger species such as *Haliotis midae* (abalone) which has a higher meat yield but low abundance. However, foraging in the intertidal zone near the low-water mark can

be dangerous and needs to be timed to coincide with the most favourable part of the daily tidal cycle and the monthly lunar cycle (De Vynck et al. 2020). In the southern Cape, at Pinnacle Point, in the 164ka layers, evidence suggests people foraged along the higher, less productive Lower to Upper Balanoid zones for *Donax serra* (white mussel), *Choromytilus meridionalis* (black mussel), *Perna perna* (brown mussel) and *Dinoplax gigas* (giant chiton) (Jerardino & Marean 2010; De Vynck *et al.* 2020: 2; Jerardino & Navarro 2021). By 100ka, prey species such as *T. sarmaticus*, *P. perna, Haliotis spp.,* and *Burnupena spp.* from the lowest tidal zone, the Cochlear zone, show up in MSA sites such as Blombos Cave, Pinnacle Point and KRM, signifying ongoing systematic exploitation of shellfish (Jerardino & Marean 2010; Wurz *et al.* 2022). Apart from the shift in prey species corresponding to deeper infiltration of tidal-zone habitats, the remains of shells increase in density, indicating that MSA people increasingly depended on these resources as a component of their diet from 110ka (Will *et al.* 2019; De Vynck *et al*. 2020: 2).

Table 2. 2: Common species found within the different Intertidal Zones (adapted from Langejans *et al.* 2012).

Tidal Zone	Species
Littorina Zone	*Oxystele spp.*
Upper Balanoid Zone	*Cymbula oculus*
Lower Balanoid Zone	*Scutellastra longicosta*
Cochlear Zone	*Turbo sarmaticus*
Sublittoral/Infratidal Fringe	*Perna perna*
Subtidal/Infratidal Zone	*Haliotis midae*

2.4.3. Nutritional Value

Shellfish are nutritionally beneficial and fit the category of so-called functional foods (De Vynck *et al*. 2020: 14). However, if shellfish lack resilience in the face of predation, their value as a primary food resource is minimal as ongoing foraging could decrease productivity (De Vynck *et al.* 2020: 2). Resilience is therefore seen as dependence or high productivity over a long period of time. Calorific gain is commonly measured through ethnographic observations combined with a quantitative assessment of the associated harvest. The results are usually expressed in terms of hourly caloric benefit ($kcal/h^{-1}$)

from pursuing various resources (De Vynck *et al.* 2020: 2). In De Vynck *et al*. (2020: Table 3, 7) the total calories for all the *T. sarmaticus* that were collected was 31 148.7 kcal which consisted of 81.9% of the total calorific percentage for the entire collection. This means that one individual *T. sarmaticus* contributed 19.22 kcal (De Vynck *et al*. 2020: 7).

Langejans *et al*. (2012: 84) looked at the ranking of species by focusing on the shellfish species that were exploited for nutrition. By combining the data on yield and handling cost, the assumption was made that the shellfish with the highest meat yield would have been preferred during collection (Langejans *et al*. 2012: 83). A quantitative framework has been set up for broader discussions on the importance and role of shellfish in the diets of MSA hunter-gatherers in two disparate coastal regions (southwestern Cape and Kwazulu-Natal) (Kyriacou 2017: 31). The two coastal regions differ in shellfish diversity due to the difference in ocean currents, nutrients in the water and sea-surface temperature (SST), with the southwestern Cape having a higher species diversity due to the cold waters upwelled by the Benguela current (Kyriacou 2017). The most energy received from shellfish meat derives from the protein and, to a lesser extent, the lipid components of edible soft tissue (Kyriacou 2017: 34).

T. sarmaticus is seen to have the highest caloric harvest values compared to all other species harvested (De Vynck *et al.* 2016: Figure 3, 106). Experiments on intertidal foraging along the southern Cape coast of South Africa suggest that foragers with simple tools could extract sufficient nutrients along stretches of the coast at rates that compare favourably with the returns from terrestrial hunting and gathering observed in modern hunter-gatherer societies (De Vynck *et al*. 2016: 109). The marine intertidal foraging habitat would often provide higher energetic returns than other foraging activities. Additionally, marine invertebrates yield protein content that is comparable (in weight ratio) to protein from terrestrial fauna. For example, the gonad of a single *Scutellastra granularis* (granular limpet) yields 8.1 g/100 g of protein, compared to the muscle of a single Kudu which yields 12.9 g/100 g of protein (Kyriacou *et al.* 2014: Table 3, 68). This means that while meeting energetic needs, marine intertidal foragers could also easily deliver sufficient protein in the diet for good health, and may need to complement the lean protein shellfish diet with carbohydrate or lipid-rich resources to avoid negative consequences of a too-high protein diet (De Vynck *et al*. 2016: 109).

2.5. *Turbo sarmaticus* operculum size and the 'predation hypothesis'

Turbo sarmaticus operculum size gives insight into the life cycle of this species (Steele & Klein 2008). *T. sarmaticus* grows in two stages. The first stage is the first few years of the species' lifecycle where it grows rapidly in size and the second stage is where the growth rate of the species slows down (Yssel 1989). For example, the shell length will be between 24 mm – 72 mm for the first three years and will be more than 112 mm after nine years (Yssel 1989).

In a study on various coastal sites along the Cape coastline comparing the *T. sarmaticus* opercula size of MSA to Later Stone Age (LSA) coastal occupation sites, Steele & Klein (2008, Klein & Steele 2013) showed that *T. sarmaticus* opercula differ in size between the LSA (median 26.3 mm) and MSA (MSA I median 37.2 mm, MSA II median 39.4 mm, and MSA III median 42.3 mm) periods at KRM. (Klein & Steele 2013: 10913). The median for *T. sarmaticus* opercula length during MSA II, the period during which layer SMONE was formed was thus 39.3 mm (see also Steele & Klein 2008). Steele & Klein (2008) argue that the larger opercula from the MSA sites are due to MSA humans not exploiting shellfish as intensively as LSA humans and therefore, the shellfish were able to develop to full size. LSA humans however are thought to have a higher population density and individuals who understood the coastal environment better and were, therefore, able to exploit more of the shellfish continuously, and as a result the shellfish were unable to develop to full size (Steele & Klein 2008; Klein & Steele 2013; Klein & Bird 2016).

2.6. *Turbo sarmaticus* operculum size, growth patterns and the 'climatic and environmental hypothesis'

The following section discusses factors other than predation that might influence opercula size. An isotopic study looked at the increments of the complex spirals seen on *T. sarmaticus* opercula (Figure 2. 3), to understand the growth patterns of the individuals (Galimberti *et al*. 2017). The opercula did not show any clear annual or sub-annual bands (Sealy & Galimberti 2011; Galimberti *et al*. 2017), as the opercula grow at a slow rate of around ca. 9 mm per/year during the first three years, slowing to ca. 2 mm per/year thereafter for the remaining years of their 10–year lifespan (Foster 1997; Galimberti *et al.* 2017). *T. sarmaticus* growth is slowed during periods of extreme temperatures (Galimberti *et al*. 2017: 65–66). During the months of winter, when the water

temperature is colder (drops to lower than 14^0C in the Mossel Bay region) the growth of the operculum and shell is slowed. The same is seen in the hottest months when the temperature of the water is greater than $23,5^0$C (Sealy & Galimberti 2011; Galimberti *et al*. 2017). Therefore, it is believed that the sea surface temperature (SST) would have a direct effect on the *T. sarmaticus* growth and would consequentially affect the size of the operculum, showing that the climate and environment play a role in their growth.

The size of *T. sarmaticus* and thus the size of the opercula is dependent on the environmental conditions and larger *T. sarmaticus* are generally associated with increased nutrient availability (Sealy & Galimberti 2011). An increase in SST would have a slowing effect on *T. sarmaticus*, as the warm water increases the metabolic rates of the mollusc (Sealy & Galimberti 2011; Langejans *et al.* 2017), resulting in a decrease in the size of the opercula due to the slowed growth rate. There is an increase in productivity in colder SST due to the increase in nutrients from algae and plankton (Langejans *et al.* 2017).

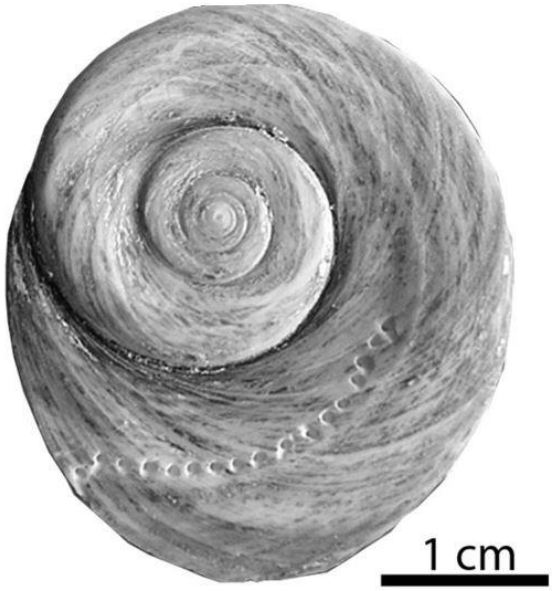


Figure 2. 3: Spirals on *T. sarmaticus* operculum (adapted from Galimberti *et al*. 2017: Fig.1, 63).

A study was conducted that documented the difference between the growth rates and reproductive fitness of *T. sarmaticus* which were kept in a controlled tank environment (Foster *et al*. 1999). The oceanic productivity, of organic matter by phytoplankton, helps

generate food for shellfish, and variations in oceanic productivity affect the marine food chain and may affect the size and distributions of shellfish species (Sealy & Galimberti 2011). The results showed that there could be a regional difference in the growth of *T. sarmaticus* due to the different algae species affecting the growth rate (Foster *et al.* 1999).

2.7. Seasonality and *Turbo sarmaticus*

Seasonality is a key dimension of subsistence behaviour based on the acquisition of resources and the occupation of sites (Loftus *et al.* 2019). In southern African archaeology, a framework on seasonal mobility has been used to explore whether hunter-gatherers exploited between coastal and inland sites due to fluctuations in seasonality and understand the different resources found between the different ecozones (Parkington 1976). The seasonal occupation of coastal sites compared to year around occupation.

Loftus *et al.* (2019) provided a perspective of shellfish foraging seasonally along the southern Cape coastline in the context of existing detailed coastal archaeological sites and records. Oxygen isotopes from marine mollusc shells can be used to reconstruct the seasonality of the sea surface temperature (SST) during the period of shell growth and seasonal climate changes to the environment (Loftus *et al*. 2019). Loftus *et al.* (2019) conducted the oxygen isotope study using *T. sarmaticus* opercula from five archaeological sites (Nelson Bay Cave, Robberg Cave, Byneskranskop 1, Klasies River Main Site and Pinnacle Point) along the southern Cape coastline within the last interglacial cycle. The *T. sarmaticus* opercula from the five assemblages showed visible growth increments on the flange surface, due to the species location in the intertidal zone, it can be used as a good indicator for SST and for palaeotemperature reconstruction as they are mostly always submerged (Loftus *et al*. 2019).

Semi-annual foraging patterns based on $\delta^{18}O$ analysis for KRM (MSA II Lower) *T. sarmaticus* opercula showed more warm water (summer and autumn) (n=7) foraging patterns but not a big difference between the cool water (winter and spring) (n=5) with the quarterly season mainly showing autumn (n=4), spring (n=3) and summer (n=3) (Loftus *et al*. 2019: 9). The majority of the MSA coastal sites showed evidence of foraging of *T. sarmaticus* during summer and spring compared to the LSA coastal sites where spring and winter were much more evident (Loftus *et al*. 2019).

The analysed assemblage from KRM during Loftus *et al.* (2019) study showed the fewest *T. sarmaticus* were harvested during winter, which is the least optimal foraging season. The KRM assemblage showed a strong seasonal signal with nearly 50% of the assemblage being foraged during spring and notably less during summer, the optimal foraging period (Loftus *et al.* 2019).

2.8. Previous work on experimental processing of *Turbo sarmaticus*

De Vynck *et al*. (2016: 102), described caloric return rates of intertidal foraging within an actualistic context along the Still Bay coastline. They found that the variables that could affect foraging returns include, the individual forager's ability, and tidal level (meters). The tide is a synthetic controlling variable, which can affect the foraging success, like an ocean swell, wind, and rain (De Vynck *et al*. 2020: 5). Statistical analysis was used to investigate the effect of tidal level, habitat type and weather patterns, as well as age and sex of the forager to measure shellfish return rates (De Vynck *et al*. 2016: 102). Overall, the harvest was mainly comprised of *T. sarmaticus* (56.1%) (De Vynck *et al*. 2016: 102).

In the experiments undertaken by De Vynck (2017), non–metal tools (bone tools and wooden sticks) were created to forage and process shellfish by indigenous coastal foragers. The 2017 methodology, similar to those used in this study and described in Chapter 3, was informed by the indigenous coastal foragers, due to their knowledge and experience with coastal foraging and processing of the shellfish species, as well as their experience with being in the intertidal zones and producing tools that would be successful during the process. The collection of material for tool production was done before the experiments, as bone and wood used needed time to dry before tool production could occur. The production of the tools was done along the protruding rocks along the Still Bay coast and only once the tools had been produced, the foraging could take place. The foraging for the shellfish took place at spring low tide and was done by experienced foragers from the local indigenous communities. After the foraging had taken place, the processing occurred in a similar style as discussed in De Vynck *et al.* (2016: 109). Both the raw and cooked processing was done by the same foragers after foraging was completed, and extraction of the edible portion was done after cooking and for some, the extraction was done raw (De Vynck 2017: Appendix 3). *T. sarmaticus* were usually cooked in batches of 15–20 shells placed directly on the coals (Figure 2. 4). The

cooking occurred in batches, as this way, the mean cooking time required was only 27 seconds per item. Extracting the meat from the shell (Figure 2. 5) and removing the guts before consumption took 18 seconds per item on average (no variance was measured because numbers are calculated from a single large batch) (De Vynck *et al.* 2016: 109). *T. sarmaticus* did not require constant attention but cooking instead took place while the foragers were conversing, socialising and repairing tools (De Vynck *et al.* 2016: 109). In this study, these experiments are expanded on, and the tools produced for the De Vynck (2017) experiments are replicated.



Figure 2. 4: Cooking of *T. sarmaticus* on the coals (De Vynck 2017: Fig. A 3.15a, Appendix 3).



Figure 2. 5: Raw extraction of the meat from *T. sarmaticus* shell with a bone tool (De Vynck 2017: Fig. A3.12, Appendix 3).

2.9. *Turbo sarmaticus* opercula and site formation

Taphonomy is the study of the biological, physical and chemical processes that change organisms after death (Lyman 1994). As there are no published papers that have studied taphonomic aspects of *T. sarmaticus* opercula, literature relating to *Turbo undulatus* (Common warrener) was used to help understand the taphonomic characteristics of shellfish within the same genus (Sherwood *et al.* 2016; see also Holmes 2020). *T. undulatus* opercula are found along the southern Australian coastline in Holocene-occupied sites. Sherwood *et al*. (2016) investigated the differences between anthropogenic, naturally occurring, and coastal gull middens. Anthropogenic middens [or in the case of Sherwood *et al.* (2016) Aboriginal middens] are defined as middens that have been created by human collection and consumption of shellfish and feature a bias towards larger shells found in the midden due to the prey selection. This means that larger opercula will be found at the site predominantly due to the selection of larger individuals (Sherwood *et al.* 2016). Naturally occurring middens are beach deposits that occur due to storm surges that wash the opercula to the shore. In beach deposits, a wide variety of sizes are seen with a higher proportion of smaller opercula. The opercula from a beach deposit will show evidence of water-wear or rounding of the edges due to the

abrasion of the sand and waves (see Chapter 4: Analytical Methods) (Sherwood *et al*. 2016).

Human depositional middens or cultural middens are formed at occupation sites where the processing of shellfish took place (in the case of KRM, the at the caves). In South Africa, few researchers have looked at understanding how cultural middens form and the possible taphonomy that goes along with the human interaction with shellfish and opercula (cf. Sherwood *et al.* 2016; 2018). A study done in southern Australian on early and late Holocene Aboriginal coastal occupation sites looked at understanding the taphonomy left on the shells of *T. undulatus*. However, there were no conclusive differences between the cultural middens' taphonomy and that of a coastal gull's midden. Burning was the only attribute that distinguished between the human and natural midden (Sherwood *et al.* 2016; Sherwood *et al.* 2018).

2.10. Conclusion

In this chapter, the literature on KRM and the context of the material analysed have been discussed. The literature on previous actualistic work associated with *T. sarmaticus*, the understanding of the influences of exploitation, coastal adaptations, the environment and the factors of SST and the presence or absence of nutrients that can affect the growth of *T. sarmaticus* and their operculum were addressed. In the next chapter the methodology and materials used in the actualistic study conducted for this paper is discussed.

Chapter 3: Experimental Materials and Methods

3.1. Introduction

An actualistic study was undertaken to investigate the subsistence behaviour and taphonomic marks that are left on *T. sarmaticus* from the MSA II layer SMONE at KRM. In this chapter, the experimental methodology is described involving the foraging practice and methods used for processing.

3.2. Foraging

The foraging experiment to collect and process *Turbo sarmaticus* (alikreukel), and three other shell species, took place at Jongensfontein, Still Bay, Western Cape, South Africa (Figure 3. 1). Three different locations were visited (Figure 3. 2). Experimentation took place over a period of seven days, between the 18 August 2021 and the 25 August 2021 (late winter), during a period of spring tide (full moon). Tidal variation occurs at several levels based on the monthly lunar cycles (spring and neap tides) and daily lunar cycles (low and high tides). The maximum monthly lunar cycle variation is classified into spring and neap tides, which are driven by a relative lunar position to the sun (Marean 2010: 432). Field research commenced after the habitat, the correct ethnographic replication of tool production and foraging, and the materials required were studied.

To conduct the foraging research, a Research fishing permit was obtained from the South African Department of Environmental Affairs [Appendix 1D.1: Research Permit (RES2021–85)] which allowed the collection of 150 individual *T. sarmaticus* that were greater than 55.5 mm in shell length. In addition, an annual Fishing licence [Appendix 1D.2: Additional Fishing Permit (1052834)] was bought from the Still Bay Post Office, allowing for the collection of additional mollusc species and an additional five individual *T. sarmaticus*.



Figure 3. 1: Jongensfontein, where the experimental foraging took place, in relation to the southern Cape coastal archaeological sites Klasies River main site (KRM), Blombos Cave (BBC) and Pinnacle Point (PP) (Google Earth Pro 2021a).

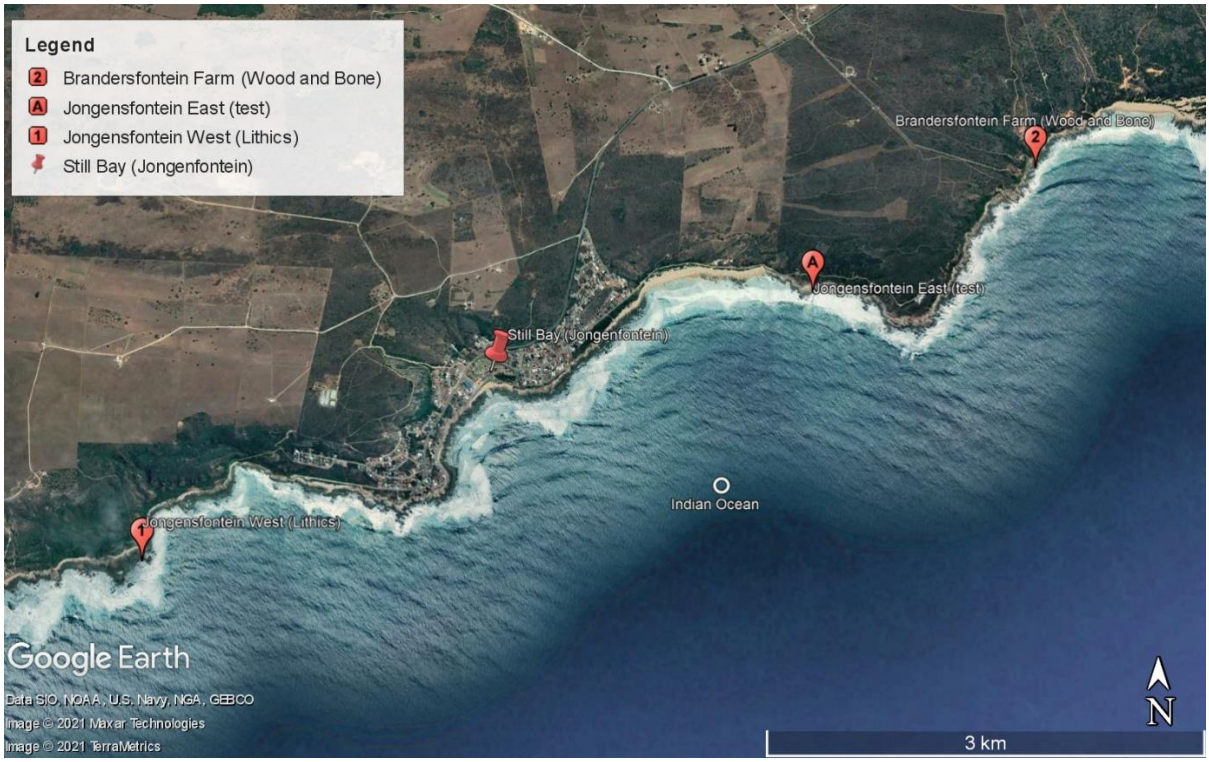


Figure 3. 2: Foraging locations for Still Bay foraging experiment, A: Test foraging day at Jongensfontein East, 1: Lithics foraging at Jongensfontein West, 2: Wooden tool and Bone tool foraging at Brandersfontein Farm (Google Earth Pro 2021b).

3.2.1. Participants and Prey

For the purposes of this study, Dr Jan De Vynck is referred to as participant 1 (P1) and I, Carl Holmes, as participant 2 (P2). P1 has experience through observations of local coastal foragers and had learnt foraging and tool–making techniques from them (De Vynck 2017). Before the experiment P2 had no foraging experience or experience making tools. P2 had to learn while foraging and could be considered to have the same skills as an adult with no foraging experience in a Middle Stone Age (MSA) context.

For the foraging, we targeted five intertidal species commonly found within the archaeological record along the southern Cape coast. The five species were targeted as they probably would have foraged at the same time in the past: *T. sarmaticus* (Figure 3. 3A and B), *Perna perna* (brown mussel) (Figure 3. 3C), *Scutellastra longicosta* (long-spined limpet) (Figure 3. 3D), *Cymbula oculus* (goat's eye limpet) (Figure 3. 3E) and *Cymbula miniata* (pink ray limpet) (Figure 3. 3F), with the processing focusing mainly on the *T. sarmaticus*.

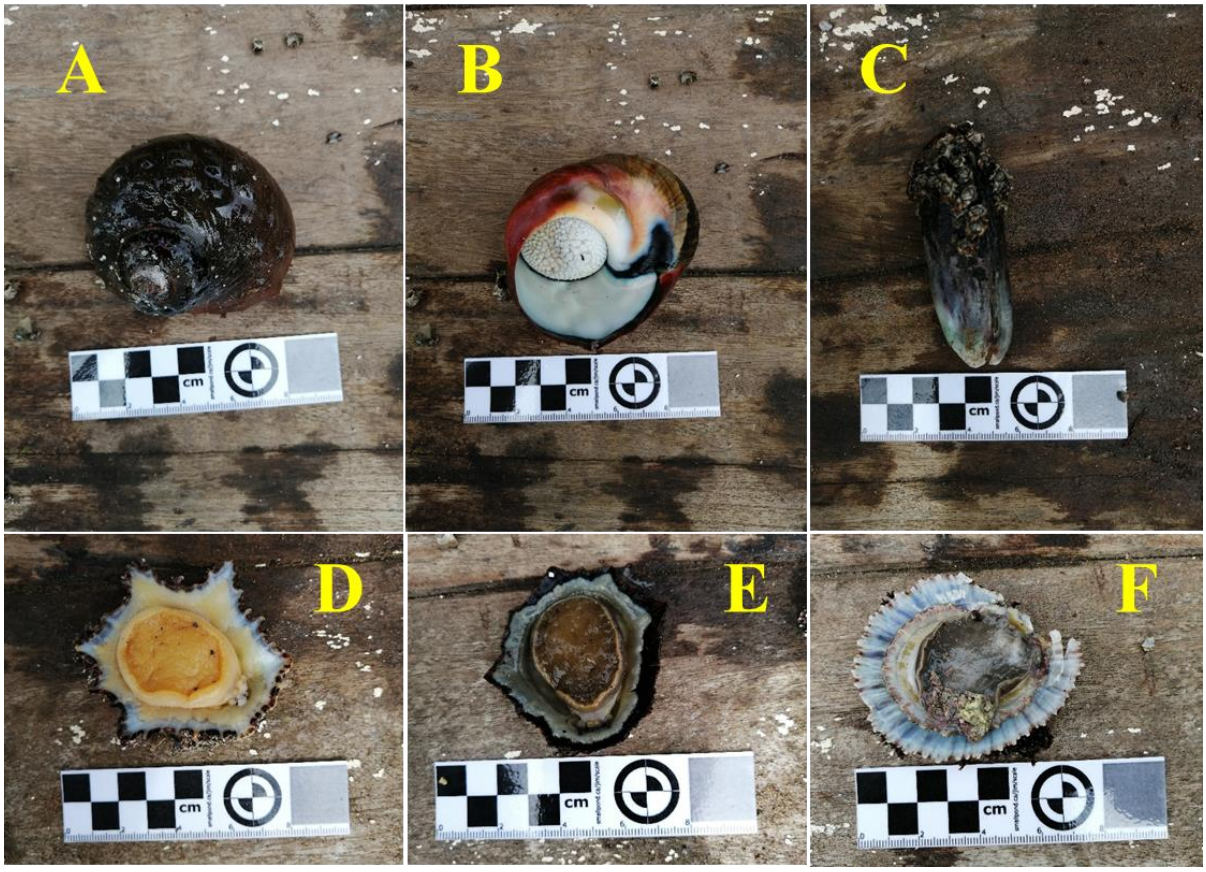


Figure 3. 3: A, the dorsal side of a *T. sarmaticus* shell, B, the ventral side of the *T. sarmaticus* shell with operculum in place. C, of an intact *P. perna* shell. D, of the ventral side of the *S. longicosta* shell. E, of the ventral side of the *C. oculus* shell. F, of the ventral side of the *C. miniata* shell.

The opercula from the *T. sarmaticus* are the focus of the study. The opercula are hard round/oval calcium carbonate disks carried on the foot of the species. The *T. sarmaticus* opercula have a rigiclaudent spiral with multiple spirals and the shape of the opercula fitting the opening (Checa & Jiménez-Jiménez 1998), where the spirals rotate in a clockwise direction. The opercula serve the purpose of protecting the molluscs head near the shell aperture (Checa & Jiménez-Jiménez 1998). The *T. sarmaticus* opercula consist of two sides, the dome (ventral) and the flange (dorsal) (see Figure 3. 4).



Figure 3. 4: A, dome (dorsal) surface of the *T. sarmaticus* opercula. B, the flange (ventral) surface of the *T. sarmaticus* opercula.

3.2.2. Habitat

The foraging of the shellfish took place between the Lower Balanoid and the Cochlear zones during low tide (Table 2. 1) (Stephenson 1939), corresponding to the accessibility of the tidal zones during the spring low tide (Marean 2010: 432). The geology of the Still Bay coastal landscape is dominated by Table Mountain Sandstone (TMS) consisting of boulders, exposed rocky headlands, and wave-cut platforms (De Vynck 2017: 7; Cawthra *et al.* 2020).

3.2.3. Foraging Tools

Three different types of tools were used over three days of foraging during low tide. One tool type was used per day: MSA lithics from the spill heap at KRM (Day 1), experimentally made wooden tools (Day 2), and experimentally made bone tools (Day 3).

Production of foraging tools

Lithics

The lithics used for the foraging experiment were MSA lithics recovered out of context from the spill heap at Klasies River Main Site (Figure 3. 5). The lithics were described by Sarah Wurz to provide a clear understanding of the types of lithics that were used and selected by each participant. The lithics in this experiment consisted of MSA points, blades, and core edge (débordant) flakes and blades, with the raw material being quartzite for all the lithics (pers. comm Wurz).



Figure 3. 5: Out of context Middle Stone Age lithics from the Klasies River main site spill heap after use, showing breakage on the lithics as a result of the experiment.

Wooden tools

The Wooden tools were produced by P1 and P2 from *Olea europaea ssp. africana* (Wild Olive) branches which were collected from the Still Bay area. This species is the wood of choice used by modern day local communities along the southern Cape coast for the making of wooden tools, due to its accessibility and density of the wood allowing it to be reused (De Vynck 2017, pers. comm De Vynck).

The production of the wooden tools took place at Morris Point above the Still Bay Harbour ($34^0$25'13,22"S, $21^0$21'49,40"E). The type of wooden and bone tools was based on replicated tools that P1 observed local community members make during his PhD research (De Vynck 2017). This was the basis for the production of the tools in this dissertation. Before the production of the tools, the branches were measured (using a standard 3m tape measure) to equal 0.45 m (Figure 3. 6A) and were then cut using a hand saw (Figure 3. 6B). Pre-historic tool producers would have cut the lengths with lithics or placed lengths in a fire to shorten the branches. We felt that there was no need to replicate either cutting method as cutting with a saw had zero effect on the outcome of the experiment. The wooden tools were produced by scraping the wood on TMS rocks with quartz veins running through the dominating quartzite base geology (Figure 3. 7, Figure 3. 8 and Figure 3. 9). Three wooden tools (Figure 3. 10) were produced by each of the participants, with the time being recorded for how long the participants took to produce each tool.



Figure 3. 6: A, the measuring of the *Olea europaea ssp. africana* branches to 0.45 m. B, the hand saw used to cut the branches before the production of the tools, and C, the cut *Olea europaea ssp. africana* branches for both participants.



Figure 3. 7: Wooden tool production by P2 using the quartzite veins on the Table Mountain Sandstone rocky headlands.

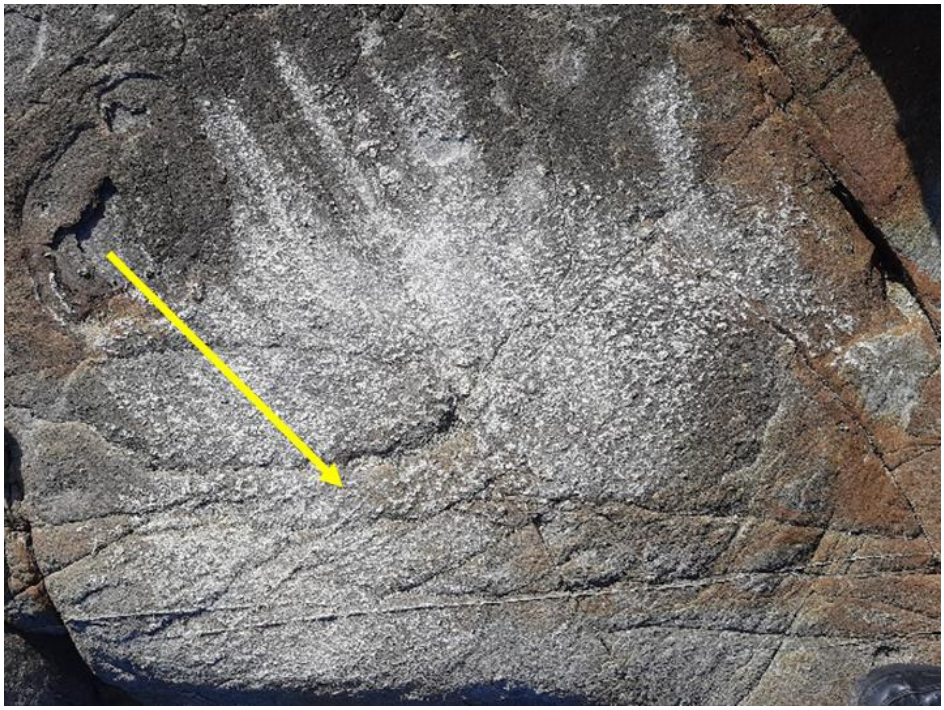


Figure 3. 8: Worksite after the tool production, in the image the quartzite veins are protruding from the Table Mountain Sandstone exposed rocky headlands.



Figure 3. 9: Worksite after the tool production, in the image the Table Mountain Sandstone exposed rocky headland surface shows the site used to refine and sharpen the tool where no quartzite veins are present.



Figure 3. 10: Wooden tools made by P2 out of *Olea europaea ssp. africana* branches.

Bone tools

Four *Tragelaphus strepiceros* (Greater Kudu) long bones (1: humerus, 2: femur, 3: radius and ulna, 4: femur, see Figure 3. 11) from the local butcher in Still Bay were used to construct the bone tools. Two long bones were baked in the oven for 60 minutes at 200^{0}C, and the remaining two bones were kept raw. Cooking bone before production was conducted under the assumption that marrow was important for MSA foragers to add to the optimal caloric gain per energy package (individual animals) (Hawkes *et al.* 1982; Hawkes & O'Connell 1992). Also, heat-treated bone is potentially denser and more

effective as a tool than raw bone (Bradfield 2015). The bones were then placed on the roof to dry for a week.



Figure 3. 11: 1, *T. strepiceros* humerus (baked). 2, *T. strepiceros* femur (raw). 3, *T. strepiceros* radius and ulna (baked). 4, *T. strepiceros* femur (raw).

The production of the bone tools took place near Still Bay in a pristine intertidal area (34°24'43.80"S, 21°22'49.40"E), along TMS exposed rocky headlands. Each participant received one cooked *T. strepiceros* long bone and 1 raw *T. strepiceros* long bone to produce as many bone tools as they could (Figure 3. 11). The hammer and anvil technique were used by both participants, with small cobbles and rocks found near the production site, to crack open the long bone (Figure 3. 12) (De Vynck 2017), so the marrow could be removed. Then the participants used the fragment from the long bone to produce the tools, by rubbing the edge of the bone fragment on the TMS rocks until the participant was satisfied with the tool produced and they were similar to the ethnographic observations (point, blade, or scraper) (Figure 3. 13) (De Vynck 2017). Tool production time, per tool and per participant, was recorded. Most of the bone tools were produced from the baked bone (Figure 3. 14), as the raw bone fragmented into small unusable fragments (Figure 3. 15B).



Figure 3. 12: Cobblestones used for the hammer and anvil technique to crack open the long bone. A is the Cobblestone used by P1, and B is the Cobblestone used by P2.



Figure 3. 13: A, the area where P2 produced the bone tools. B, the remains left behind postproduction (bone marrow, skin, bone fragments).



Figure 3. 14: A, bone tools made by P2 out of *T. strepiceros* long bones. B, bone tools made by P1 out of *T. strepiceros* long bones.



Figure 3. 15: A, the tool produced by P2 from the baked long bone. B, the bone fragments produced by P2 from the raw long bone.

3.2.4. Foraging Process

Before the foraging took place each day, the following data were recorded as affecting variables (Appendix 1A Table 1), the Geographical Positioning System (GPS) coordinates for the start and stop location of the foraging patch (using a Garmin eTrex®10 handheld GPS), the habitat type, the swell size, period and direction (Windy.com 2011), the low tide and high tide times and tidal heights (tides4fishing.com 2021), the phase of the moon, the

wind direction and speed (Windy.com 2011), the aspect of the shoreline, the ocean condition rating (Table 3. 1), and the water temperature (Windy.com 2011).

Table 3. 1: Ocean Condition rating scale, calibrated to the Beaufort scale, showing the optimal and suboptimal conditions for shellfish foraging.

Ocean Condition Rating	Beaufort Scale	Wind (kph)	Swell (m)	Status
1	0–2	0–11	0–0.3	Good
2	3	12–19	0.4–1	Good
3	4–5	20–38	1.1–2.4	Average
4	6	39–50	2.5–5.8	Poor
5	7–12	51+	5.9+	Unsafe

The Ocean Condition rating (Table 3. 1) was correlated to the Beaufort scale rating system (De Vynck 2017), based on wind speed, and swell size. These conditions affect the condition of the sea and the ability of a forager to successfully forage in the intertidal zones. The Ocean Condition Rating is ranked on a score of 1 (the best) to 5 (the worst).

Foraging time was recorded to measure caloric return rates ($Kcal/Hr^{-1}$) related to the effectiveness and the effects on the shell damage of the various foraging tool media. 30 individuals of *T. sarmaticus* were collected per participant, 10 of each of the limpet species (*S. longicosta*, *C. oculus*, and *C. miniata*) and 20 *P. perna*. Each participant used ethnographic observations (De Vynck 2017), to conduct foraging methods within the intertidal zone and foraging time elapsed when the above volumes per species were collected per foraging event. The foraging tools were used to extract the prey species from the intertidal zone as per ethnographic observations.

3.2.5. Processing

Processing methods of *T. sarmaticus* were consistent throughout the research experiment. Each day processing took place immediately after foraging was completed. The foraging tools were used during the processing with the aim to measure the operculum damage variations between each tool. *T. sarmaticus* operculum damage was investigated subsequently in the laboratory. The first step in the processing commenced by weighing out 10 kg of *Acacia cyclops* (Rooikrans) firewood (using a Pelouze® Rubbermaid 45 kg x 50 g digital hanging scale) and lighting the fire within a container (one fire was made per day, and the fire was shared by both participants) (Figure 3. 16).

Pre-historic replications of cooking shellfish directly on the fire embers (De Vynck 2017). However, *T. sarmaticus* were placed on a grid above the fire to ensure practical field research methods for allometric conversions and did not result in a variation from pre-historic cooking results (pers. comm De Vynck). Total cooking time was recorded for each fire each day from when the fire was started to when the fire was ready for cooking and cooking time was recorded as a variable affecting the total cost–benefit ratios of caloric gain (De Vynck 2017).



Figure 3. 16: Fire for cooking *T. sarmaticus*.

Raw and Cooked Processing

Processing *T. sarmaticus* was twofold: raw extraction and cooked extraction of edible portions using the three types of tools. The processing started by recording the following information for both participants: the total weight of the combined foraged shellfish (using an AWS-SR-20 20 000 g x 10 g digital hanging scale), along with the total count for each species individually (*T. sarmaticus, P. perna, S. longicosta, C. oculus and C. miniata*), and the weight and count for the raw and cooked *T. sarmaticus* edible portions (Appendix 1A.2. Processing Data).

Raw Processing

For the processing of the raw *T. sarmaticus*, the following was recorded during the processing for each shell by each participant: the shell length in millimetres (Figure 3.

17A), the shell width in millimetres (Figure 3. 17B), the operculum length in millimetres (mm), the operculum width in millimetres, the gross weight in grams (g) (using an AWS-SR-5 5 000 g x 5 g digital hanging scale), the edible portion raw weight in grams (using an AWS-70 70 g x 0.01 g digital pocket scale), the gonad weight in grams (using an AWS-70 70 g x 0.01 g digital pocket scale), the gonad colour, and the shell colour (possible gender difference), and the total time it took to process the 15 individual shells (Figure 3. 18). After the *P. perna* and limpet species weights were recorded the *P. perna* were kept aside to be consumed later and the limpet species were released back into the nearby rock pools.

Cooked Processing

For the processing of the cooked *T. sarmaticus*, the following was recorded during the processing for each shell by each participant: the shell length in millimetres (Figure 3. 17A), the shell width in millimetres (Figure 3. 17B), the operculum length in millimetres, the operculum width in millimetres, the gross weight in grams (using an AWS-SR-5 5 000 g x 5 g digital hanging scale), the edible portion cooked weight in grams (using an AWS-70 70 g x 0.01 g digital pocket scale), the cooked gonad weight in grams (using an AWS-70 70 g x 0.01 g digital pocket scale), the gonad colour (yellow vs green gonad indicates gender), and the shell colour (possible gender difference related to gonad colour), and the total time it took to process the 15 individual shells (Figure 3. 18), and the time it took for each shellfish to cook (Figure 3. 19). Once P1 completed his processing for his 15 individual *T. sarmaticus*, P2 would begin to process his 15 individual *T. sarmaticus* with the same information being recorded.



Figure 3. 17: A, the shell length measurement technique by P1. B, the shell width measurement technique by P1.

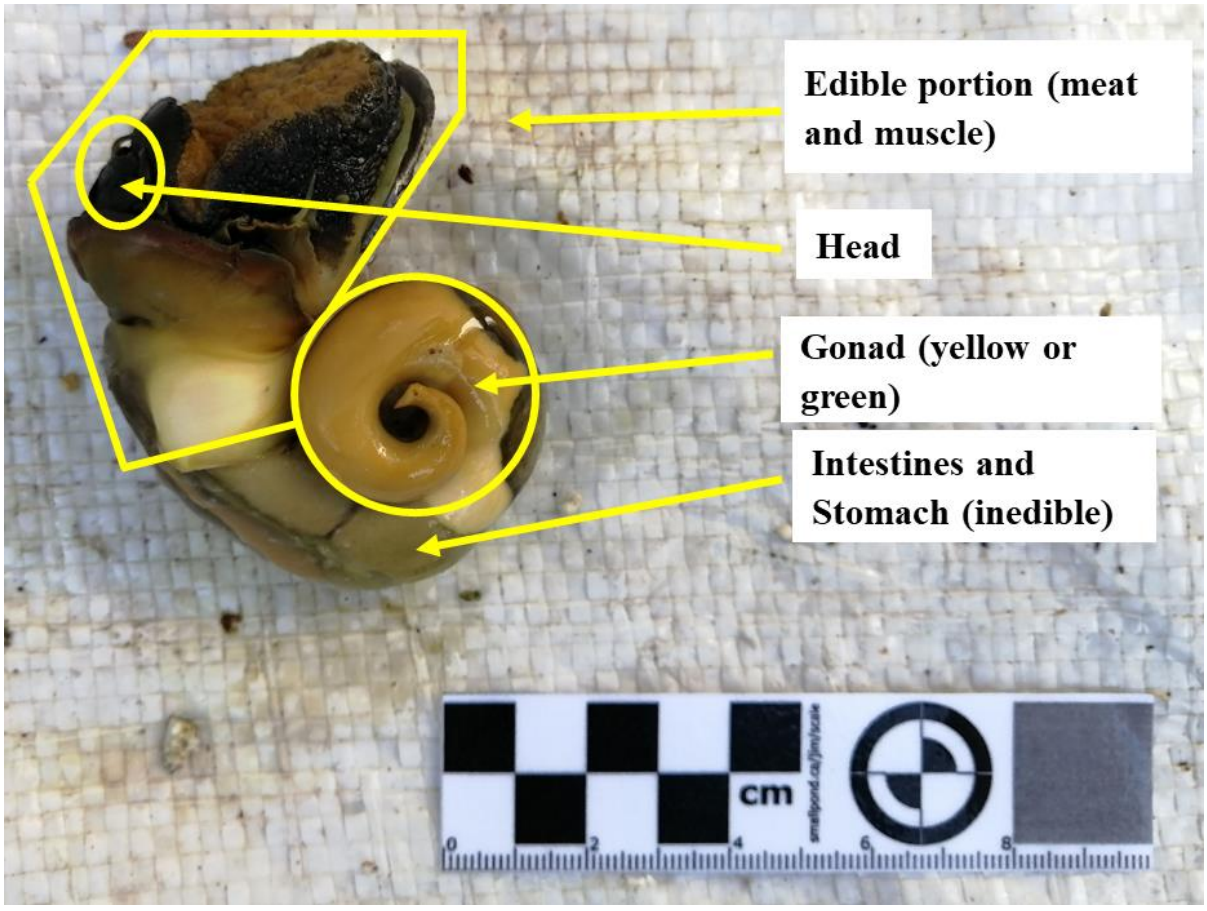


Figure 3. 18: Labelled diagram of the internal portion of the *T. sarmaticus*.



Figure 3. 19: A, how the cooked *T. sarmaticus* individuals bubble when done. B, the cooking of the *T. sarmaticus* shells in batches of 15.

3.3. Conclusion

In this chapter the actualistic study that took place was described, with the methodology used for the experiment for both the foraging and processing with MSA tools. The processing methods were discussed on how P1 and P2 approached the raw and cooked extraction of the *T. sarmaticus*. In the next chapter the methods used to analyse the experimental and archaeological samples will be compared to interpret the taphonomic similarities and differences.

Chapter 4: Analytical Methods

4.1. Introduction

Techniques used for the identification of *Turbo sarmaticus* (alikreukel) within the archaeological deposits follow those used by Henshilwood (2008) to identify shellfish at Blombos Cave (BBC) in the southern Cape. Branch *et al.* (2010) are used as a reference for the descriptive details of *T. sarmaticus* along with the comparative shellfish collection housed at the University of the Witwatersrand (Holmes 2020).

The analytical methods are relevant to the *T. sarmaticus* opercula from both the experimental sample and the archaeological sample. The opercula were measured, weighed, and analysed according to taphonomic criteria to investigate processes that influenced it in the past and to compare the experimental and the archaeological sample.

4.2. Opercula Size

The size of the *T. sarmaticus* opercula for both samples was determined through multiple variables. The length, width, thickness, and weight were measured for each operculum or operculum fragment.

4.2.1. Opercula Length

The length of the longest side of the opercula was measured in millimetres (mm) using a digital calliper (accurate to 0.01 mm) (Assefa *et al.* 2008; Sherwood *et al.* 2016; Brenner *et al.* 2022). All archaeological *T. sarmaticus* opercula fragments that were equal to and/or larger than 2 cm were classified as identifiable and were analysed as an individual, but size was determined only for complete or almost complete individuals. All archaeological *T. sarmaticus* opercula with a centre spiral present were classified as identifiable irrespective of the size and were analysed as individuals. Length measurements were recorded according to the placement model and not just according to size (Figure 4. 1). This was based on the spiral model where each spiral can be seen, as the spirals are relatively similar for all *T. sarmaticus* opercula. All the *T. sarmaticus* opercula fragments smaller than 2 cm were weighed as a group for Layer SMONE.

4.2.2. Opercula Width

Opercula width is not routinely measured, but we observed that many of them are oval–shaped and therefore attempted to capture this by measuring the width as well. The measurement of the shorter dimension of the opercula was measured in millimetres (mm) using a digital calliper (accurate to 0.01 mm) (Figure 4. 1).

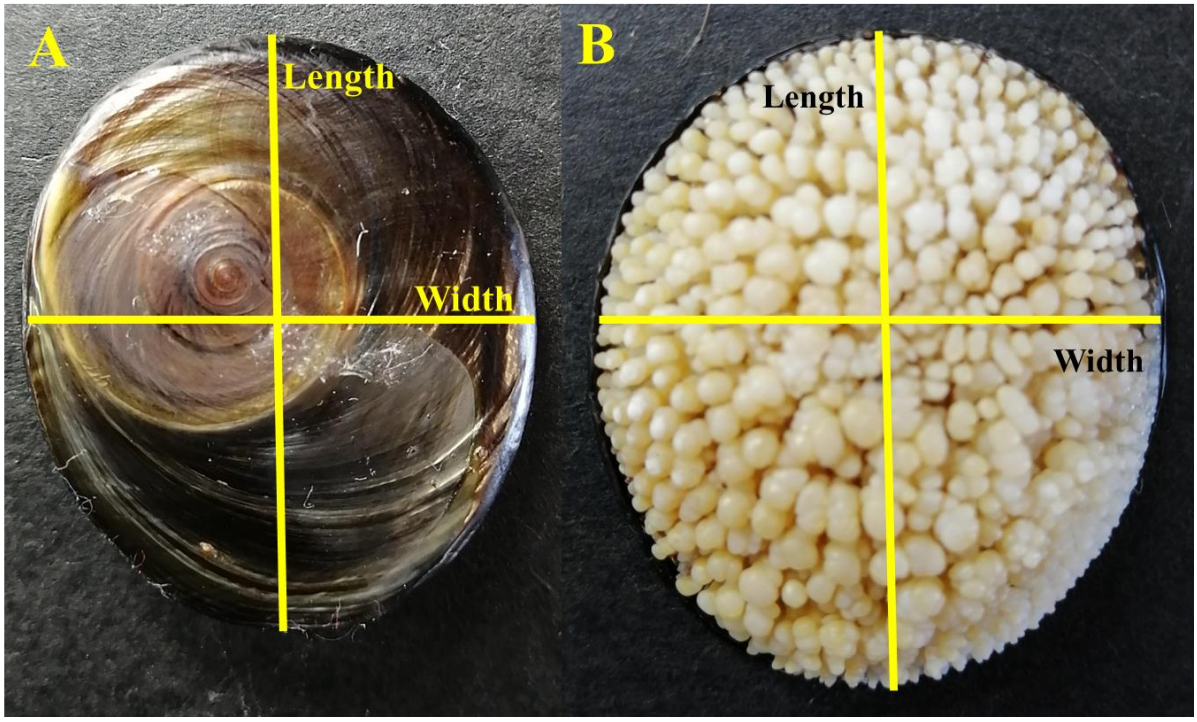


Figure 4. 1: A, how the length and width are measured on the ventral (flange) of the *T. sarmaticus* operculum. B, how the length and width are measured on the dorsal (dome) of the *T. sarmaticus* operculum.

4.2.3. Opercula Thickness and Weight

The measurement of the thickness of the opercula across the flange (dorsal) and dome (ventral) surfaces was done in millimetres (mm) using a digital calliper (accurate to 0.01 mm). The individual weight of each operculum in grams (g) was recorded using a digital scale (accurate to 0.01 g).

In order to investigate the relationship between the archaeological sample and the experimental sample, a T–Test was conducted to allow for the understanding of the correlation between the different measurements (Drennan 2010). A Two–Sample Assuming Unequal Variances T–Test was conducted in order to calculate the p–value (https://www.socscistatistics.com/tests/studentttest/default.aspx; Accessed on the

04/12/2022). The p–value is the value at which the two variances correlate and is shown as a percentage, the smaller the percentage the more the two variances correlate and the less random the outcome was (Drennan 2010).

4.3. Opercula Age

The animal age of the *T. sarmaticus* opercula was derived from the method used by Yssel (1989) who determined age based on the length of the shell as the shell grows continuously throughout the shellfish life span (Figure 4. 2). However, in the archaeological material, complete shells are rare due to the crushing and trampling that occurs over thousands of years. For this study the shell lengths from the experimental sample were recorded, along with the opercula length (see Table 4. 1) and the operculum length and shell length relationship were determined (Ilano *et al.* 2004).

A Spearman's Rho correlation test was conducted using the Social Science Statistics website (https://www.socscistatistics.com/tests/spearman/default.aspx; Accessed on the 04/12/2022). and the results were $r_s = 0.89$ with a p–value (2–tailed) = 0, meaning that there is a significant positive statistical correlation between the operculum length and the shell length. Yssel (1989), developed an age system for *T. sarmaticus* based on their mortality, production, and recruitment statistics. Yssel (1989) provided an 11-year age system (see Table 4. 2) based on a 16-year cycle of measuring *T. sarmaticus* shell length.

Table 4. 1: Summary of statistics for the experimental *T. sarmaticus* shell and opercula length.

Variables	Shell Length	Opercula Length
Mean	**81.3**	**35.1**
Median	**81.0**	**35.3**
Standard Deviation	**10.5**	**4.0**
Range	**57.0**	**19.0**
Minimum	**55.0**	**24.8**
Maximum	**112.0**	**43.7**
Count	**180**	**180**

Table 4. 2: Relative age for *T. sarmaticus* shell length (from Yssel 1989: Table 11, 77).

Relative Age	Shell Length (mm)
Age 1+	24
Age 2+	43
Age 3+	59
Age 4+	72
Age 5+	83
Age 6+	98
Age 7+	104
Age 8+	109
Age 9+	112
Age 10+	115
Age 11+	118

The archaeological sample's operculum length was used to infer the age of the *T. sarmaticus* (see Appendix 1B Table 1). This was done as there is other previous literature describing the age of the *T. sarmaticus* based on the operculum size.

The *T. sarmaticus* opercula can be described in four age categories: 0 to 3 years, 3 to 6 years, 6 to 9 years and 9 plus years (Table 4. 3). The average lifespan of the *T. sarmaticus* is ca. 11 years (Yssel 1989).

Table 4. 3: *T. sarmaticus* age index based on operculum length and inferred shell length (adapted from Yssel 1989: Table 11, 57).

Age (Years)	Operculum Length (mm)	Shell Length (mm)
0–3	24–30	24–72
3–6	30–40	72–98
6–9	40–44	98–112
9+	44+	112+



Figure 4. 2: P1 measuring the length of the *T. sarmaticus* shell in the actualistic study.

4.4. Opercula Shape

The shape of the opercula is determined by the width relative to the length (W/L) x 100. Relative size measurement of the length and the width of the opercula is expressed as a percentage.

Opercula Width (mm) / Opercula Length (mm) x 100 = Relative size (%)

According to the formula above if the outcome is a larger percentage, the rounder the opercula. For the purpose of this study, an operculum with a relative size percentage >80% is seen as round in shape and the opercula with a relative size percentage <80 is seen as oval in shape.

4.5. Opercula Taphonomy Criteria

The criteria described below were used to analyse both the experimental and archaeological sample.

4.5.1. Completeness of Opercula Dome and Flange

The completeness of the *T. sarmaticus* operculum dome and flange is determined by whether the dome and flange retain their original shape. A complete flange will show all the spirals on the ventral surface (Sherwood *et al.* 2016), and the complete dome will show the complete convex surface.

4.5.2. Breakage Type shown on Opercula

The breakage type is split into four categories. Intact (no break), Eroded break, Transverse break and an Irregular break. This is based on the bone breakage system set out by Driver (2005) due to there being no literature specific to the breakage that occurs to opercula.

4.5.3. Incisions on Opercula

The convex surface of the dome or dome fragment was inspected for small roughly linear incisions. These extent of the incisions, for example whether they start from the edge of the flange where the outer edge intersects the growth spiral of the operculum, has been noted(Sherwood *et al.* 2016: Table 2, 18).

4.5.4. Colouration of Opercula

The colour of the opercula was recorded as shades of white, brown, black, yellow/green and the natural colour of the periostracum. The natural opercula could show colour from cream to brown patches. Colouration on archaeological opercula specimens may occur as a result of carbonisation during the heating process, where the surface changes colour to a variation of white, brown and shades of black (Assefa *et al.* 2008). Black and grey colours are common, brown less so (Sherwood *et al.* 2016: Table 2, 18; Sherwood *et al*. 2018).

4.5.6. Percussion Marks on Opercula

Pits and notches have been recorded (see Figure 4. 3). A pit is circular in shape and has evidence of internal microstriations in bone. Such pit marks are interpreted as anthropogenic percussion marks in bone. Percussion notches are closely associated with the impact from a hammerstone and show micromorphological features (Blumenschine & Selvaggio 1988). This trait was used to infer anthropogenic percussion related to processing of the *T. sarmaticus* based on observations during the processing of the

experimental sample where percussion marks were observed (after Blumenschine 1995; Domínguez-Rodrigo *et al*. 2009).

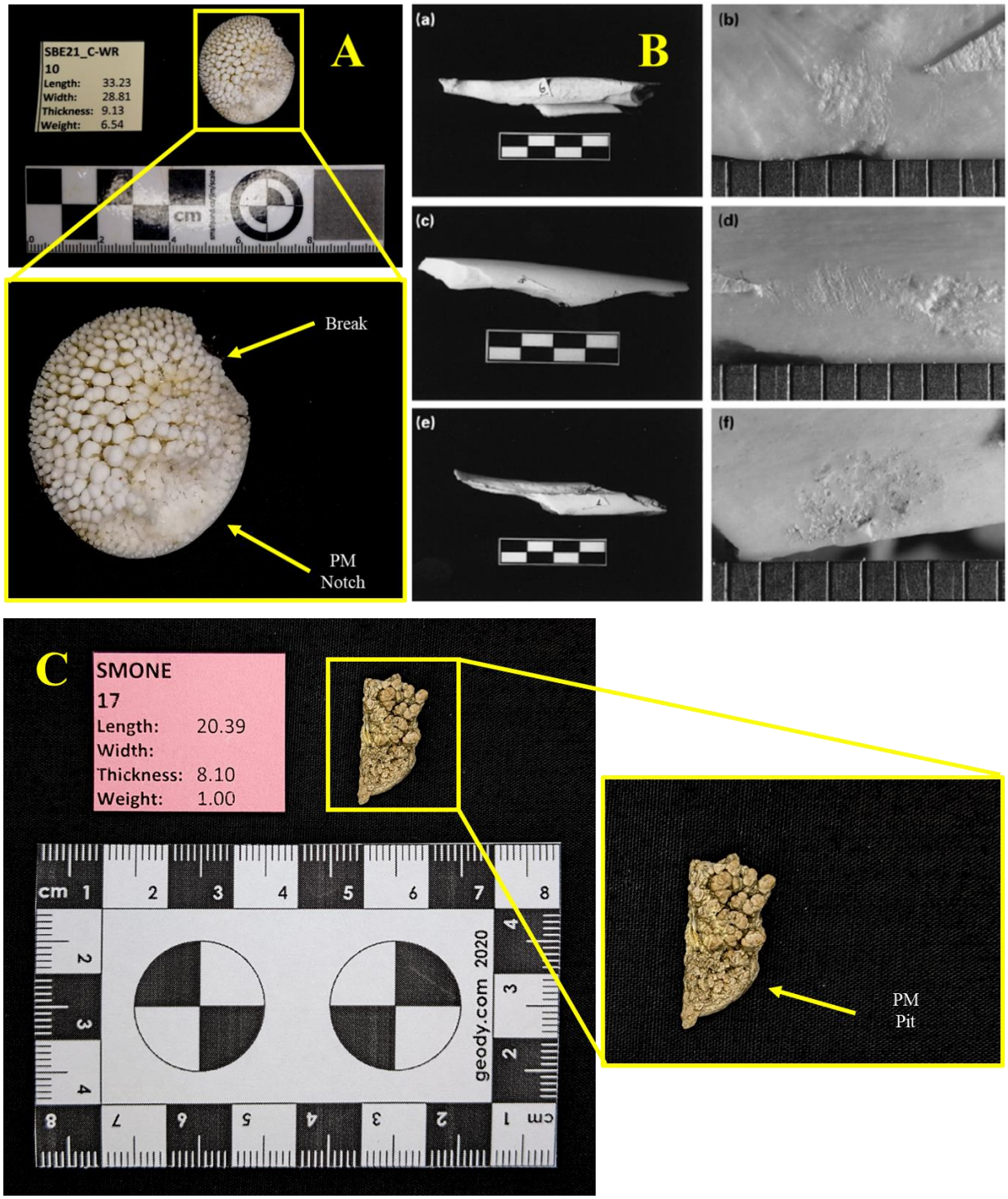


Figure 4. 3: A, an experimental *T. sarmaticus* opercula showing percussion notch marks (PM) on the dome surface with a break. B, bone percussion marks caused by hammer and anvil techniques (from Blumenschine *et al.* 1996: Figure 2, 498). C, an archaeological *T. sarmaticus* opercula showing percussion pit marks (PM) on the dorsal surface.

4.5.7. Bore marks

These are small and round holes occurring on the ventral surface in line with the central spiral. There is no literature that describes these marks, and these are based on observations in the samples.

4.5.8. Etching

Etching is the surface modification caused by roots, soils and other natural processes on a bone (Akman *et al.* 2005). The soil could cause etching due to its acidity or alkalinity. Etching is the porous holes that form on the dome surface of the operculum and is evident on the ventral surface of the opercula (after Behrensmeyer 1978; Andrews & Cook 1990; Fernandez-Jalvo & Andrews 2016; Sherwood *et al.* 2016).The absence of aspects of the dome surface was inferred to be related to etching, similar to that seen on bone (after Behrensmeyer 1978; Andrews & Cook 1990; Fernandez-Jalvo & Andrews 2016; see also Sherwood *et al.* 2016).

4.5.9. Encrustation of Opercula

A layer of hardened sand or crust occurring on either the flange or dome surface of the operculum (after Karkanas & Goldberg 2010).

4.5.10. Surface Condition

The surface condition is described as Chalky, Porous or Smooth. These conditions have not been described in the literature before.

4.5.11. Abrasion

Sheen marks are visible marks primarily found on the dorsal (flange) surfaces of the opercula's elevated spiral ridges. Edges of chips and breaks that are rounded or smoothed can be caused by abrasion known as water–wear (Sherwood *et al.* 2016: Table 2, 18). This was recorded, as the flanges are greatly reduced or missing (Assefa *et al*. 2008; Sherwood *et al*. 2016).

4.5.12. Preservation of Opercula

The state of the surface is based on how well the specimen is preserved and can be analysed.

4.5.13. Perforations on Opercula

Perforations are small holes in the flange surface of the opercula (D'Errico & Villa 1997; Assefa *et al*. 2008).

4.5.14. Periostracum on Operculum

The flat interior surface of the opercula has a brown/black membrane coating when removed from the animal's foot. This coating either completely or partially covered the flange on some opercula from the bird middens (Sherwood *et al.* 2016: Table 2, 18).

4.6. Opercula Placement Model

A placement model has been developed based on a model from Sherwood *et al.* (2016), that allows for the taphonomic caused marks to be given an exact location relative to each operculum. Two placement models have been developed, a spiral placement model (mimicking the spirals seen on the opercula) and the wedge placement model (where the opercula have been divided into eight wedges) (see Figure 4. 4 and Figure 4. 5).

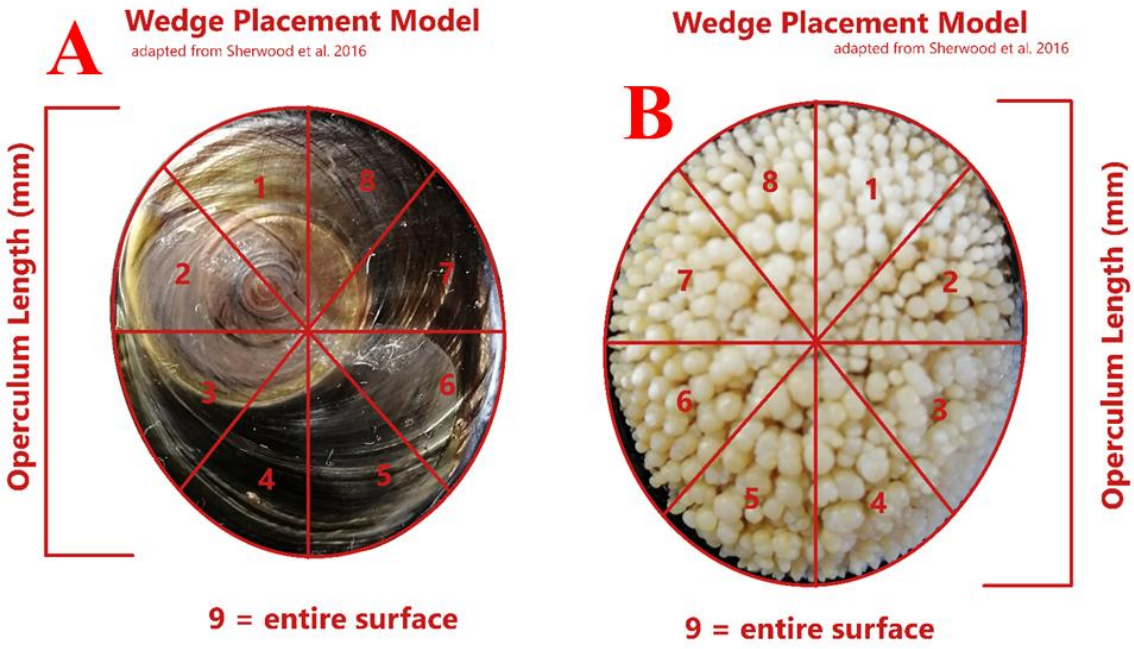


Figure 4. 4: Wedge Placement Model (Sherwood *et al.* 2016). A, the dorsal side wedge model 1–8. B, the ventral side wedge model 1–8.

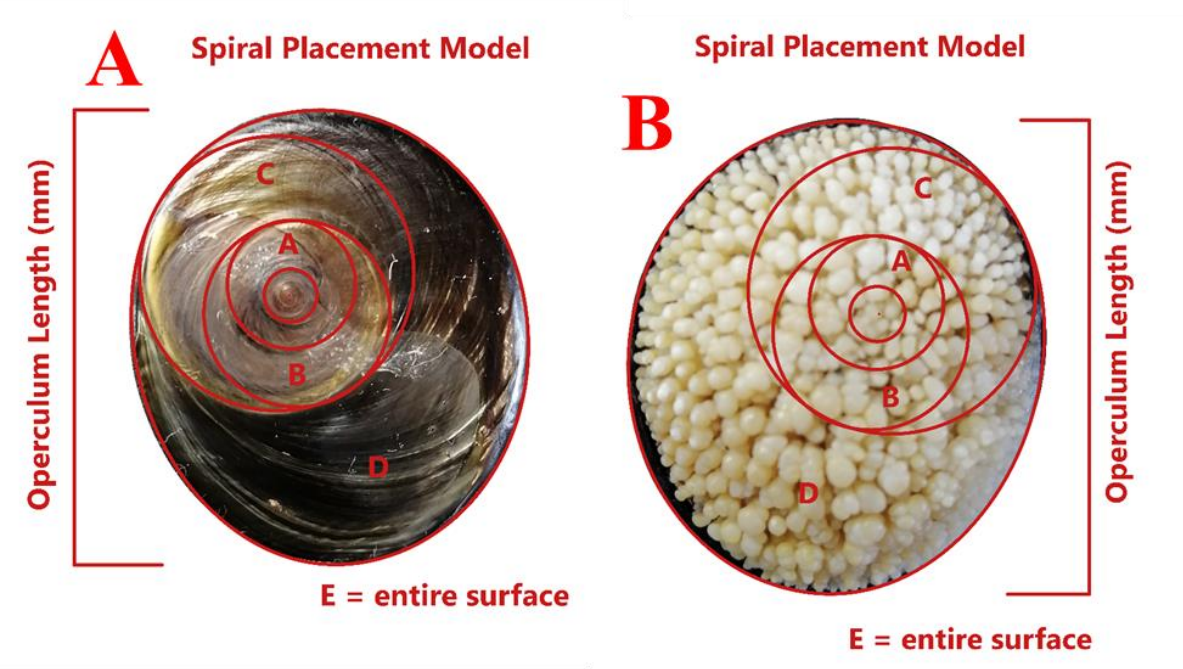


Figure 4. 5: Spiral Placement Model. A, the dorsal spiral placement model A–D. B, the ventral spiral placement model A–D.

4.7. Conclusion

In this chapter the analytical methods used to analyse the taphonomy of the archaeological and experimental opercula was stated. In Chapter 5 the results from the analysis using the methods described in the previous two chapters are presented. The archaeological and modern opercula collected are compared.

Chapter 5: Results

5.1. Introduction

This chapter presents the results of the analysis of the archaeological and experimental *Turbo sarmaticus* opercula, by discussing opercula size, age, shape and the taphonomy of the opercula.

5.2. Opercula size

As discussed in Chapter 4: Analytical Methods the *T. sarmaticus* opercula for both the experimental and archaeological samples were measured in four different aspects (Length, Width, Thickness and Weight). Table 5. 1 shows the summary statistics for the experimental sample as a whole (a combination of both participants 1 and 2, and the combination of all three tool types), and the archaeological opercula. The mean length of the experimental sample is 2 mm longer than the archaeological sample. The width and thickness are also larger than the archaeological sample. The SMONE sample has a wider range of lengths than the experimental sample, with the range being 21.5 compared to the 19.0 for the experimental sample. Table 5. 1 shows that there are similarities in the opercula lengths between the two samples, however, the medians for both the length and width differ with the archaeological sample being 2 mm smaller, and with the minimum and maximum being within a few millimetres of one another.

Table 5. 1: A, Summary statistics for *T. sarmaticus* opercula with a combination of both P1 and P2, and the combination of all three tool types. B, Summary statistics for *T. sarmaticus* opercula from layer SMONE.

Table A	**Experimental**			
Variables	**Length (mm)**	**Width (mm)**	**Thickness (mm)**	**Weight (g)**
Mean	35.1	30.2	9.6	8.6
Median	35.3	30.3	9.6	8.4
Standard Deviation	4.0	3.3	1.3	3.0
Range	19.0	15.1	7.8	14.7
Minimum	24.7	21.9	4.7	1.7
Maximum	43.7	37.0	12.5	16.5
Count	180	180	180	180
Table B	**SMONE**			
Variables	**Length (mm)**	**Width (mm)**	**Thickness (mm)**	**Weight (g)**
Mean	33.6	28.4	7.8	3.0
Median	32.6	29.7	7.9	2.0
Standard Deviation	6.1	7.5	1.7	2.6
Range	21.5	28.8	9.0	12.6
Minimum	23.3	9.3	2.7	0.1
Maximum	44.7	38.1	11.7	12.6
Count	36	62	189	189

A t–test was undertaken to investigate if the lengths of the opercula of the experimental and archaeological samples are significantly different from each other. The results show that the lengths of the experimental sample and archaeological samples are not statistically significantly different at $p < .05$ (t-value=-1.88252, p=0.061). The t-tests in this chapter were calculated through the social science statistics website (https://www.socscistatistics.com/tests/studentttest/default2.aspx). A t–test was also undertaken to compare the operculum length of specimens collected by Participant 1 (P1) and Participant 2 (P2) respectively, to compare the samples. The results show a statistically significant difference between the opercula lengths as collected by P1 and P2 (t-value=3.13008, p-value =0.002043).

Although the mean lengths of the archaeological and experimental samples of *T. sarmaticus* opercula are similar, there is an outlier in the experimental sample (light green and green) with P2's lithics foraging showing a slight decrease in the operculum length (Figure 5. 1). This shows the effects the ocean conditions have on foraging. The

ocean conditions affected the ability to forger deeper into the ocean due to the intensity of the waves and swells. This meant that on days with a lower ocean condition rating both P1 and P2 were able to forge deeper into the ocean where the larger *T. sarmaticus* specimens are, and *vice versa* for higher ocean condition ratings (see Appendix 1A.1. Foraging Data).

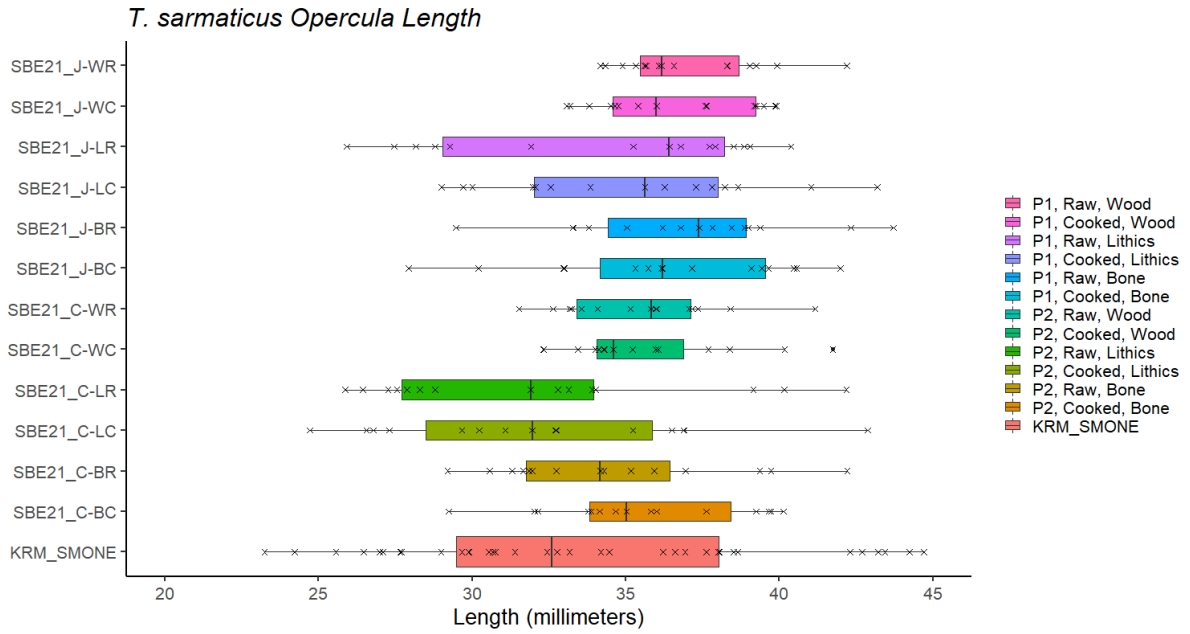


Figure 5. 1: *T. sarmaticus* opercula length of raw and cooked from all three tool types from the experimental sample and the archaeological sample.

A t–test was undertaken to test if the experimental and archaeological samples are significantly different from each other with regards to the width. The results show a significant difference (t-value=-2.60441,p-value=0.00978). There are a few outliers seen in both the archaeological sample and the experimental sample. For the archaeological sample (salmon colour) there is an outlier of under 10 mm. For the experimental sample P2 bone cooked extraction (orange colour) has an outlier compared to the rest of the sample from that participant on that day. Overall, from the experimental sample the results are similar between P1 and P2 with P2's samples having a wider range in size than P1's sample.

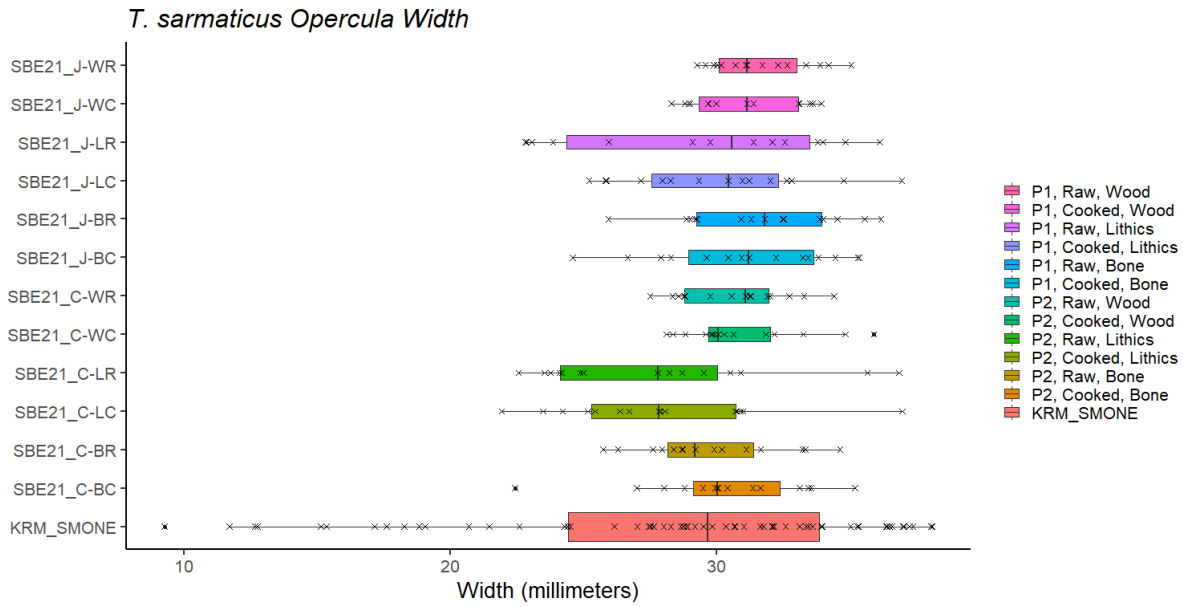


Figure 5. 2: *T. sarmaticus* opercula width of raw and cooked from all three tool types from the experimental sample and the archaeological sample.

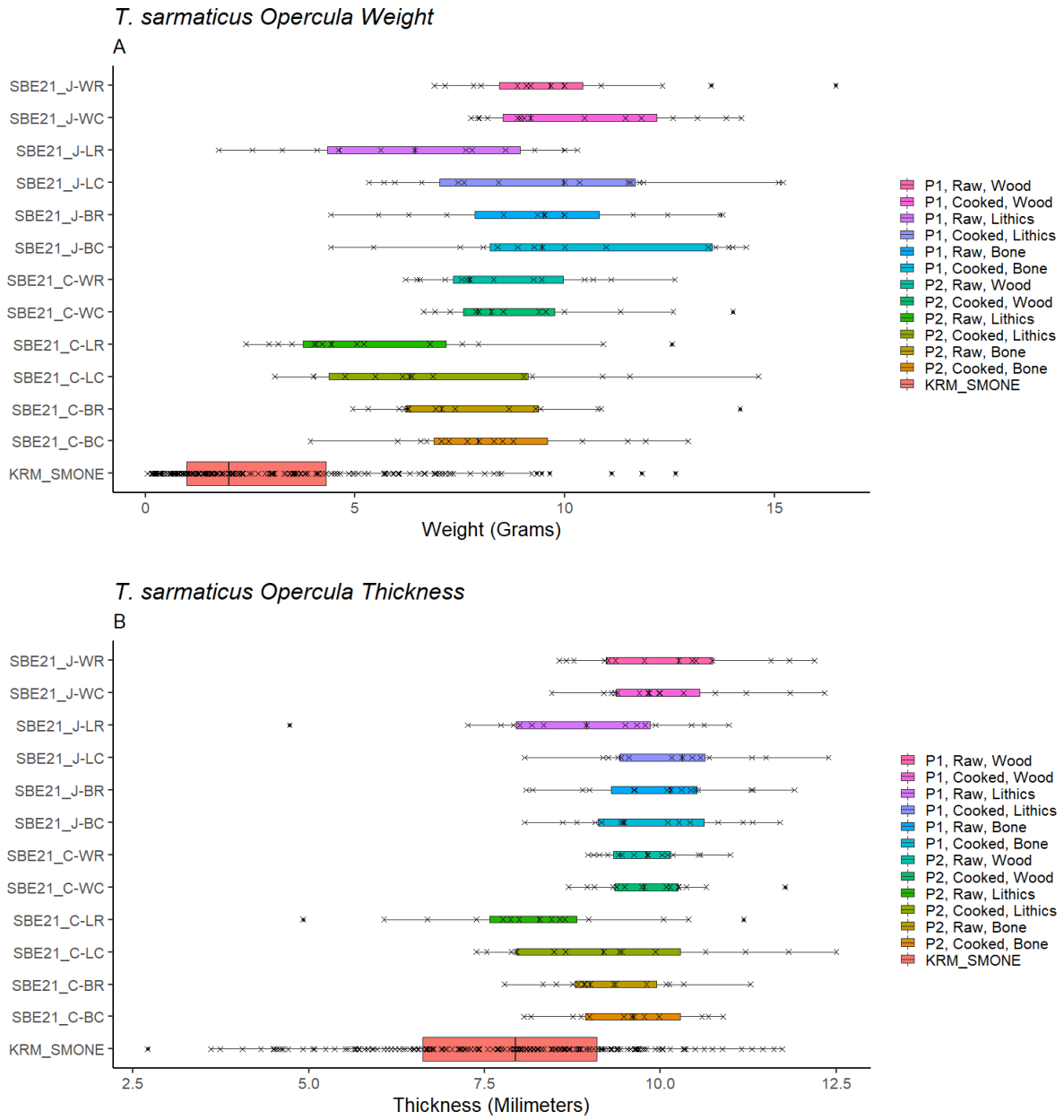


Figure 5. 3: A, weight of the *T. sarmaticus* opercula. B, thickness of the *T. sarmaticus* opercula of raw and cooked from all three tool types from the experimental sample and the archaeological sample.

T-tests were also undertaken to determine whether the thickness and weight of the archaeological and experimental opercula are significantly different. For thickness there is a significant difference (t-value=-11.37966; p-value is < 0.00001). For weight there is also a significant difference between the samples (t-value=-19.05361; p-value is < 0.00001). The archaeological sample weighs less than the experimental sample, and the experimental sample for both P1 and P2 has a much wider range. For the thickness, the

experimental sample has a few outliers, with both outliers coming from the raw extraction from both P1 (purple colour) and P2 (green colour).

5.3. Opercula Shape

As discussed in Chapter 4: Analytical Methods, during the foraging experiment, it was realised that there are two shapes of opercula. Some opercula are rounder in shape and others are more oval in shape. The results of the archaeological sample are slightly skewed due to the fragmentation that occurs in the archaeological record. There are very few opercula that are complete and allow for complete width measurement. The shape could only be determined for the complete operculum. A width-to-length ratio (W/L x 100) of >80 indicates round, and <80 indicates oval. More than 90% of both the archaeological and the experimental opercula are round in shape with very few being oval (see Table 5. 2 and Appendix 1B Table 2).

Table 5. 2: *T. sarmaticus* operculum shape for the experimental and archaeological sample.

Operculum Shape	Experimental	%	SMONE	%
Oval	5	2.9	3	9.4
Round	174	97.2	29	90.6
Grand Total	**179**	**100.0**	**32**	**100.0**

5.4. Opercula Age

The experimental sample shows 77.8% (n=140) have an estimated age of 3 to 6 years. The archaeological sample shows that 42.9% (n=18) had an estimated age of between 0 to 3 years and 3 to 6 years, with 14.3% (n=6) between the age of 6 to 9 years (see Table 5. 3 and Figure 5. 4).

Table 5. 3: *T. sarmaticus* opercula length and age index with experimental and SMONE n values.

Age	Operculum length (mm)	Experimental (n)	SMONE (n)
0 to 3 years	24–30	23	18
3 to 6 years	30–40	140	18
6 to 9 years	40–44	17	6
9 + years	44 +	0	0
Count		**180**	**42**

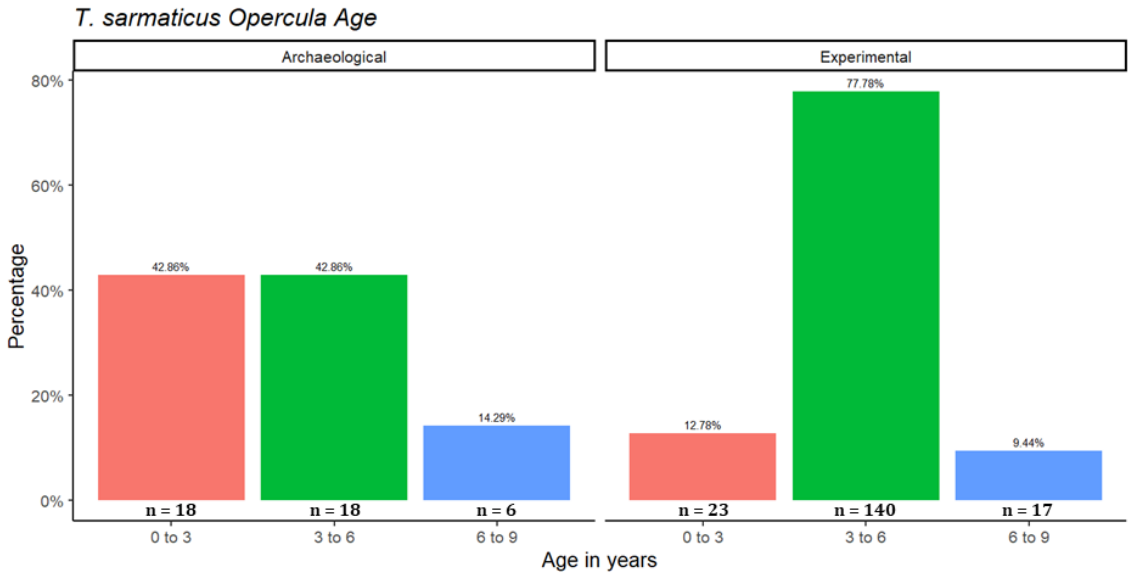


Figure 5. 4: Age distribution for the *T. sarmaticus* based on the opercula measurements of the experimental and archaeological sample (see Table 4. 3).

5.5. Opercula Taphonomy

In this section, the taphonomic indicators of incisions, breakage, colouration, etching, encrustation, surface-condition, abrasion and preservation are discussed.

5.5.1. Incisions of opercula

The convex surfaces of the *T. sarmaticus* operculum domes or fragments shows small roughly linear incisions. This has been seen in the opercula from the experimental sample (Sherwood *et al*. 2016: Table 2, 18). The incision that was present was measured. There was a total of n = 9 experimental opercula that showed this (Table 5. 4).

Table 5. 4: Experimental *T. sarmaticus* opercula incision measurements, with tool type and participant.

Opercula Number	Tool type	Participant	Length of incision (mm)
2	Lithic (raw)	P1	15.8
4	Lithic (raw)	P1	10.9
6	Lithic (raw)	P1	7.0
11	Lithic (raw)	P1	12.2
15	Lithic (raw)	P1	9.2
3	Lithic (raw)	P2	12.5
8	Lithic (raw)	P2	5.9
10	Lithic (raw)	P2	8.5
1	Bone (raw)	P1	6.7

5.5.2. Completeness of Opercula

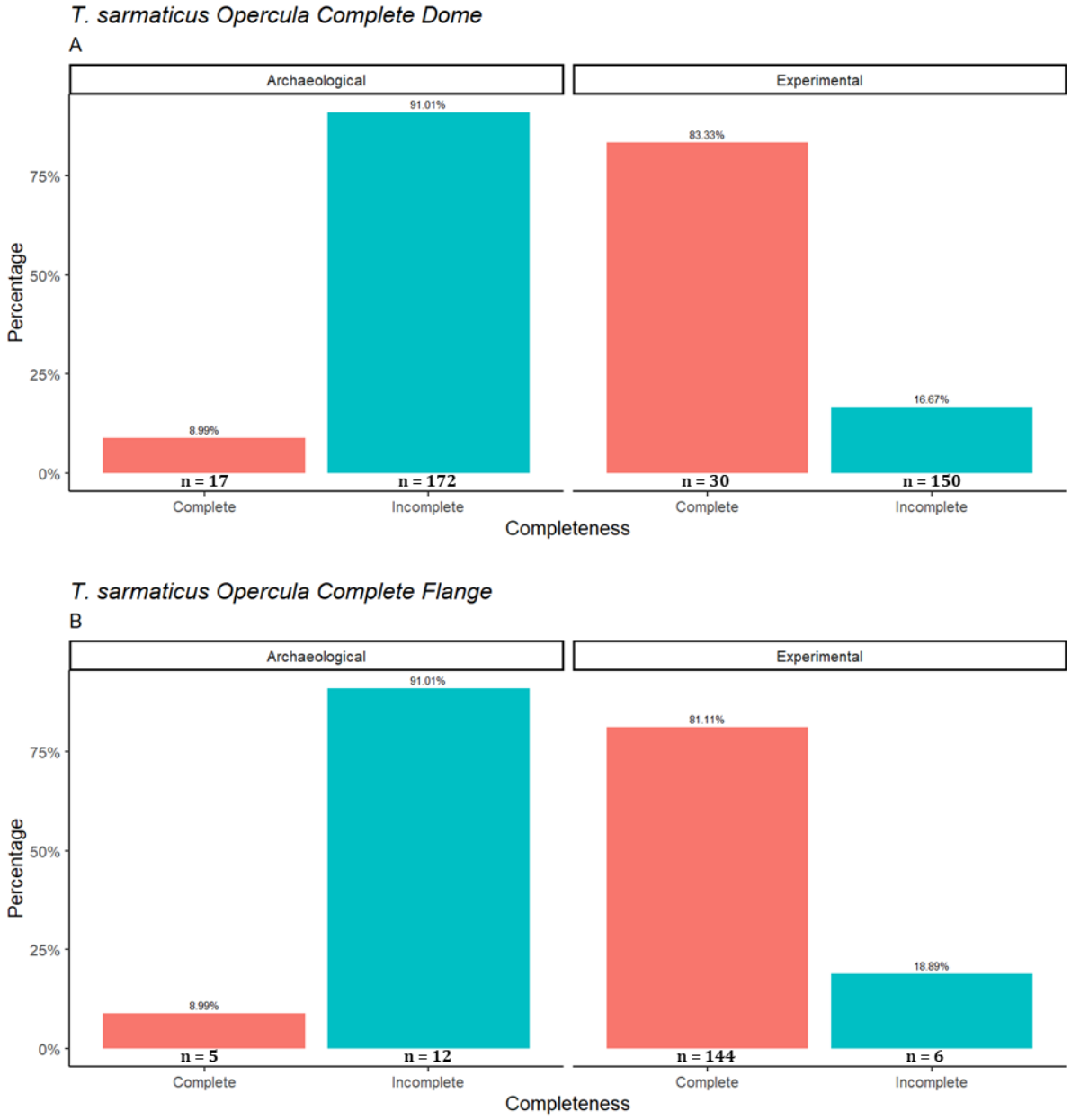


Figure 5. 5: A, complete dome (ventral surface) on *T. sarmaticus* opercula for combining the experimental sample and the archaeological sample. B, complete flange (dorsal surface) on *T. sarmaticus* opercula for combining the experimental sample and the archaeological sample.

The archaeological sample contains few complete opercula, with only 9.0% (n=17) with a complete dome and 9.0% (n=5) with a complete flange. This is in contrast to the experimental sample with only 83.3% (n=30) with a complete dome and 81.1% (n=144) with a complete flange, after processing (Figure 5. 5).

5.5.3. Breakage of Opercula

The breakage type is split into three categories (Eroded, Transverse and Irregular), as discussed in Chapter 3: Experimental Materials and Methods Opercula were classified as 'intact' if no breakage was evident. In the experimental sample, eroded and recent breaks did not occur, but transverse and irregular breaks occurred frequently with a pointed bone, lithic or wooden tools (Table 5. 5)Table 5. 5. This is particularly evident during extraction using lithics as 6.1% (n=11) of the raw opercula were intact during the raw process, and 17.2% (n=31) were intact during the cooked processing with the same tool. The processing with the use of lithics on a raw specimen revealed the most opercula with irregular 3.9% (n=7) and transverse 6.7% (n=12) breakage compared to the wooden tools with 1.1% (n=2) irregular breaks and 1.7% (n=3) with transverse breaks, similarly for the bone tools, 1.7% (n=3) showed irregular breaks and 0.6% (n=1) with transverse breaks (Table 5. 5).

In the archaeological sample 42.3% (n=79) exhibit transverse breaks and 30.0% (n=56) irregular breaks. Less than a quarter (24.1%; n=15) of opercula in the archaeological sample exhibit eroded breaks (see Figure 5. 6 for the different breakage types and Figure 5. 7 for the differences in the breakage types in the two samples).

Table 5. 5: Instrument vs breakage type for the experimental sample with P1 and P2 combined.

Instrument	Breakage Type	Extraction Type	n	%
Lithics	Intact	Raw	11	6.1
		Cooked	31	17.2
	Irregular	Raw	7	3.9
		Cooked	0	0.0
	Transverse	Raw	12	6.7
		Cooked	0	0.0
Wooden Tools	Intact	Raw	25	13.9
		Cooked	30	16.7
	Irregular	Raw	2	1.1
		Cooked	0	0.0
	Transverse	Raw	3	1.7
		Cooked	0	0.0
Bone Tools	Intact	Raw	29	16.1
		Cooked	26	14.4
	Irregular	Raw	1	0.6
		Cooked	2	1.1
	Transverse	Raw	0	0.0
		Cooked	1	0.6

Less than a quarter of the archaeological sample is intact whereas most of the opercula (84.4%; n=151) in the experimental sample are intact. The majority of the breaks in the archaeological and experimental samples are transverse and irregular, however, the archaeological sample has relatively more breakage types. Less than half (42.3%; n=23) of the archaeological sample has transverse breaks as 8.9% (n=16) of the experimental sample show evidence of the same breakage. The breaks mainly occurred during the raw extraction sample (Table 5. 5). In the archaeological sample, 24.1% (n=15) of the opercula show eroded breakage. Ten percent (n=56) of the archaeological sample have irregular breaks (Figure 5. 7).

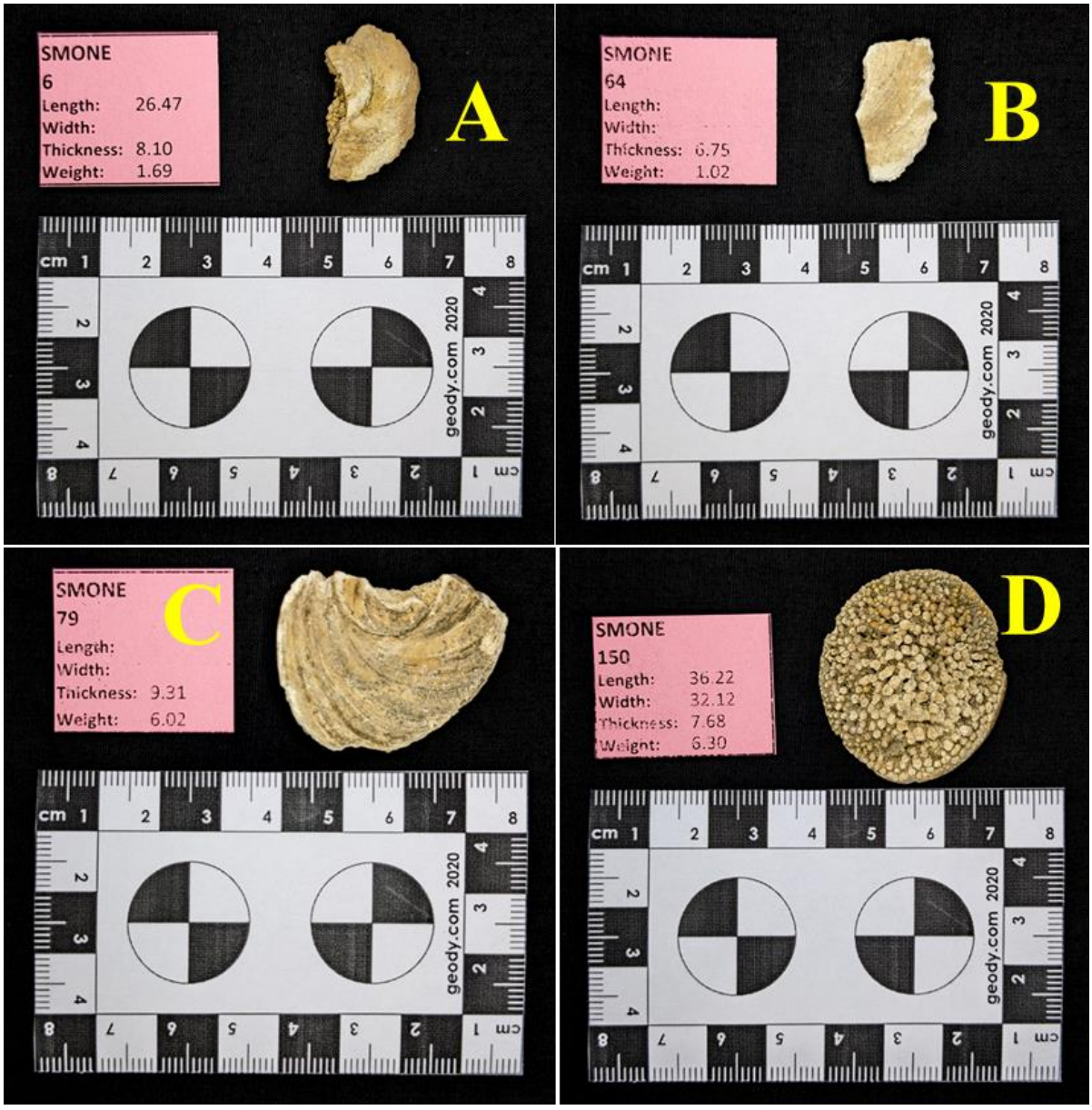


Figure 5. 6: Breakage types seen on the SMONE samples: A, transverse break, B, eroded break, C, irregular break, D, Intact.

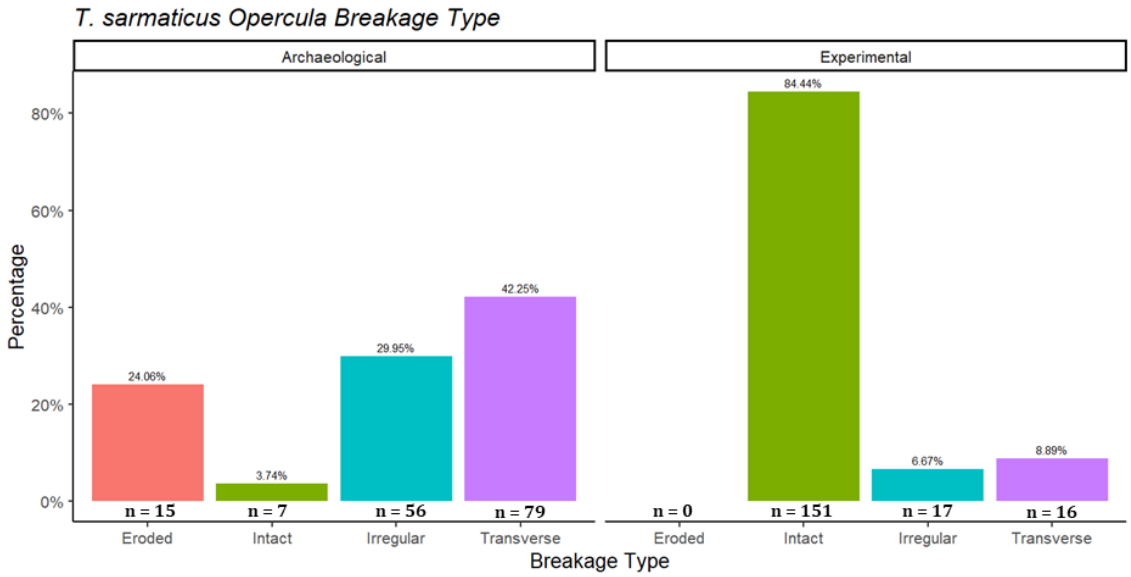


Figure 5. 7: Breakage type on the archaeological and experimental *T. sarmaticus* opercula.

5.5.4. Percussion marks on Opercula

Evidence of percussion marks in the experimental sample is mainly evident on the T. sarmaticus opercula that were extracted raw (Table 5. 6). The experimental sample shows that with raw extraction percussion notches occur on 35.0% (n=63) of the specimens. For the cooked extraction 6.1% (n=11) of the specimens display percussion marks. In comparison, in the archaeological sample both percussion notches and pits are near equal frequency (

Table 5. 7 and Figure 5. 8). Percussion marks are thus less frequent in the archaeological sample with 45.0% (n=81) of the experimental sample showing evidence of percussion marks and 40.0% (n=72) of the percussions are percussion notches (after Blumenschine 1995; Domínguez-Rodrigo *et al*. 2009). In layer SMONE 18.0% (n=34) show percussion marks with there being 10.6% (n=20) for percussion notches and 7.4% (n=14) for percussion pits.

Table 5. 6: Percussion marks on Experimental and SMONE *T. sarmaticus* opercula.

Percussion Mark	Experimental Raw		Experimental Cooked		SMONE	
	n	%	n	%	n	%
Present	68	37.8	13	7.2	34	18.0
Absent	22	12.2	47	26.1	155	82.0

Table 5. 7: Percussion mark details on Experimental and SMONE *T. sarmaticus* opercula.

Percussion Mark	Experimental Raw		Experimental Cooked		SMONE	
	n	%	n	%	n	%
Percussion Pit	5	2.77	2	1.11	14	7.41
Percussion Notch	63	35.00	11	6.11	20	10.58

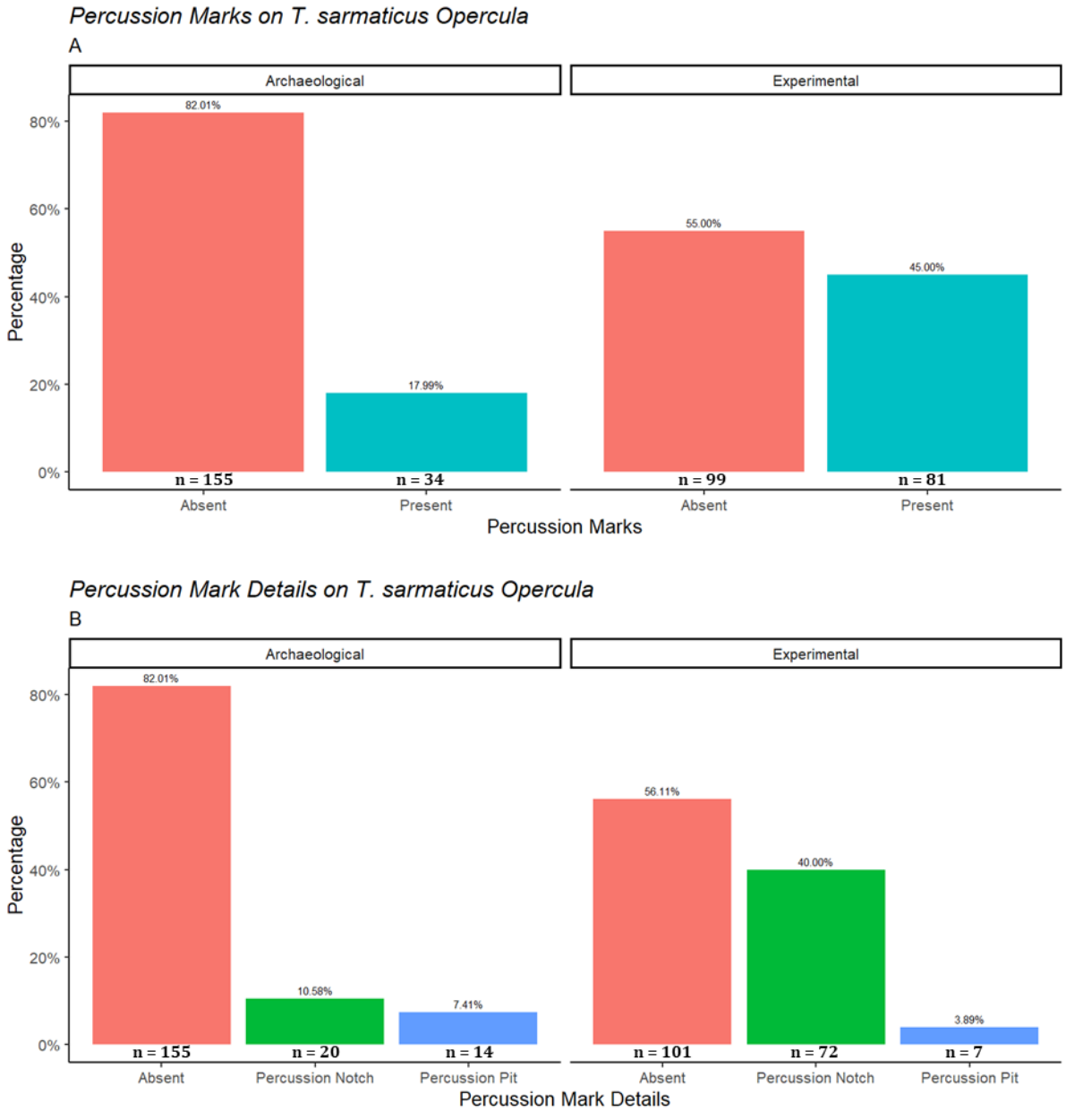


Figure 5. 8: A, percussion marks on the ventral surface of the *T. sarmaticus* opercula, B, percussion mark details on the *T. sarmaticus* operculum.

5.5.5. Placement of percussion marks

A placement model was created to help with the accuracy of the taphonomic analysis of the operculum (Figure 5. 9 and Figure 5. 10). The majority of the placements of the percussion marks in the experimental sample 30.0% (n=54) are in the 3rd wedge and 30.0% (n=54) in the 4th wedge. For layer SMONE the majority of the placements, 7.4% (n=14) is in the 3rd wedge and 10.6% (n=20) in the 4th wedge, with the major difference being that the SMONE sample shows percussion marks in all wedges of the placement model where the experimental sample does not have marks in the 6th and 8th wedge. However, during the analysis of the archaeological sample, the majority of the opercula in the SMONE sample were missing the 3rd and 4th wedge (Table 5. 8).

Table 5. 8: *T. sarmaticus* opercula percussion mark placement statistics.

Percussion Wedge Placement	Experimental	%	SMONE	%
1	5	2.8	1	0.5
2	14	7.8	2	1.1
3	54	30.0	14	7.4
4	54	30.0	20	10.6
5	16	8.9	9	4.8
6	0	0.0	2	1.1
7	1	0.6	1	0.5
8	0	0.0	1	0.5
9	4	2.2	0	0.0

The majority of the placements of the percussion marks in the experimental sample mentioned above fall within the d spiral with 36.1% (n=65). For layer SMONE the majority of the percussion marks concur with the experimental with 14.8% (n=28) in the d spiral (Table 5. 9).

Table 5. 9: *T. sarmaticus* operculum percussion marks localised statistics (Figure 5. 9 and Figure 5. 10).

Percussion Spiral Placement	Experimental	%	SMONE	%
A	5	2.8	0	0.0
B	14	7.8	1	0.5
C	6	3.3	1	0.5
D	65	36.1	28	14.8
E	6	3.3	1	0.5

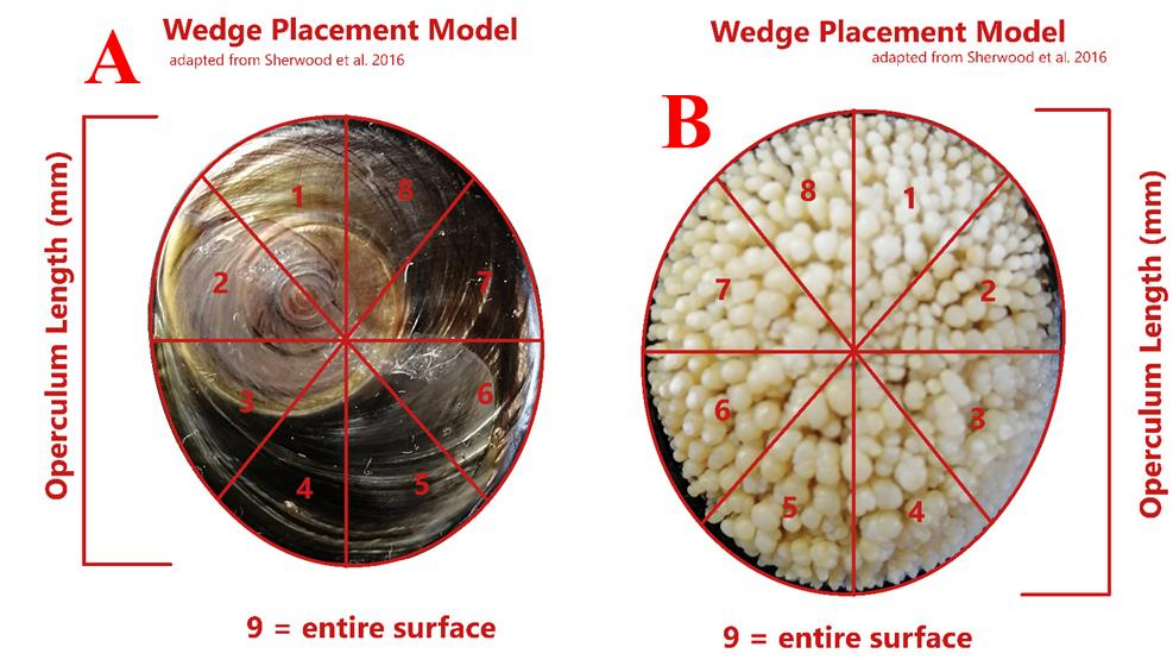


Figure 5. 9: Wedge Placement Model (Sherwood et al. 2016). A, the dorsal side wedge model 1–8. B, the ventral side wedge model 1–8.

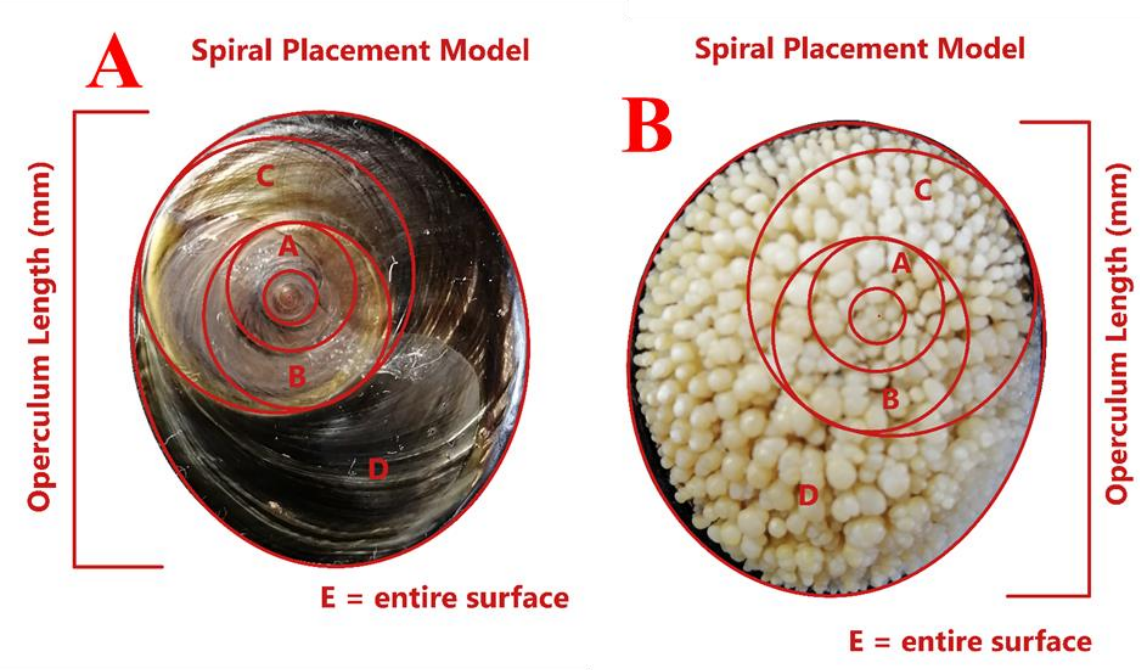


Figure 5. 10: Spiral Placement Model. A, the dorsal spiral placement model A–D. B, the ventral spiral placement model A–D.

5.5.6. Bore marks

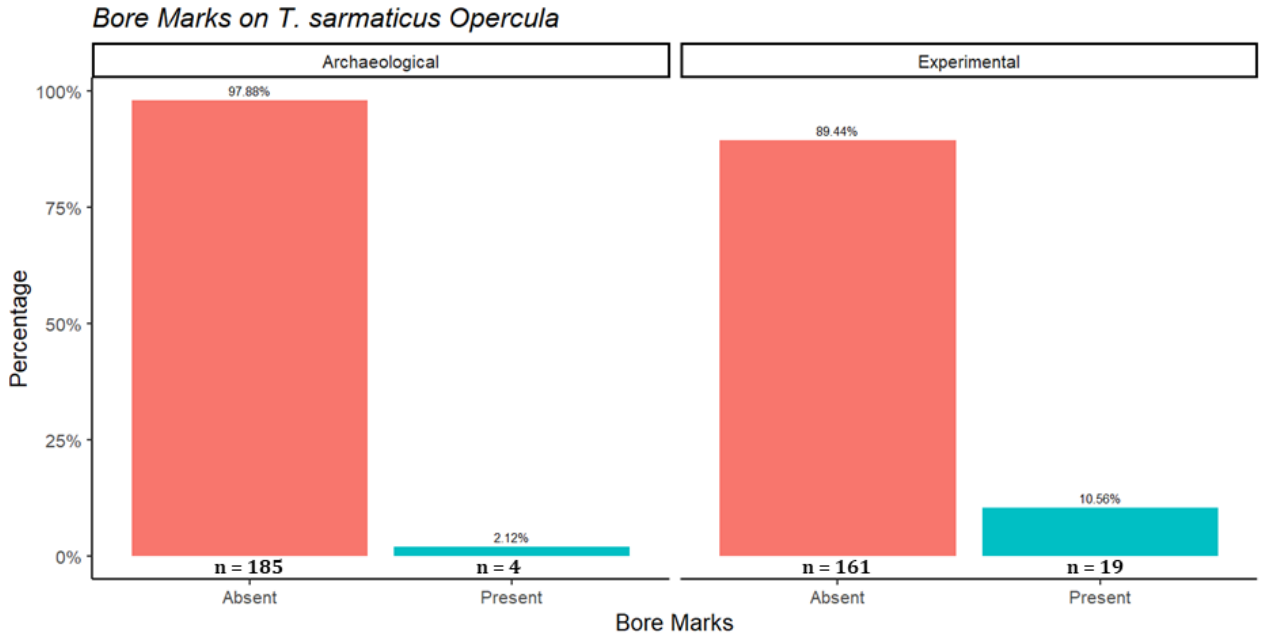


Figure 5. 11: Bore Marks were seen on the ventral surface of the *T. sarmaticus* operculum.

In both the archaeological (2.1%; n=4) and the experimental (10.6%; n=19) samples, there is a low frequency of these marks (Figure 5. 12) and further investigation is required to understand what the cause of these marks might be.

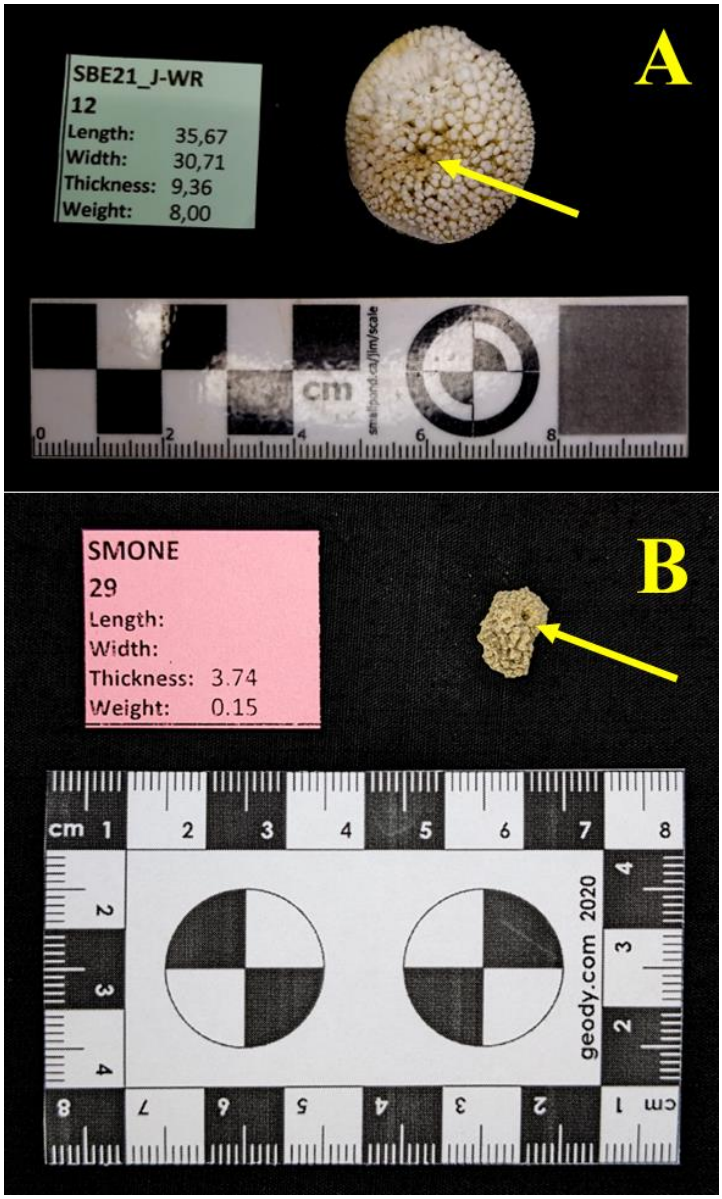


Figure 5. 12: A, bore mark seen on the experimental opercula. B, bore mark seen on the SMONE opercula.

5.5.7. Opercula Colouration

The majority of the archaeological sample, 61.9% (n=117), shows brown colouration, 34.4% (n=65) are white and 3.7% (n=7) are black (Figure 5. 13).

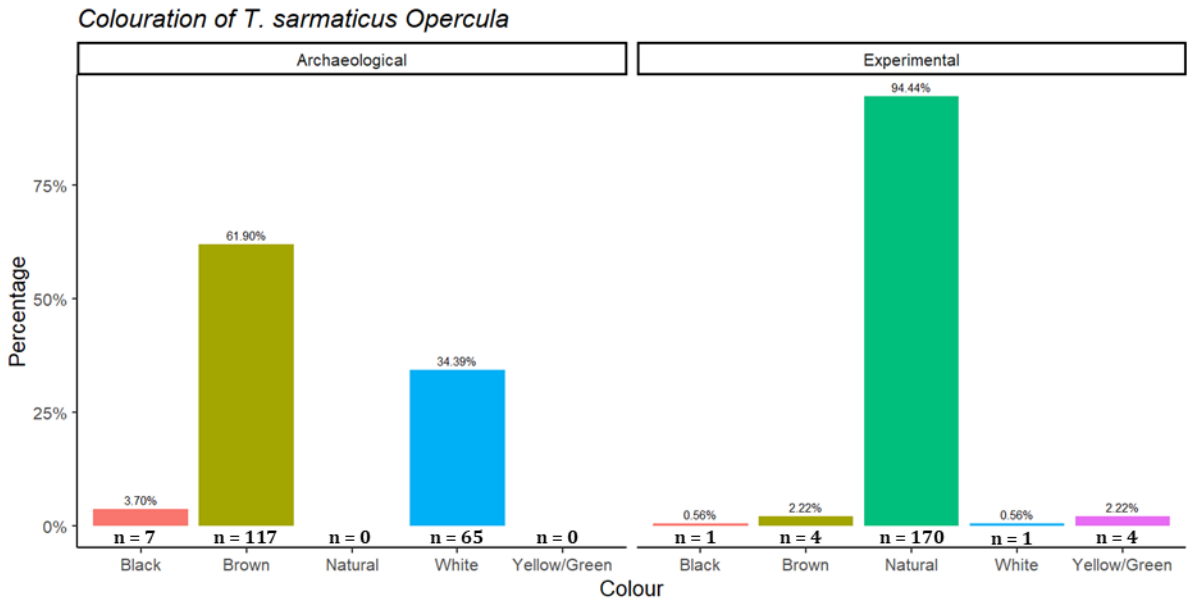


Figure 5. 13: Colouration on *T. sarmaticus* opercula.

5.5.8. Etching of Opercula

The majority, 88.4% (n=167) of the *T. sarmaticus* opercula in the archaeological sample have etching present on the ventral surface. The experimental sample show etching on 33.9% (n=61) of the opercula (Figure 5. 14).

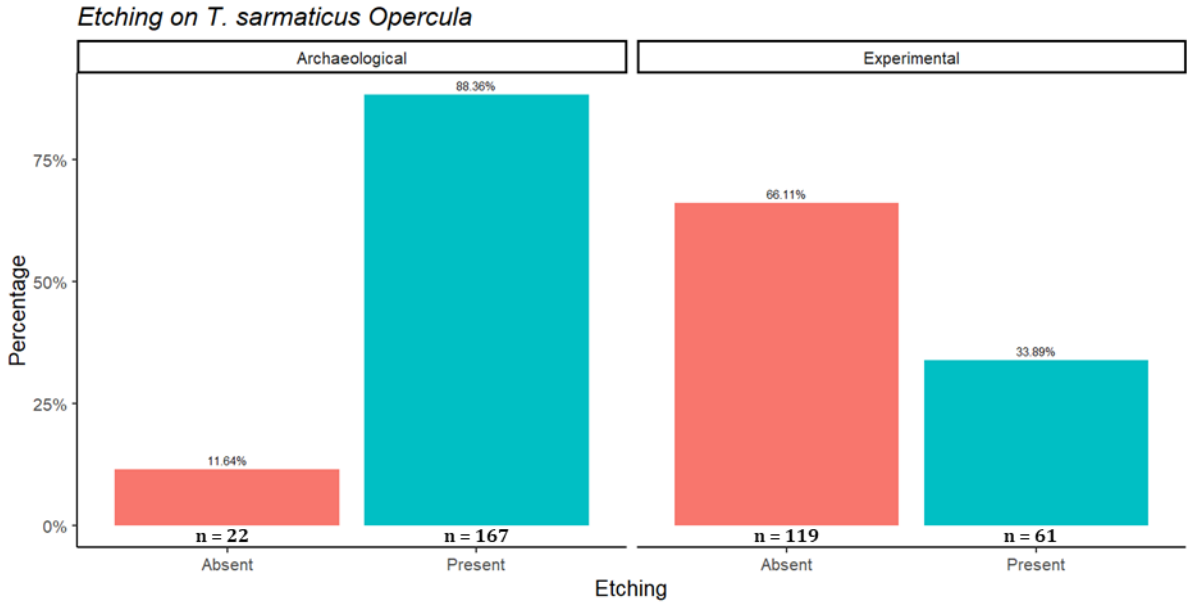


Figure 5. 14: Evidence of etching on the ventral surface of the *T. sarmaticus* operculum.

5.5.9. Encrustation of opercula

Encrustation on the *T. sarmaticus* operculum is evident in about a third of the archaeological sample (36.5%; (n=69) (Figure 5. 15). The majority of the placements of the encrustation in the SMONE sample occur in the 4th, 5th, 7th, and 9th wedges, based on the varying degrees of encrustation. In the case of the experimental sample, 1.7% (n=3) of the sample showed evidence of encrustation, however, this could be cemented sand that has gathered on the dome of the opercula. The placements of the encrustation in the experimental sample were split between the 1st, 3rd, 4th, and 8th wedges (see Table 5. 10; Figure 5. 9 and Figure 5. 10).

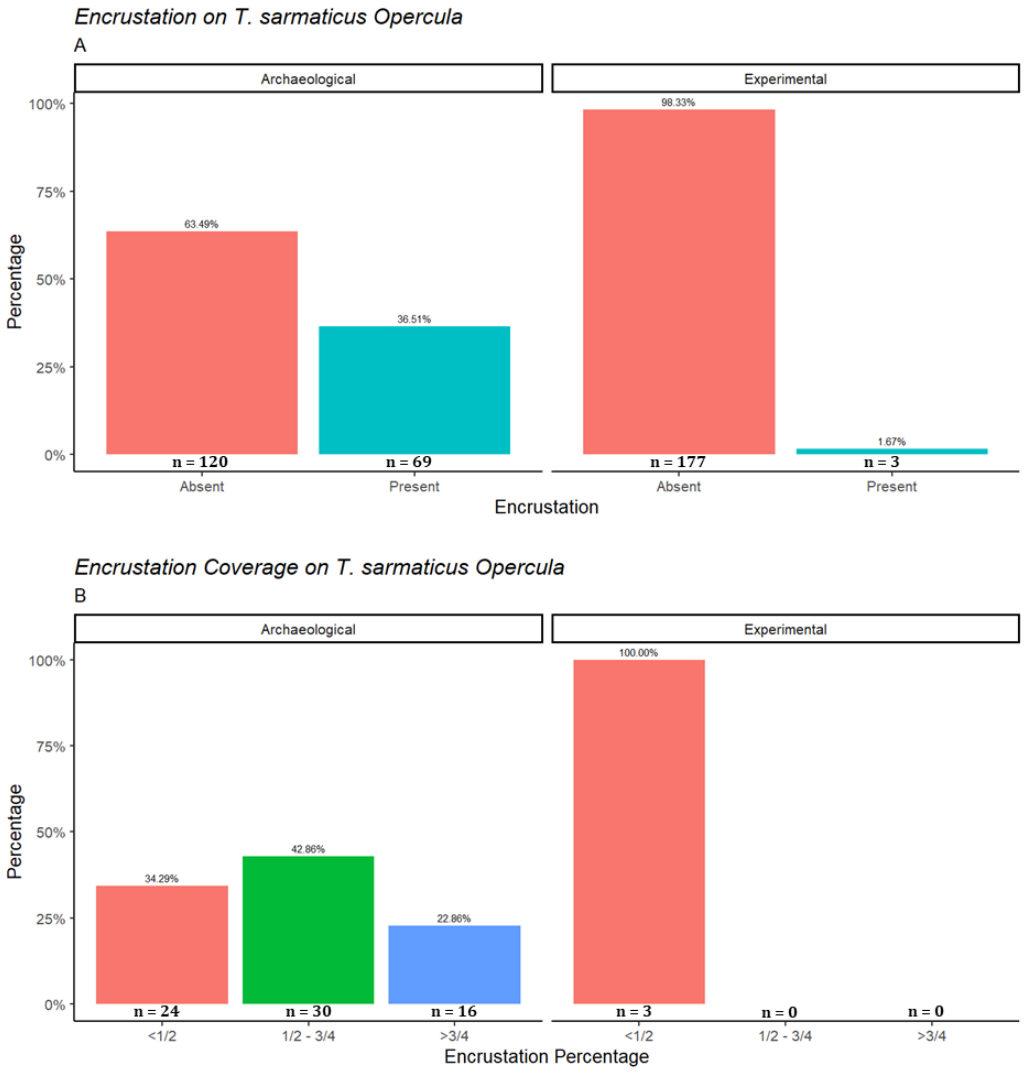


Figure 5. 15: A, encrustation on the dome of the *T. sarmaticus* opercula. B, coverage of the encrusting on the *T. sarmaticus* opercula.

Table 5. 10: *T. sarmaticus* opercula encrustation placement statistics.

Encrustation Wedge Placement	Experimental			SMONE		
	< 1/2	½ - 3/4	> 3/4	< 1/2	½ - 3/4	> 3/4
1	2	0	0	1	1	0
2	0	0	0	0	1	0
3	1	0	0	1	0	0
4	2	0	0	4	1	0
5	0	0	0	6	2	0
6	0	0	0	3	2	0
7	0	0	0	1	3	0
8	1	0	0	2	2	0
9	0	0	0	13	26	15

The majority of the placements of the encrustation in the experimental sample fall within the c and d spiral. For layer SMONE, the majority of the encrustation occurs within the e-spiral (Table 5. 11; Figure 5. 9 and Figure 5. 10).

Table 5. 11: *T. sarmaticus* opercula encrustation localised numbers (Figure 4. 4 and Figure 4. 5).

Encrustation Spiral Placement	Experimental			SMONE		
	< 1/2	½ - 3/4	> 3/4	< 1/2	½ - 3/4	> 3/4
A	0	0	0	0	0	0
B	0	0	0	0	0	0
C	1	0	0	0	0	0
D	2	0	0	3	0	0
E	0	0	0	17	29	15

5.5.10. Abrasion of Opercula

Abrasion is very uncommon on the *T. sarmaticus* operculum flange in both the experimental with 96.1% (n=173) showing no evidence and 97.4% (n=184) for the archaeological sample (Figure 5. 16).

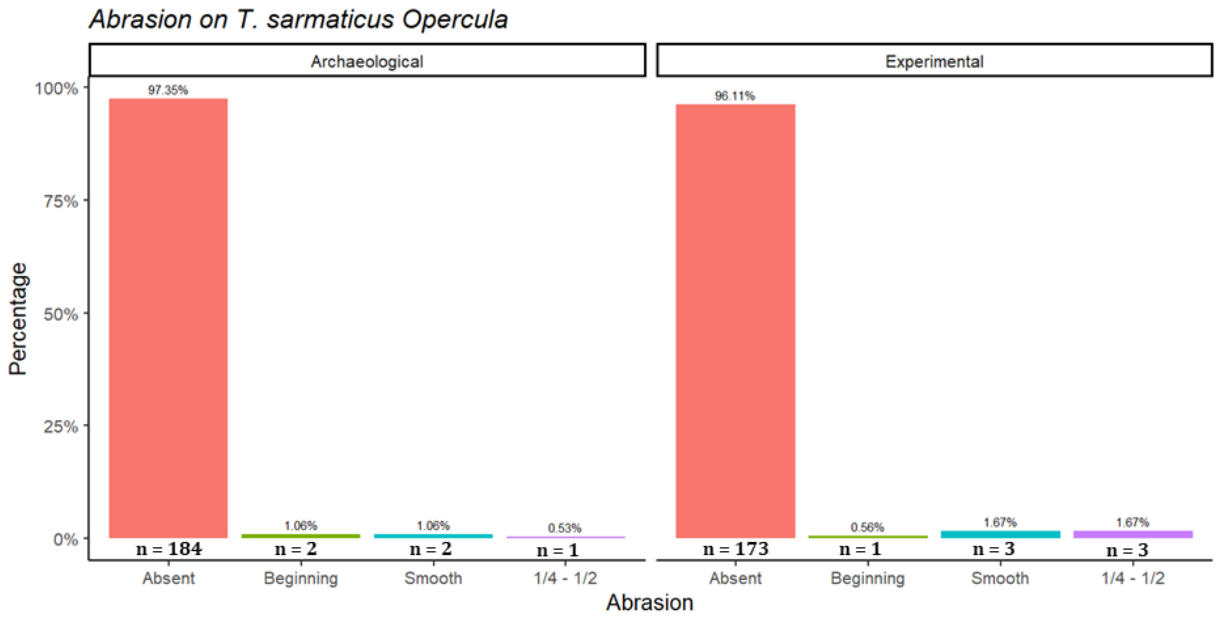


Figure 5. 16: Abrasions on the flange of the *T. sarmaticus* operculum.

5.5.11. Preservation of Opercula

T. sarmaticus opercula from the experimental sample were well preserved. In the archaeological sample, 22.2% (n=42) of the opercula were well preserved and 22.2% (n=42) were not well preserved. Further investigation into the post–depositional processing will increase the understanding of the site formation processes (Figure 5. 17).

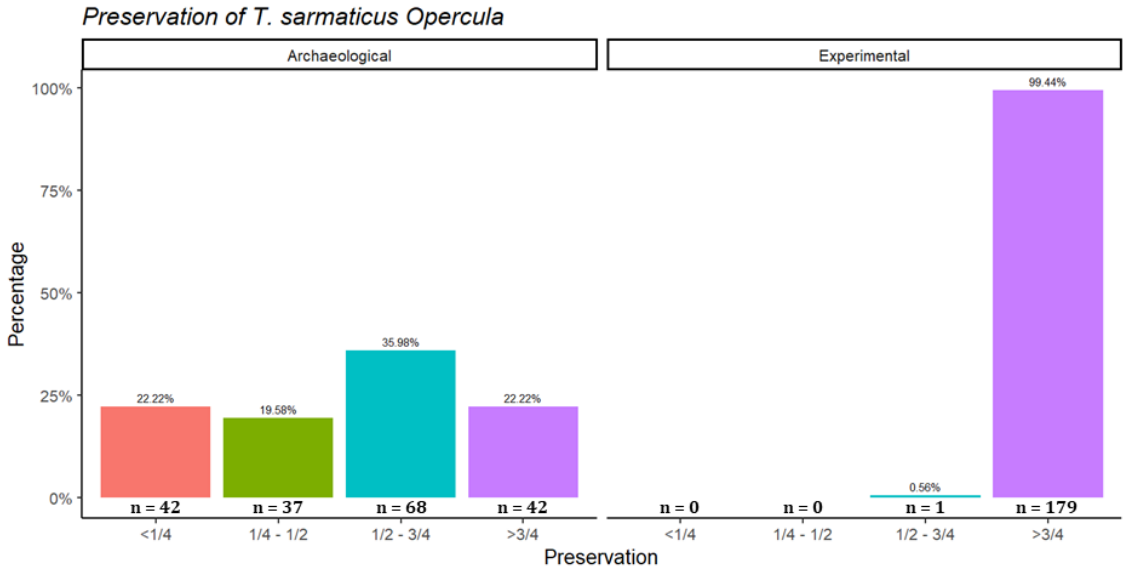


Figure 5. 17: Preservation of the experimental and archaeological *T. sarmaticus* opercula.

5.6. Conclusion

This chapter discussed the results of the analysis of the experimental and archaeological opercula samples. It was shown that the archaeological opercula are smaller than the experimental opercula in all respects, apart from lengths. Most archaeological opercula were incomplete and some post depositional altering took place. The next chapter will interpret the results of this study according to the results from this study according to the literature.

Chapter 6: Discussion

6.1. Introduction

This chapter discusses the implications of the results of the analysis of the experimental and archaeological opercula samples. Discussions on *T. sarmaticus* opercula size, age, opercula processing, and opercula taphonomy will be related to relevant literature.

6.2. Opercula Size and shape

The experimental and archaeological opercula are similar in length, however, are significantly different in width and thickness, with the archaeological sample being somewhat lighter than the experimental sample.

In the 'predation hypothesis,' it is suggested that the MSA opercula are larger than the opercula from the LSA due to more intensive exploitation patterns in the LSA. This might lead to the expectation that the modern opercula should also be smaller than the MSA opercula if the frequency of foraging was more intense in the present day than in the MSA (c.f. Steele & Klein 2008). In Table 6.1 the experimental and archaeological opercula median lengths obtained in this study are compared to those from the MSA II and LSA from KRM and BBC (Table 6. 1), to further explore differences in median length. The SMONE opercula are smaller than those from the MSA II (as a whole) at KRM, and the broadly contemporary MSA II (M3) at BBC. The MSA II opercula are larger than the LSA opercula from both KRM and BBC, as predicted by the predation hypothesis. Although the opercula from the experimental sample is somewhat larger than the LSA and more similar in length to the opercula from SMONE, the collection of only relatively larger opercula was allowed by the permit. It is thus premature to interpret the median length of the experimental sample in relation to the predation hypothesis. It is interesting, however, that the SMONE opercula are somewhat smaller than those from the rest of the MSA II. This needs to be further investigated in relation to exploitation levels and/or environmental and climatic factors that affected the growth of the *T. sarmaticus* opercula. As noted in Chapter 2: Literature Review, opercula size may vary due to environmental conditions such as sea surface temperature, seasonal variations and shifts in nutrient availability (Sealy & Galimberti 2011).

Table 6. 1: Comparison of opercula length measurement (mm) statistics from various MSA II and LSA opercula from KRM and the experimental sample from this study.

		(Klein & Steele 2013: 10913)				
	SMONE	**KRM MSA II**	**BBC M3 (MSA II)**	**KRM LSA**	**BBC LSA**	**Experimental**
Median	32.6	39.4	43.6	26.3	28.5	35.3
Minimum	23.3	14.6	20.0	14.4	14.4	24.7
Maximum	44.7	55.0	57.2	42.2	45.7	43.7
n	36	1832	463	166	198	180

Ryano (2014), in the analysis of the *T. sarmaticus* opercula found at Klipdrift Cave (KDC) in the Later Stone Age, saw a variation in the sizes between the LSA layers at KDC. The *T. sarmaticus* opercula from KDC showed a maximum of 47 mm, with a minimum of 10 mm, with the average median across the various LSA layers being 30 mm to 39 mm (Ryano 2014: 174). This difference also needs to be further investigated in relation to the predation hypothesis (Steele & Klein 2008; Klein & Steele 2013

The foraging for the experiment was conducted during a non-optimal time of the year. This was due to foraging taking place in winter, which is the time of spawn for the *T. sarmaticus* (Loftus *et al*. 2019). It needs to be further investigated whether with the same results would be obtained if there is now restriction on the size of *T. sarmaticus* collected and when collection takes place during a different season. *T. sarmaticus* is still the species of choice for the local communities in the southern Cape (De Vynck *et al*. 2020).

Another factor of interest is the experience of the collector. The difference in experience of the two participants in this study resulted in clear differences in the foraging efficiency with the expert forager being able to select specific *T. sarmaticus* compared to the novice collecting the *T. sarmaticus* which he randomly came across. The experience level also was seen with the foragers' abilities to handle harsher conditions (expert) compared to the struggle of having to stick to the shallow intertidal zones (novice).

The investigation into the shape of the opercula was based on observations during the experimental process. There is a small difference seen in the shape of the *T. sarmaticus* opercula between round and oval, and a minor percentage (9.38%) of the archaeological opercula turned out to be oval. This may vary between regions and be influenced by a number of factors besides prey choice, such as seasonality and environmental conditions. Further investigation would reveal why opercula shape differences occur.

6.3. Opercula Age

The results from the experimental sample show that the majority of experimental *T. sarmaticus* is older than the archaeological sample. The archaeological sample's ages are estimated between 0 to 3 years and 3 to 6 years, and those of the experimental sample is between 3 to 6 years.

As mentioned, there was a restriction on the size of the *T. sarmaticus* that could be collected, but seasonality may play an important role in opercula size. The time of the year during which *T. sarmaticus* is foraged would affect the age of the individuals captured. The season upwelling and shift in the Benguela current northward towards the equator during winter leads to more nutrient-rich water helping the growth of the *T. sarmaticus*. Therefore, foraging during spring and early summer would yield larger *T. sarmaticus* (Sealy & Galimberti 2011; Langejans *et al.* 2017). The experiment in this study took place in August near the time period when *T. sarmaticus* spawn. Should the collected species have been representative of a normal sample, one would expect the individuals foraged to be younger. Factors that can be considered in future are the possible effects of climate change, the upwelling of the Benguela current may have occurred earlier in the year, causing the growth of the *T. sarmaticus* to begin earlier (Loftus *et al.* 2019). Another possibility may be selective foraging practice, with the foragers spending more time looking for larger *T. sarmaticus*. A major factor that could have affected the shell size of the experimental sample is the regulations set out by the South African Department of Environmental Affairs. Research permits restrict the size to a minimum of 55mm in length across the shell for *T. sarmaticus* that is allowed to be foraged. Therefore larger *T. sarmaticus* had to be selected by the foragers.

As mentioned above, for the archaeological sample, there is an even split between those observed between the estimated age of 0 to 3 years and 3 to 6 years. Studies of *T saramaticus* age need to take the foraging season into account. Very few T*. sarmaticus* were collected during winter in the KRM MSA II sample as determined by $\delta^{18}O$ analysis done by Loftus *et al.* (2019). Winter is the period of bigger sea swells and adverse weather conditions so access to the Cochlear zone is limited. The biggest *T. sarmaticus* occur in this zone and smaller individuals occur in the adjacent zone, the Lower Balanoid, which is still accessible during big sea swells. The faunal remains from the SASL at KRM during the MIS 5c period indicate a possible colder interglacial period during which *T. sarmaticus*

were foraged (Reynard & Wurz 2020). However, non-environmental factors based on socio-economical divisions of labour among the hunter-gatherers may have affected the mollusc size since it was more dangerous collecting from the deeper intertidal zones (McLachlan & Lombard 1980).

Seasonality may have played a role in opercula size. It has been suggested that cooler water temperatures during winter and spring result in an increased growth rate of opercula compared to a decreasing growth rate linked to warmer waters temperature during summer and autumn (Loftus *et al.* 2019). Thus, if foraging occurs during the winter and spring the *T. sarmaticus* are in a period of growth, possibly resulting in smaller opercula compared to *T. sarmaticus* foraged during summer and autumn where the period of growth has already occurred, possibly relating to larger opercula (Loftus *et al.* 2019).

6.4. Opercula Processing

Breakage in the experimental sample was generally due to the extraction of the meat from the shell when it was not cooked. Lithics caused most of the breakage in the experimental sample. For lithics the most common breakage type is the transverse break. For bone and wooden tools, few of the opercula show breakage. The dominance of the transverse and irregular breaks in the archaeological sample suggests raw extraction with stone tools. This may be due to breaks occurring due to damage using tools as 6.67% (n=12) of the experimental sample shows evidence of the same breakage, and this mainly occurred in the raw extraction sample. However, the archaeological sample also showed evidence of eroded breaks, which suggests post–depositional processes. This could be due to a number of factors including site formation processes.

Percussion marks in the experimental sample may also indicate raw extraction. The archaeological sample shows notable frequencies of percussion marks, and it is assumed that, like those in the experimental sample, these marks represent raw extraction. The placement model shows that percussion marks on opercula from the experimental sample were placed in the 3rd and 4th wedge (see Figure 4. 4) near the outer spiral (see Figure 4. 5). For the archaeological sample, percussion marks showed a similar pattern of placement. This shows that the opercula in the archaeological sample with the

percussion marks were also likely extracted raw, as the cooked extraction lacked percussion marks and breakage.

Another aspect of processing is whether the *T. sarmaticus* was cooked directly on the coals where the shell acts as a 'pot' in which the meat cooks. The operculum is then not exposed to the coals but is exposed to the boiling moisture content. This causes a colour change from white to brown. When meat is extracted raw, the operculum still adheres to the meat. The meat would have been placed on the coals causing possible colouration on the operculum as a result of carbonisation during the heating process, where the surface would change colour to a variation of white, brown and shades of black (Assefa *et al.* 2008). In this case, the expectation would be that the opercula might show signs of burning. None of the archaeological opercula retained their natural colour on both the flange and dome with many opercula (62%) displaying brown colouring. There is minimal literature on the colouration observed in archaeological opercula. The assumption here is that the colour change observed is either due to heating or staining in the soil. From field observations, some opercula are coloured when live. This is especially evident with older individuals. Further investigation and analysis are required.

In the archaeological sample, there was one interesting example that indicates some relationship with charcoal. An operculum from the SMONE layer showed evidence of a possible line of charcoal (15.72 mm long) along the flange surface (Figure 6. 1). The line appears as if it could have been made intentionally as the line goes from thick to thin. Further microscopic analysis is required to investigate whether the line seen is intentional. If intentional, this may be interpreted as complex behaviour (Langley *et al*. 2008) at this early stage of the Middle Stage Age.

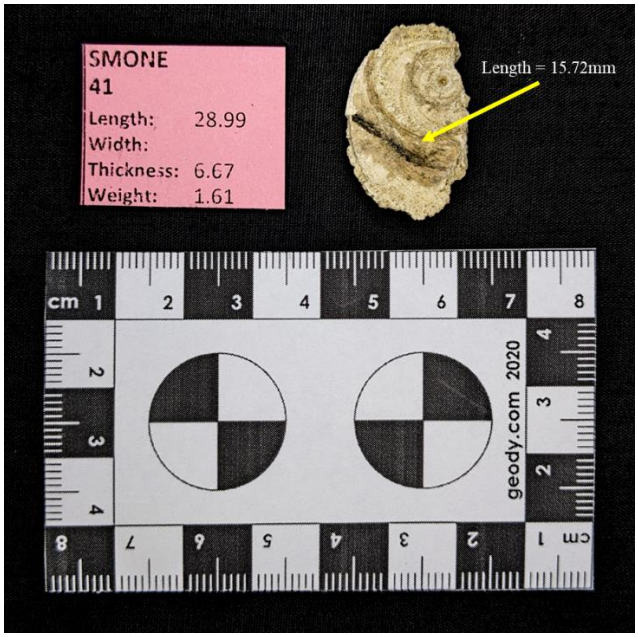


Figure 6. 1: *T. sarmaticus* operculum #41 from the SMONE layer at KRM, showing a charcoal line on the flange.

6.5. Opercula Taphonomy

Etching, encrustation, and abrasion give an indication of post-depositional processes. The etching is only evident on the archaeological sample and only on the dome surface of the opercula and it is most likely that post–depositional effects caused by roots, soils, and other natural processes lead to the etching. The soil could cause etching due to its acidity or alkalinity (Malinsky-Buller *et al*. 2011; Reynard 2022).

The encrustation observed on some of the archaeological opercula (36.51%) may have been caused by the cementation of soil after the opercula were deposited. In some cases, the experimental sample showed evidence of "encrustation", but this could have been caused by the accumulation of beach sand in the dome of the opercula during the migration process of *T. sarmaticus*.

A taphonomic analysis of the large mammal faunal remains from layer SMONE was done by Lap (2020: 67). The bone showed evidence of a high frequency of fragmentation, with breakage that occurred due to above sediment pressure, trampling, or excavator damage. On the faunal remains from SMONE, 19.6% showed evidence of percussion marks, with some evidence of acid etching, and rodent gnaws marks. These results from the faunal remains from layer SMONE reflect similarities to the results on the opercula from the same layer. With the evidence of breakage and percussion marks dominating in the

archaeological sample, with the evidence of etching that has occurred post–depositionally.

Abrasion on the *T. sarmaticus* operculum flange is very uncommon in both the experimental and archaeological samples. This could be due to a process in the soil that has affected the surface of the flange making the sheen marks unclear. The preservation of the *T. sarmaticus* opercula from the archaeological sample varies greatly between near-perfect preservation and terrible preservation. Further investigation into the post–depositional processing will further help understand the site formation processes.

Chapter 7: Conclusion

This actualistic study involved three different tool types associated with the MSA (lithic, bone and wooden tools). The experiment conducted in this project differed from other experiments undertaken in other context because in this study, raw and cooked processing was conducted using various tool types. More damage was seen on the raw extracted opercula than the cooked extracted opercula, but the cooked opercula showed some evidence of colouration that was not associated with burning. One of the results of the actualistic study was the demonstration that the experience level of the participants, with one being a novice level and one being an expert forager, made a difference in the size of the *T. sarmaticus* collected.

The archaeological opercula show some differences compared to the experimental opercula. The two samples have similar lengths, but the width, thickness and weight are significantly different. The reason for this should be investigated further.

The taphonomic conditions on the experimental and archaeological opercula show evidence of a variety of processing marks and taphonomic marks. The archaeological sample shows that post–depositional processes affected the opercula that were not evident in the experimental opercula. The archaeological opercula show similarity in the breakage patterns observed with the raw extracted opercula from the experimental sample. There is a clear difference seen between the *T. sarmaticus* opercula that were cooked versus the raw ones. The cooked *T. sarmaticus* show little to no damage to the opercula whereas the raw *T. sarmaticus* showed major breakage or damage to the opercula.

Future Avenues of Research

The opercula from various MSA and LSA coastal sites can be investigated using the criteria developed in this study. The colour changes caused by the burning of *Turbo sarmaticus* opercula need to be investigated further. Further study into the breakage patterns caused by the various tool types could be undertaken, and post–depositional breakage patterns caused by possible trampling and compaction also need to be understood. Further investigation is needed to explore the differences in the

experimental and archaeological *T. sarmaticus* opercula shape, size and bore marks. The age range index that has been developed in this study may be useful in investigating the links between age and collection patterns in relation to the 'predation hypothesis' and the 'climatic and environmental hypothesis'.

References

Akman, A.C., Demiralp, B., Güncü, G.N., Kiremitçi, A. & Sengün, D. 2005. Necrosis of Gingiva and Alveolar bone caused by acid etching and its treatment with subepithelial connective tissue graft. *Journal of the Canadian Dental Association* 71 (7): 3.

Andrews, P. & Cook, J. 1990. *Owls, caves and fossils: predation, preservation and accumulation of small mammal bones in caves, with an analysis of the pleistocene cave faunas from Westbury-Sub-Mendip, Somerset.* UK: University of Chicago Press.

Assefa, Z., Lam, Y.M. & Mienis, H.K. 2008. Symbolic use of terrestrial gastropod opercula during the Middle Stone Age at Porc-Epic Cave, Ethiopia. *Current Anthropology* 49 (4): 746–756.

Behrensmeyer, A.K. 1978. Taphonomic and ecologic information from bone weathering. *Paleobiology* 4 (2): 150–162.

Blumenschine, R. J. 1995. Percussion marks, tooth marks, and experimental determinations of the timing of hominid and carnivore access to long bones at FLK Zinjanthropus, Olduvai Gorge, Tanzania. *Journal of Human Evolution* 29 (1): 21–51.

Blumenschine, R.J., Marean, C.W. & Capaldo, S.D. 1996. Blind tests of inter-analyst correspondence and accuracy in the identification of cut marks, percussion marks, and carnivore tooth marks on bone surfaces. *Journal of Archaeological Science* 23 (4): 493–507.

Blumenschine, R.J. & Selvaggio, M.M. 1988. Percussion marks on bone surfaces as a new diagnostic of hominid behaviour. *Nature* 333 (6175): 763–765.

Bradfield, J. 2015. Use-trace analysis of bone tools: a brief overview of four methodological approaches. *The South African Archaeological Bulletin 70* (201): 3–14.

Branch, G., Branch, M., Griffiths, C. & Beckley, L. 2022. *Two Oceans: a guide to the marine life of Southern Africa*. Penguin Random House South Africa.

Branch, G.M., Griffiths, C.L., Branch, M.L. & Beckley, L.E. 2010. *Two Oceans: a guide to the marine life of Southern Africa*. Cape Town, South Africa: Struik Nature.

Brenner, M.J., Ryano, K. & Wurz, S. 2022. Coastal adaptations at Klasies River main site during MIS 5c/d (93 – 110 000 years ago) from a southern Cape perspective. *Journal of Island and Coastal Archaeology*, https://doi.org/10.1080/15564894.2020.1774444.

Brenner, M.J. & Wurz, S. 2019. A high-resolution perspective on MIS 5c-d lithic assemblages from Klasies River main site Cave 1. *Journal of Archaeological Science: Reports* 26 (101891): 1–33.

Bustamante, R.H. & Branch, G.M. 1996. Large scale patterns and trophic structure of southern African rocky shores: The roles of geographic variation and wave exposure. *Journal of Biogeography* 23 (3): 339–351.

Carr, A.S., Bateman, M.D., Cawthra, H.C. & Sealy, J. 2019. First evidence for onshore marine isotope stage 3 aeolianite formation on the southern Cape coastline of South Africa. *Marine Geology* 407: 1–15.

Cawthra, H.C., Anderson, R.J., De Vynck, J.C., Jacobs, Z., Jerardino, A., Kyriacou, K. & Marean, C.W. 2020. Migration of Pleistocene shorelines across the Palaeo-Agulhas Plain: Evidence from dated sub-bottom profiles and archaeological shellfish assemblages. *Quaternary Science Reviews* 235: 106107.

Chandler, G. & Merry, C.L. 2010. The South African geoid 2010: SAGEOID10. *Position IT*, 29–33.

Checa, A.G. & Jiménez-Jiménez, A.P. 1998. Constructional morphology, origin, and evolution of the gastropod operculum. *Paleobiology* 24 (1): 109–132.

Cold Water. 2016. Windmill beach Alikreukel or Giant periwinkle, Cape Town. https://www.youtube.com/watch?v=B7C8WoiJwZY. (Accessed 20 November 2022).

Da Silva, C.M. 2004. The spring full moon. *Journal for the History of Astronomy* 35 (4): 475–478.

De Vynck, J.C. 2017. Productivity and resilience of intertidal resources available to extant human foragers on South Africa's Cape south coast: behavioural implications for early Homo sapiens. (*Doctoral dissertation, Nelson Mandela Metropolitan University)*, 1–243.

De Vynck, J.C., Anderson, R., Atwater, C., Cowling, R.M., Fisher, E.C., Marean, C.W., Walker, R.S. & Hill, K. 2016. Return rates from intertidal foraging from Blombos Cave to Pinnacle Point: Understanding early human economies. *Journal of Human Evolution* 92: 101–115.

De Vynck, J.C., Difford, M., Anderson, R., Marean, C.W., Cowling, R.M. & Hill, K. 2020. The resilience to human foraging of intertidal resources on the south Cape coast of South Africa and the implications for pre-historic foragers. *Quaternary Science Reviews* 235: 106041.

Deacon, H.J. 1995. Two Late Pleistocene-Holocene Archaeological Depositories from the Southern Cape, South Africa. *The South African Archaeological Bulletin* 50 (162): 121–131.

Deacon, H.J. & Geleijnse, V.B. 1988. The stratigraphy and sedimentology of the Main Site Sequence, Klasies River, South Africa. *The South African Archaeological Bulletin* 43 (147): 5–14.

D'Errico, F. & Villa, P. 1997. Holes and grooves: the contribution of microscopy and taphonomy to the problem of art origins. *Journal of Human Evolution* 33 (1): 1–31.

Domínguez-Rodrigo, M., de Juana, S., Galán, A.B. & Rodríguez, M. 2009. A new protocol to differentiate trampling marks from butchery cut marks. *Journal of Archaeological Science* 36 (12): 2643–2654.

Drennan, R. D. 2010. *Statistics for Archaeologists*. New York: Springer.

Driver, J.C. 2005. Manual for description of vertebrate remains. Unpublished manual. Crow Canyon Archaeological Center: Cortez.

Fernandez-Jalvo, Y. & Andrews, P. 2016. *Atlas of Taphonomic Identifications: 1001+ Images of Fossil and recent mammal bone modification*. Springer.

Foster, G.G. 1997. Growth, reproduction and feeding biology of Turbo sarmaticus (Mollusca : Vetigastropoda) along the coast of the Eastern Cape Province of South Africa. Unpublished PhD dissertation: Rhodes University.

Foster, G.G., Hodgson, A.N. & Balarin, M. 1999. Effect of diet on growth rate and reproductive fitness of Turbo sarmaticus (Mollusca: Vetigastropoda: Turbinidae). *Marine Biology* 134 (2): 307–315.

Fu, L.-L. & Pihos, G. 1994. Determining the response of sea level to atmospheric pressure forcing using TOPEX/POSEIDON data. *Journal of Geophysical Research: Oceans* 99 (C12): 24633–24642.

Galimberti, M., Loftus, E. & Sealy, J. 2017. Investigating δ18O of Turbo sarmaticus (L. 1758) as an indicator of sea surface temperatures. *Palaeogeography, Palaeoclimatology, Palaeoecology* 484: 62–69.

Garzoli, S.L. & Gordon, A.L. 1996. Origins and variability of the Benguela Current. *Journal of Geophysical Research: Oceans* 101 (C1): 897–906.

Google Earth Pro. 2021a. Still Bay experimental foraging trip in Jongensfontein, Western Cape, South Africa. In relations to the southern Cape coastal archaeological sites Klasies River main site (KRM), Blombos Cave (BBC) and Pinnacle Point (PP). *Google Inc.*

Google Earth Pro. 2021b. Foraging locations for Still Bay Foraging Experiment, A: Test foraging day at Jongensfontein East, 1: Lithics Foraging at Jongensfontein West, 2: Wooden Tool and Bone Tool foraging at Brandersfontein Farm. *Google Inc.*

Hawkes, K, Hill, K. & O'Connell, J. F. 1982. Why hunters gather: optimal foraging and the Aché of eastern Paraguay. *American Ethnologist* 9 (2): 379–398.

Hawkes, K. & O'Connell, J. 1992. On Optimal Foraging Models and Subsistence Transitions. *Current Anthropology* 33 (1): 63–66.

Helm, C., Cawthra, H., Cowling, R., De Vynck, J., Marean, C., McCrea, R. & Rust, R. 2018. Palaeoecology of giraffe tracks in Late Pleistocene aeolianites on the Cape south coast. *South African Journal of Science* 114 (1/2).

Henshilwood, C.S. 2008. Holocene Prehistory of the Southern Cape, South Africa. Excavations at Blombos Cave and the Blombosfontein Nature reserve. 1–187.

Holmes, C.L. 2020. Shellfish use at Klasies River Main Site: an investigation of layer SMONE. Unpublished Honours Thesis: University of the Witwatersrand, 1–61.

Hutchings, L., van der Lingen, C.D., Shannon, L.J., Crawford, R.J.M., Verheye, H.M.S., Bartholomae, C.H., van der Plas, A.K., Louw, D., Kreiner, A., Ostrowski, M., Fidel, Q., Barlow,

R.G., Lamont, T., Coetzee, J., Shillington, F., Veitch, J., Currie, J.C. & Monteiro, P.M. S. 2009. The Benguela Current: An ecosystem of four components. *Progress in Oceanography* 83 (1): 15–32.

Ilano, A.S., Ito, A., Fujinaga, K. & Nakao, S. 2004. Age determination of Buccinum isaotakii (Gastropoda: Buccinidae) from the growth striae on operculum and growth under laboratory conditions. *Aquaculture* 242 (1): 181–195.

Jerardino, A. & Marean, C.W. 2010. Shellfish gathering, marine paleoecology and modern human behavior: perspectives from cave PP13B, Pinnacle Point, South Africa. *Journal of Human Evolution* 59 (3–4): 412–424.

Jerardino, A. & Navarro, R. 2021. Pleistocene and Holocene procurement of the clam Donax serra (Bivalvia: Donacidae) along the southern Cape coast of south Africa. *Journal of Archaeological Science: Reports* 38: 103062.

Karkanas, P. & Goldberg, P. 2010. Site formation processes at Pinnacle Point Cave 13B (Mossel Bay, Western Cape Province, South Africa): resolving stratigraphic and depositional complexities with micromorphology. *Journal of Human Evolution* 59 (3): 256–273.

Kilburn, R. & Rippey, E. 1982. *Sea Shells Of Southern Africa*. Johannesburg, South Africa: Macmillan South Africa.

Klein, R.G. & Bird, D.W. 2016. Shellfishing and human evolution. *Journal of Anthropological Archaeology* 44: 198–205.

Klein, R.G. & Steele, T.E. 2013. The Middle and Later Stone Age faunal remains from Diepkloof Rock Shelter, Western Cape, South Africa. *Journal of Archaeological Science* 40 (9): 3453–3462.

Kvale, E.P. 2006. The origin of neap–spring tidal cycles. *Marine Geology* 235 (1): 5–18.

Kyriacou, K., Parkington, J.E., Will, M., Kandel, A.W. & Conard, N.J. 2015. Middle and Later Stone Age shellfish exploitation strategies and coastal foraging at Hoedjiespunt and Lynch Point, Saldanha Bay, South Africa. *Journal of Archaeological Science* 57: 197–206.

Kyriacou, K. 2017. Intertidal shellfish as a source of protein and energy for the Middle Stone Age inhabitants of the southwestern Cape and northern KwaZulu-Natal, South Africa. *Quaternary International* 438: 30–39.

Kyriacou, K., Parkington, J.E., Marais, A.D. & Braun, D.R. 2014. Nutrition, modernity and the archaeological record: Coastal resources and nutrition among Middle Stone Age hunter-gatherers on the western Cape coast of South Africa. *Journal of Human Evolution* 77: 64–73.

Langejans, G.H.J., Dusseldorp, G.L. & Thackeray, J.F. 2017. Pleistocene molluscs from Klasies River (South Africa): Reconstructing the local coastal environment. *Quaternary International* 427: 59–84.

Langejans, G.H.J., van Niekerk, K.L., Dusseldorp, G.L. & Thackeray, J.F. 2012. Middle Stone Age shellfish exploitation: Potential indications for mass collecting and resource intensification at Blombos Cave and Klasies River, South Africa. *Quaternary International* 270: 80–94.

Langley, M. C., Clarkson, C. & Ulm, S. 2008. Behavioural Complexity in Eurasian Neanderthal Populations: A Chronological Examination of the Archaeological Evidence. *Cambridge Archaeological Journal* 18 (3): 289–307.

Lap, A.L.V. 2020. Bones for Thought: A taphonomic study of the faunal remains from early MIS 5 at Klasies River main site. Unpublished Master's Thesis: University of the Witwatersrand, 1–222.

Lidour, K., Béarez, P., Beech, M., Charpentier, V. & Méry, S. 2021. Intensive exploitation of marine crabs and sea urchins during the middle holocene in the eastern Arabian peninsula offers new perspectives on ancient maritime adaptations. *The Journal of Island and Coastal Archaeology*, 1–29.

Loftus, E., Lee-Thorp, J., Leng, M., Marean, C. & Sealy, J. 2019. Seasonal scheduling of shellfish collection in the Middle and Later Stone Ages of southern Africa. *Journal of Human Evolution* 128: 1–16.

Lyman, R.L. 1994. Quantitative Units and Terminology in Zooarchaeology. *American Antiquity* 59 (1): 36–71.

MacArthur, R.H. & Pianka, E.R. 1966. On optimal use of a patchy environment. *The American Naturalist* 100 (916): 603–609.

Malinsky-Buller, A., Hovers, E. & Ofer, M. 2011. Making time: "Living floors", "palimpsests" and site formation processes - A perspective from the open-air Lower Paleolithic site of Revadim Quarry, Israel. *Journal of Anthropological Archaeology* 30: 89–101.

Marean, C.W. 2010. Pinnacle Point Cave 13B (Western Cape Province, South Africa) in context: The Cape Floral kingdom, shellfish, and modern human origins. *Journal of Human Evolution* 59 (3): 425–443.

Mather, A.A., Garland, G.G. & Stretch, D.D. 2009. Southern African sea levels: corrections, influences and trends. *African Journal of Marine Science* 31 (2): 145–156.

McLachlan, A. & Lombard, H.W. 1980. Seasonal variations in energy and biochemical components of an edible gastropod, Turbo sarmaticus (Turbinidae). *Aquaculture* 19 (2): 117–125.

Meehan, B. 1982. Shell bed to shell midden: Australian Institute of Aboriginal Studies. *Atlantic Highlands, NJ, distributed by Humanities Press*.

Morrissey, P., Mentzer, S.M. & Wurz, S. 2022. A Critical Review of the Stratigraphic Context of the MSA I and II at Klasies River Main Site, South Africa. *Journal of Paleolithic Archaeology* 5 (5): 47.

Nami, H.G., de la Pefia, P., Vásquez, C.A., Feathers, J. & Wurz, S. 2016. Palaeomagnetic results and new dates of sedimentary deposits from Klasies River Cave 1, South Africa. *South African Journal of Science* 112 (11–12): 1–12.

Outram, A.K. 2008. Introduction to experimental archaeology. *World Archaeology* 40 (1): 1-6. DOI: 10.1080/00438240801889456

Parkington, J. 1976. Coastal Settlement between the Mouths of the Berg and Olifants Rivers, Cape Province. *The South African Archaeological Bulletin* 31 (123/124): 127–140.

Pulfrich, A. & Branch, T.A. 2002. Population dynamics and potential yield of three species of giant winkles in the Western Cape, South Africa. *African Journal of Marine Science* 24: 161–183.

Reynard, J.P. 2022. Tracking Occupational Intensity Using Archaeo-faunal Data: Case Studies from the Late Pleistocene in the Southern Cape of South Africa. *Journal of Archaeological Method and Theory* 29 (1): 214–250.

Reynard, J.P. & Wurz, S. 2020. The palaeoecology of Klasies River, South Africa: An analysis of the large mammal remains from the 1984–1995 excavations of Cave 1 and 1A. *Quaternary Science Reviews* 237: 106301.

Ryano, K.P. 2014. The later Stone Age in the Southern Cape, South Africa, during the terminal pleistocene/early holocene with a focus on Klipdrift cave. Unpublished PhD Thesis: University of the Witwatersrand.

Sealy, J. & Galimberti, M. 2011. Shellfishing and the Interpretation of Shellfish Sizes in the Middle and Later Stone Ages of South Africa. In: N. F. Bicho, J. A. Haws, & L. G. Davis (eds.) *Trekking the Shore: Changing Coastlines and the Antiquity of Coastal Settlement*: 405–419. New York: Springer.

Sherwood, J., McNiven, I.J., Laurenson, L., Richards, T. & Bowler, J. 2016. Prey selection, size, and breakage differences in Turbo undulatus opercula found within Pacific Gull (Larus pacificus) middens compared to Aboriginal middens and natural beach deposits, southeast Australia. *Journal of Archaeological Science: Reports* 6: 14–23.

Sherwood, J.E., McNiven, I.J. & Laurenson, L. 2018. The Moyjil site, south-west Victoria, Australia: shells as evidence of the deposit's origin. *Proceedings of the Royal Society of Victoria* 130 (2): 50.

Singer, R. & Wymer, J. 1982. *The Middle Stone Age at Klasies River Mouth in South Africa*. Chicago and London: The University of Chicago Press.

Steele, T.E. & Klein, R.G. 2008. Intertidal shellfish use during the middle and later stone age of South Africa. *Archaeofauna* 17 (6): 63–76.

Stephenson, T.A. 1939. The constitution of the intertidal fauna and flora of South Africa.–Part I. *Journal of the Linnean Society of London, Zoology* 40 (273): 487–536.

Stephenson, T.A. & Stephenson, A. 1949. The Universal Features of Zonation Between Tide-Marks on Rocky Coasts. *Journal of Ecology* 37 (2): 289–305.

tides4fishing.com. 2021. Tide times and charts for Mossel Bay, South Africa and weather forecast for fishing in Mossel Bay in 2021, accessed November 16, 2021, available at https://tides4fishing.com/af/south-africa/mossel-bay/.

Toth, N. & Schick, K. 2009. The importance of actualistic studies in the early Stone Age research: some personal reflections. *The Cutting Edge: New Approaches to the Archaeology of Human Origins:* Chapter 13, 267-344. Stone Age Archaeology Institute Press.

Will, M., Kandel, A.W., Kyriacou, K. & Conard, N.J. 2016. An evolutionary perspective on coastal adaptations by modern humans during the Middle Stone Age of Africa. *Quaternary International* 404: 68–86.

Will, M., Kandel, A.W. & Conard, N.J. 2019. Midden or Molehill: The Role of Coastal Adaptations in Human Evolution and Dispersal. *Journal of World Prehistory* 32 (1): 33–72.

Windy.com. 2011. Windy as forecasted, accessed November 16, 2021, available at https://www.windy.com/-34.390/21.431?-34.905,21.431,8/.

Wurz, S., Bentsen, S.E., Reynard, J., Van Pletzen-Vos, L., Brenner, M., Mentzer, S., Pickering, R. & Green, H. 2018. Connections, culture and environments around 100 000 years ago at Klasies River main site. *Quaternary International* 495: 102–115.

Wurz, S., Pickering, R. & Mentzer, S. 2022. U-Th dating, taphonomy and taxonomy of shell middens at Klasies River main site indicate stable and systematic coastal exploitation by MIS 5c-d. *Frontiers in Earth Science*, *Special volume: "Living on the Edge-Interdisciplinary Perspectives on Coastal and Marine Ecosystems in Human Prehistory"*.

Yssel, S.G. 1989. *Long Term Trends in a Population of Turbo Sarmaticus, Linneaus 1758, in the Tsitsikamma Coastal National Park*. Unpublished Master's Thesis, University of Port Elizabeth.

Appendices

Appendix 1A: Modern-day experimental data

Appendix 1A.1. Foraging Data

Appendix 1A.1.1. Foraging Notes

Notes from Lithic foraging Day 1

The foraging was undertaken on Day 1 over a period of one hour and twenty-three minutes for P1, and one hour and forty-two minutes for P2 (Appendix 1A Table 1). With a condition rating of 4, the conditions according to the Ocean Condition Rating (Appendix 1C Figure 1) showed the water conditions were tough, especially for an inexperienced forager. The foraging with the lithic was a good learning experience for the future days. Due to the water conditions, the size of the *T. sarmaticus* shells was smaller than during the most optimal conditions.

Notes from Wooden tool foraging Day 2

The foraging was undertaken on Day 2 over a period of twenty-five minutes for P1, and forty-six minutes for P2 (Appendix 1A Table 1). With a condition rating of 2, the conditions according to the Ocean Condition Rating (Appendix 1C Figure 1) showed the water conditions were optimal for foraging, the time foraging was less to reach the total amount and the foragers were able to be more selective about the size of the shellfish.

Notes from Bone tool foraging Day 3

The foraging was undertaken on Day 3 over a period of forty-five minutes for P1, and forty minutes for P2 (Appendix 1A Table 1). With a condition rating of 2, the conditions according to the Ocean Condition Rating (Appendix 1C Figure 1) showed the water conditions were optimal for foraging, the time foraging was less to reach the total amount and the foragers were able to be more selective about the size of the shellfish.

Appendix 1A.2. Processing Data

Appendix 1A Table 1: Experimental Opercula processing time for P1 and P2.

Processing Tool	P1 – Processing Time (min)		P2 – Processing Time (min)	
	Raw Processing	Cooked Processing	Raw Processing	Cooked Processing
Lithics	0:31:00	1:23:00	2:33:00	1:41:00
Wooden	0:30:00	1:30:00	0:45:00	1:29:00
Bone	0:40:00	1:39:00	0:49:00	1:25:00

*Cooked extraction time includes time spent on the fire

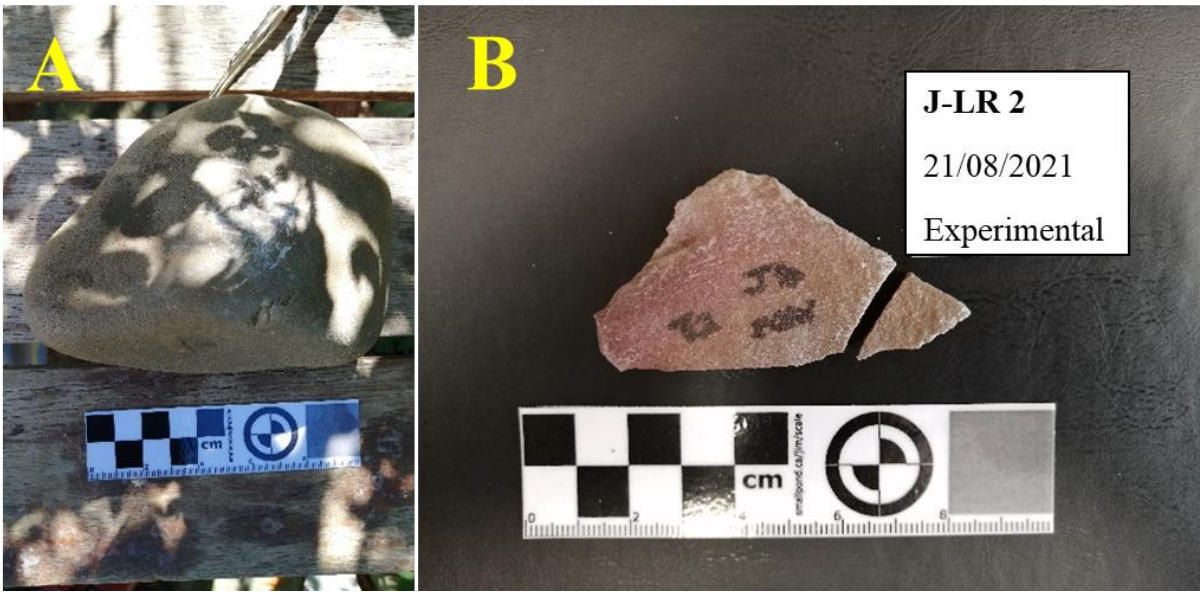
Appendix 1A Table 2: Experimental Opercula cooking time for P1 and P2.

Processing Tool	P1 – Cooking Time (min)	P2 – Cooking Time (min)
Lithics	0:42:00	0:29:00
Wooden	0:50:00	0:42:00
Bone	0:19:00	0:10:00

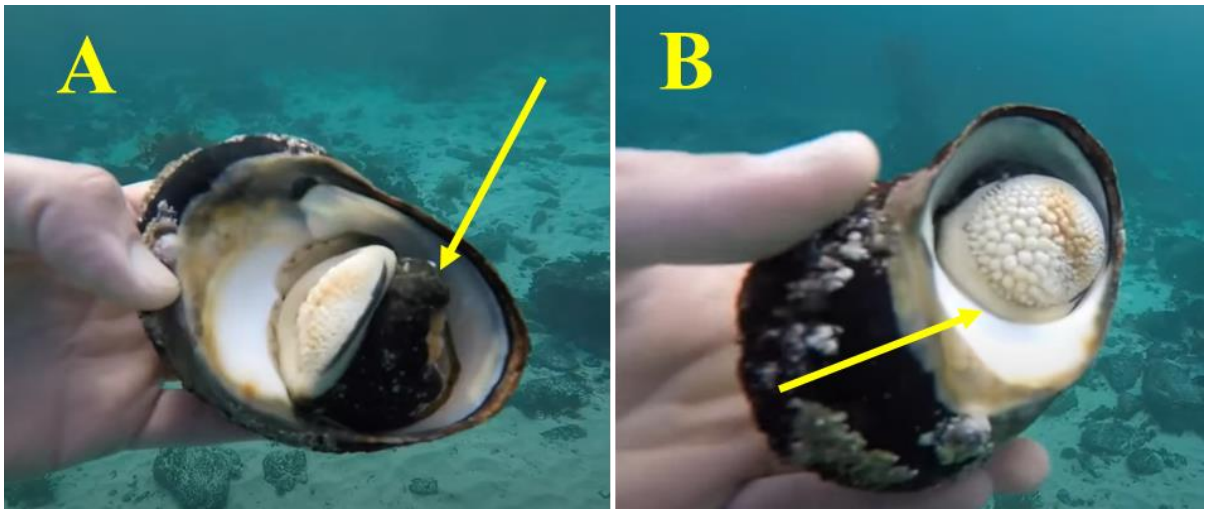
Appendix 1A.2.1. Processing Notes

Notes from Lithic processing Day 1

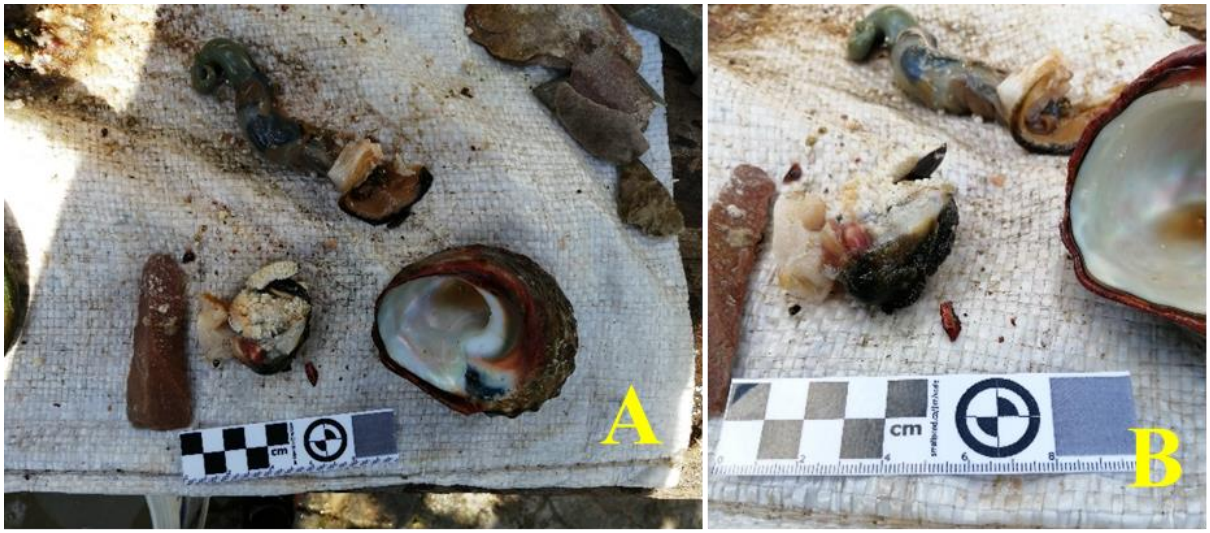
It was found that during raw extractions the lithics will break or fracture (Appendix 1A Figure 1A) if the *T. sarmaticus* is not relaxed (Appendix 1A Figure 2B), a hammer and anvil were used with a quartzite cobble by P2 (Appendix 1A Figure 1B). Some opercula remain glued onto the foot of the *T. sarmaticus* (Appendix 1A Figure 3). For smaller shells, the operculum would fragment on extraction. Three tools were used at one time, one was used as a point with the cobblestone, and one tool was used as a blade to remove the edible portion of meat from the guts.



Appendix 1A Figure 1: A, cobblestone used by P2 for Hammer and Anvil technique. B, lithic (J-LR 2) used by P1 that broke while raw processing the *T. sarmaticus*.



Appendix 1A Figure 2: A, the foot of the *T. sarmaticus*. B, the muscle near the head sealing the operculum in place (Cold Water 2016).



Appendix 1A Figure 3: A, the workspace during raw processing using lithics. B, the operculum that fragmented and remained glued to the *T. sarmaticus* foot.

For cooked extraction, a spiral technique was used to remove the meat from the shell as a complete specimen (Appendix 1A Figure 4). During the raw extraction, a specific tool was used to move around the spiralled centre of the shell to remove the flesh intact, if this was ineffective the participants would use their finger to remove the attaching muscle. With P2 a technique of a hammer stone straight onto the shell was used on one shell, this caused the shell to shatter and allowed for easy extraction and caused minimal damage to the operculum.



Appendix 1A Figure 4: The complete extraction of the *T. sarmaticus* meat from the shell due to cooked extraction.

Notes from Wooden tool processing Day 2

Placing the *T. sarmaticus* foot down (Appendix 1A Figure 5) before raw processing made the processing easier, allowing for the tool to get underneath the operculum. Similar to the lithics processing three wooden tools were used during the processing (the tools were random sticks and twigs picked up). The wooden tool seemed to be the most effective tool for foraging and processing combined due to its flexibility.



Appendix 1A Figure 5: A, the foot-up technique used for the lithic raw processing. B, the new foot–down approach used for wooden and bone tool raw processing.

In the cooking of the *T. sarmaticus*, the heat of the fire does depend on the ability to extract the gonad (Appendix 1A Table 1 and Appendix 1A Table 2).

Notes from Bone tool processing Day 3

Placing the *T. sarmaticus* foot down before raw processing made the processing easier, allowing for the tool to get underneath the operculum. Similar to the lithic and wooden tools, multiple bone tools were used during the processing (pointed, flat edged). Bone tools broke on the operculum, no raw bone tools were used as they were too small and fragile to form a functioning tool.

Appendix 1B: Analytical Data

Appendix 1B.1: Experimental Age Index

Appendix 1B Table 1: Experimental *T. sarmaticus* shell length age and opercula length age.

Order	Shell Length	Shell Length Age	Opercula Length	Opercula Age
SBE21_C-LC-3	55.00	0 to 3	24.73	0 to 3
SBE21_C-LR-11	62.00	0 to 3	26.45	0 to 3
SBE21_C-LC-15	62.00	0 to 3	26.57	0 to 3
SBE21_C-LR-14	62.00	0 to 3	27.27	0 to 3
SBE21_J-LR-5	62.00	0 to 3	27.47	0 to 3
SBE21_C-LR-12	63.00	0 to 3	25.88	0 to 3
SBE21_C-LC-10	63.00	0 to 3	26.78	0 to 3
SBE21_C-LR-15	63.00	0 to 3	27.56	0 to 3
SBE21_J-BC-13	63.00	0 to 3	27.94	0 to 3
SBE21_J-LR-15	63.00	0 to 3	28.17	0 to 3
SBE21_J-LR-14	65.00	0 to 3	25.92	0 to 3
SBE21_C-LR-9	65.00	0 to 3	27.88	0 to 3
SBE21_C-LR-13	65.00	0 to 3	28.31	0 to 3
SBE21_C-LR-7	65.00	0 to 3	28.79	0 to 3
SBE21_J-LC-11	65.00	0 to 3	29.00	0 to 3
SBE21_C-LC-14	66.00	0 to 3	27.31	0 to 3
SBE21_J-BR-11	66.00	0 to 3	29.48	0 to 3
SBE21_C-LC-11	66.00	0 to 3	29.67	0 to 3
SBE21_J-LR-12	67.00	0 to 3	28.80	0 to 3
SBE21_J-LC-12	68.00	0 to 3	29.71	0 to 3
SBE21_C-BC-15	72.00	3 to 6	29.24	0 to 3
SBE21_J-LR-10	75.00	3 to 6	29.28	0 to 3
SBE21_C-BR-14	76.00	3 to 6	29.20	0 to 3
SBE21_C-LR-6	68.00	0 to 3	31.91	3 to 6
SBE21_C-BC-9	68.00	0 to 3	34.16	3 to 6
SBE21_C-LC-13	69.00	0 to 3	30.23	3 to 6
SBE21_C-BC-14	69.00	0 to 3	33.79	3 to 6
SBE21_J-LC-15	70.00	0 to 3	30.01	3 to 6
SBE21_J-BC-14	70.00	0 to 3	30.21	3 to 6
SBE21_C-LC-9	70.00	0 to 3	31.08	3 to 6
SBE21_C-BR-15	70.00	0 to 3	31.31	3 to 6
SBE21_J-LR-4	70.00	0 to 3	31.92	3 to 6
SBE21_C-WC-9	70.00	0 to 3	32.33	3 to 6
SBE21_J-LC-4	71.00	0 to 3	31.99	3 to 6
SBE21_C-LC-2	72.00	3 to 6	31.96	3 to 6
SBE21_C-BC-13	72.00	3 to 6	32.03	3 to 6
SBE21_C-BC-11	72.00	3 to 6	32.14	3 to 6
SBE21_C-WR-12	73.00	3 to 6	31.53	3 to 6
SBE21_C-WC-15	73.00	3 to 6	32.34	3 to 6

SBE21_C-WR-11	73.00	3 to 6	33.18	3 to 6
SBE21_J-BR-7	73.00	3 to 6	33.28	3 to 6
SBE21_C-BC-10	73.00	3 to 6	34.67	3 to 6
SBE21_J-LC-7	74.00	3 to 6	32.56	3 to 6
SBE21_C-WR-9	74.00	3 to 6	32.63	3 to 6
SBE21_C-LR-10	74.00	3 to 6	32.80	3 to 6
SBE21_J-WC-13	74.00	3 to 6	33.20	3 to 6
SBE21_C-LC-7	74.00	3 to 6	36.90	3 to 6
SBE21_C-BR-9	75.00	3 to 6	30.57	3 to 6
SBE21_C-BR-11	75.00	3 to 6	31.66	3 to 6
SBE21_C-BR-13	75.00	3 to 6	31.96	3 to 6
SBE21_C-LC-6	75.00	3 to 6	32.74	3 to 6
SBE21_C-WR-10	75.00	3 to 6	33.23	3 to 6
SBE21_C-WR-3	75.00	3 to 6	34.09	3 to 6
SBE21_C-BC-5	75.00	3 to 6	36.01	3 to 6
SBE21_J-LC-14	76.00	3 to 6	32.06	3 to 6
SBE21_J-BC-2	76.00	3 to 6	33.00	3 to 6
SBE21_C-WC-6	76.00	3 to 6	33.45	3 to 6
SBE21_C-WR-2	76.00	3 to 6	33.56	3 to 6
SBE21_C-BC-8	76.00	3 to 6	33.88	3 to 6
SBE21_C-LR-8	76.00	3 to 6	33.90	3 to 6
SBE21_J-BC-12	77.00	3 to 6	32.97	3 to 6
SBE21_J-WC-10	77.00	3 to 6	33.08	3 to 6
SBE21_C-LR-4	77.00	3 to 6	33.15	3 to 6
SBE21_J-BR-4	78.00	3 to 6	33.29	3 to 6
SBE21_J-LC-6	78.00	3 to 6	33.85	3 to 6
SBE21_C-LR-5	78.00	3 to 6	34.02	3 to 6
SBE21_C-BR-8	78.00	3 to 6	34.17	3 to 6
SBE21_J-WR-8	78.00	3 to 6	34.18	3 to 6
SBE21_J-WR-13	78.00	3 to 6	34.33	3 to 6
SBE21_J-WC-7	78.00	3 to 6	34.51	3 to 6
SBE21_C-BR-2	78.00	3 to 6	39.36	3 to 6
SBE21_J-BR-13	79.00	3 to 6	33.80	3 to 6
SBE21_C-WC-13	79.00	3 to 6	34.29	3 to 6
SBE21_J-WC-14	79.00	3 to 6	34.65	3 to 6
SBE21_J-BR-12	79.00	3 to 6	35.04	3 to 6
SBE21_C-WC-1	79.00	3 to 6	35.22	3 to 6
SBE21_C-WR-8	79.00	3 to 6	35.83	3 to 6
SBE21_C-BR-10	80.00	3 to 6	32.74	3 to 6
SBE21_C-WC-3	80.00	3 to 6	34.01	3 to 6
SBE21_J-WR-15	80.00	3 to 6	34.90	3 to 6
SBE21_J-LR-7	80.00	3 to 6	35.25	3 to 6
SBE21_J-WC-4	80.00	3 to 6	35.41	3 to 6
SBE21_J-WR-12	80.00	3 to 6	35.67	3 to 6
SBE21_C-WR-1	80.00	3 to 6	36.01	3 to 6
SBE21_C-BC-3	80.00	3 to 6	37.62	3 to 6
SBE21_C-WC-12	81.00	3 to 6	34.31	3 to 6
SBE21_C-WC-14	81.00	3 to 6	34.60	3 to 6

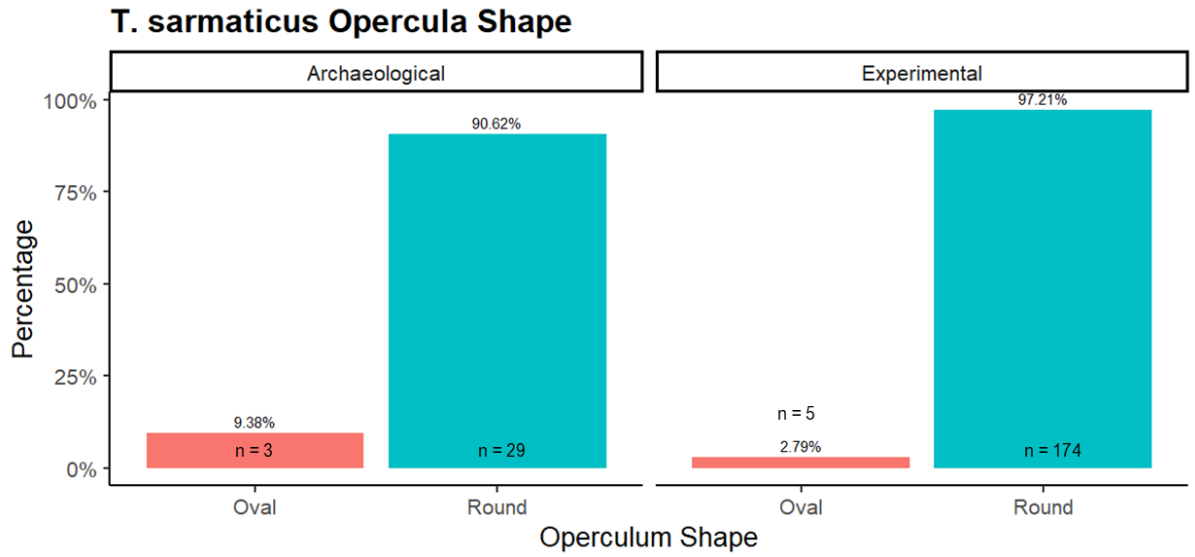
SBE21_J-WC-15	81.00	3 to 6	34.77	3 to 6
SBE21_C-LC-4	81.00	3 to 6	35.24	3 to 6
SBE21_J-WR-11	81.00	3 to 6	35.32	3 to 6
SBE21_C-BC-6	81.00	3 to 6	39.24	3 to 6
SBE21_J-WC-12	82.00	3 to 6	33.81	3 to 6
SBE21_C-WC-7	82.00	3 to 6	34.12	3 to 6
SBE21_C-BR-5	82.00	3 to 6	34.30	3 to 6
SBE21_C-WR-15	82.00	3 to 6	35.16	3 to 6
SBE21_J-LC-2	82.00	3 to 6	35.63	3 to 6
SBE21_C-WR-4	82.00	3 to 6	35.98	3 to 6
SBE21_C-WC-10	82.00	3 to 6	35.98	3 to 6
SBE21_J-WR-10	83.00	3 to 6	35.61	3 to 6
SBE21_J-WC-5	83.00	3 to 6	36.00	3 to 6
SBE21_J-BC-8	83.00	3 to 6	36.16	3 to 6
SBE21_J-LR-6	83.00	3 to 6	36.42	3 to 6
SBE21_J-BR-8	83.00	3 to 6	36.79	3 to 6
SBE21_J-LC-1	83.00	3 to 6	37.80	3 to 6
SBE21_J-LR-9	83.00	3 to 6	38.85	3 to 6
SBE21_C-BR-7	83.00	3 to 6	39.73	3 to 6
SBE21_C-BC-4	83.00	3 to 6	39.73	3 to 6
SBE21_J-BC-3	84.00	3 to 6	35.31	3 to 6
SBE21_C-WC-11	84.00	3 to 6	36.06	3 to 6
SBE21_J-WR-9	84.00	3 to 6	36.09	3 to 6
SBE21_J-BC-4	84.00	3 to 6	36.20	3 to 6
SBE21_J-BC-9	85.00	3 to 6	35.73	3 to 6
SBE21_J-WR-14	85.00	3 to 6	36.57	3 to 6
SBE21_C-WR-6	85.00	3 to 6	37.06	3 to 6
SBE21_J-LC-5	85.00	3 to 6	37.29	3 to 6
SBE21_J-WC-11	85.00	3 to 6	37.64	3 to 6
SBE21_C-BR-3	86.00	3 to 6	35.17	3 to 6
SBE21_J-LC-3	86.00	3 to 6	36.27	3 to 6
SBE21_C-LC-5	86.00	3 to 6	36.51	3 to 6
SBE21_C-WR-13	86.00	3 to 6	37.16	3 to 6
SBE21_C-LC-8	87.00	3 to 6	32.71	3 to 6
SBE21_J-WR-5	87.00	3 to 6	36.17	3 to 6
SBE21_C-WR-14	87.00	3 to 6	37.35	3 to 6
SBE21_J-BR-15	87.00	3 to 6	37.39	3 to 6
SBE21_J-WR-4	87.00	3 to 6	38.29	3 to 6
SBE21_J-WR-2	87.00	3 to 6	38.31	3 to 6
SBE21_J-LC-8	87.00	3 to 6	38.66	3 to 6
SBE21_J-LR-8	87.00	3 to 6	39.05	3 to 6
SBE21_J-BC-11	88.00	3 to 6	37.16	3 to 6
SBE21_J-WC-6	88.00	3 to 6	37.60	3 to 6
SBE21_C-WC-4	88.00	3 to 6	37.69	3 to 6
SBE21_C-WR-5	88.00	3 to 6	38.41	3 to 6
SBE21_J-BR-6	88.00	3 to 6	38.87	3 to 6
SBE21_J-BR-3	89.00	3 to 6	36.20	3 to 6
SBE21_J-BR-2	89.00	3 to 6	38.45	3 to 6

SBE21_J-WC-8	89.00	3 to 6	39.25	3 to 6
SBE21_C-BR-12	90.00	3 to 6	31.86	3 to 6
SBE21_J-LR-13	90.00	3 to 6	36.79	3 to 6
SBE21_C-BR-4	90.00	3 to 6	36.94	3 to 6
SBE21_J-LR-11	90.00	3 to 6	37.73	3 to 6
SBE21_J-LR-2	90.00	3 to 6	37.92	3 to 6
SBE21_J-WC-9	90.00	3 to 6	39.19	3 to 6
SBE21_J-BC-1	90.00	3 to 6	39.42	3 to 6
SBE21_J-WC-1	90.00	3 to 6	39.89	3 to 6
SBE21_C-LC-12	91.00	3 to 6	36.88	3 to 6
SBE21_J-BR-5	91.00	3 to 6	37.82	3 to 6
SBE21_C-LR-3	91.00	3 to 6	39.15	3 to 6
SBE21_J-WC-3	91.00	3 to 6	39.49	3 to 6
SBE21_C-BC-2	92.00	3 to 6	35.03	3 to 6
SBE21_J-WR-3	92.00	3 to 6	39.03	3 to 6
SBE21_J-WR-1	92.00	3 to 6	39.24	3 to 6
SBE21_J-BC-10	92.00	3 to 6	39.65	3 to 6
SBE21_J-WR-7	92.00	3 to 6	39.92	3 to 6
SBE21_J-LC-9	93.00	3 to 6	38.23	3 to 6
SBE21_J-LR-3	93.00	3 to 6	38.51	3 to 6
SBE21_J-BR-10	93.00	3 to 6	38.99	3 to 6
SBE21_J-BR-14	93.00	3 to 6	39.38	3 to 6
SBE21_C-WC-2	94.00	3 to 6	38.39	3 to 6
SBE21_J-BC-6	94.00	3 to 6	39.09	3 to 6
SBE21_C-BC-1	94.00	3 to 6	39.66	3 to 6
SBE21_C-BR-6	95.00	3 to 6	35.92	3 to 6
SBE21_J-WC-2	95.00	3 to 6	39.86	3 to 6
SBE21_C-BC-7	98.00	6 to 9	35.83	3 to 6
SBE21_C-BC-12	70.00	0 to 3	40.14	6 to 9
SBE21_C-WR-7	91.00	3 to 6	41.16	6 to 9
SBE21_C-BR-1	93.00	3 to 6	42.21	6 to 9
SBE21_J-BC-5	94.00	3 to 6	40.48	6 to 9
SBE21_C-WC-5	96.00	3 to 6	41.74	6 to 9
SBE21_C-LR-2	97.00	3 to 6	40.16	6 to 9
SBE21_C-WC-8	97.00	3 to 6	40.17	6 to 9
SBE21_J-BC-7	97.00	3 to 6	40.56	6 to 9
SBE21_J-BR-9	100.00	6 to 9	42.32	6 to 9
SBE21_J-LC-10	101.00	6 to 9	41.03	6 to 9
SBE21_C-LR-1	101.00	6 to 9	42.18	6 to 9
SBE21_J-WR-6	102.00	6 to 9	42.20	6 to 9
SBE21_J-LR-1	103.00	6 to 9	40.38	6 to 9
SBE21_J-BR-1	103.00	6 to 9	43.71	6 to 9
SBE21_J-BC-15	104.00	6 to 9	41.99	6 to 9
SBE21_C-LC-1	106.00	6 to 9	42.87	6 to 9
SBE21_J-LC-13	112.00	9 +	43.18	6 to 9

Appendix 1B.2: Opercula Shape

Appendix 1B Table 2: *T. sarmaticus* opercula shape for both experimental and archaeological samples.

Operculum Shape	Experimental	%	SMONE	%
Oval	5	2.8	3	9.4
Round	174	97.2	29	90.6
Grand Total	**180**	**100.0**	**189**	**100.0**



Appendix 1B Figure 1: Graph of the *T. sarmaticus* opercula shape for the experimental and archaeological samples.

Appendix 1B.3: Opercula Age

Appendix 1B Table 3: Age of *T. sarmaticus* for both experimental and archaeological samples.

Age	Experimental	%	SMONE	%
0 to 3	23	12.8	18	42.9
3 to 6	140	77.8	18	42.9
6 to 9	17	9.4	6	14.3
9+	0	0.0	0	0.0
Grand Total	**180**	**100.0**	**189**	**100.0**

Appendix 1B.4: Opercula Processing

Opercula Completeness

Complete Dome

Appendix 1B Table 4: Dome completeness for experimental and archaeological *T. sarmaticus* opercula.

Complete Dome	Experimental	%	SMONE	%
Absent	30	16.7	172	91.0
Present	150	83.3	17	9.0
Grand Total	**180**	**100.0**	**189**	**100.0**

Complete Flange

Appendix 1B Table 5: Flange completeness for experimental and archaeological *T. sarmaticus* operculum.

Complete Flange	Experimental	%	SMONE	%
Absent	34	18.9	172	91.1
Present	146	81.1	17	9.0
Grand Total	**180**	**100.0**	**189**	**100.0**

Breakage Type

Appendix 1B Table 6: Type of breakage seen in the experimental and archaeological *T. sarmaticus* opercula

Breakage Type	Experimental	%	SMONE	%
Eroded	0	0.0	15	24.1
Intact	151	83.3	7	3.7
Irregular	12	6.7	56	30.0
Transverse	16	10.0	79	42.3
Grand Total	**180**	**100.0**	**189**	**100.0**

Colouration of T. sarmaticus opercula

Appendix 1B Table 7: Colouration seen on the experimental and archaeological *T. sarmaticus* operculum.

Colouration	Experimental	%	SMONE	%
Black	1	0.6	7	3.7
Brown	4	2.2	117	61.9
Natural	170	94.4	0	0.0
White	1	0.6	65	34.4
Yellow/Green	4	2.2	0	0.0
Grand Total	**180**	**100.0**	**189**	**100.0**

Percussion Marks on T. sarmaticus opercula

Appendix 1B Table 8: Percussion marks seen on *T. sarmaticus* opercula.

Percussion Marks	Experimental	%	SMONE	%
Absent	99	55.0	155	82.0
Present	81	45.0	34	18.0
Grand Total	**180**	**100.0**	**189**	**100.0**

Percussion Marks details

Appendix 1B Table 9: Percussion mark details for the experimental and archaeological *T. sarmaticus* opercula.

Percussion Mark Details	Experimental	%	SMONE	%
Absent	101	56.1	155	82.0
Percussion Notch	72	40.0	20	10.6
Percussion Pit	7	3.9	14	7.4
Grand Total	**180**	**100.0**	**189**	**100.0**

Bore Marks on Opercula

Appendix 1B Table 10: Bored marks on *T. sarmaticus* opercula.

Bore Mark	Experimental	%	SMONE	%
Absent	161	89.4	185	97.9
Present	19	10.6	4	2.1
Grand Total	**180**	**100.0**	**189**	**100.0**

Appendix 1B.5: Opercula Taphonomy

Etching on Opercula

Appendix 1B Table 11: Etching seen on the dome of the experimental and archaeological *T. sarmaticus* opercula.

Etching	Experimental	%	SMONE	%
Absent	119	66.1	22	11.6
Present	61	33.9	167	88.4
Grand Total	**180**	**100.0**	**189**	**100.0**

Encrustation on Opercula

Appendix 1B Table 12: Encrustation of *T. sarmaticus* opercula.

Encrustation	Experimental	%	SMONE	%
Absent	177	98.3	120	63.5
Present	3	1.7	69	36.5
Grand Total	**180**	**100.0**	**189**	**100.0**

Encrustation percentage

Appendix 1B Table 13: Percentage of *T. sarmaticus* opercula encrusted.

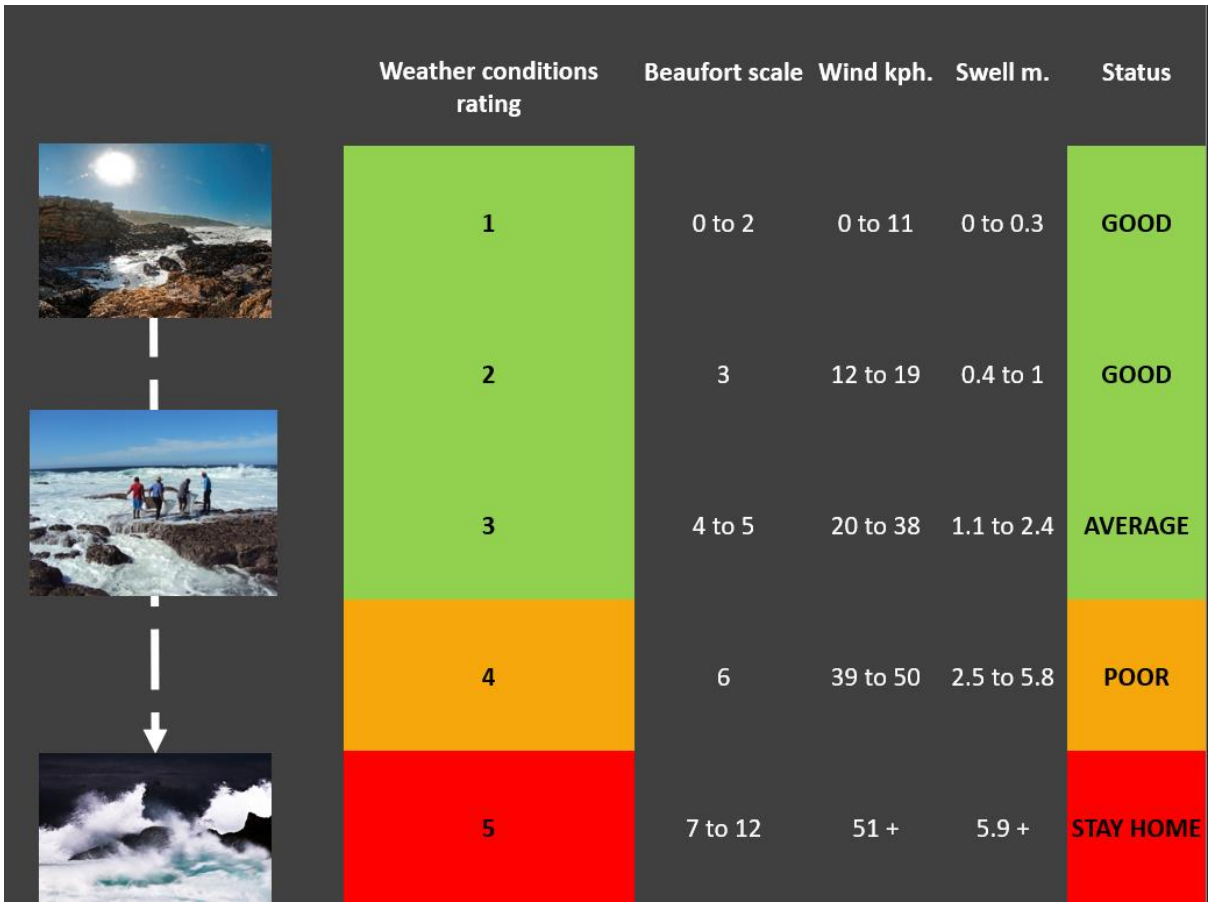
Encrusting Percentage	Experimental	%	SMONE	%
<1/2	3	1.7	24	34.3
1/2 - 3/4	0	0.0	30	42.9
>3/4	0	0.0	16	22.9
Grand Total	**180**	**100.0**	**189**	**100.0**

Abrasion on Opercula

Appendix 1B Table 14: Abrasion on archaeological *T. sarmaticus* opercula.

Abrasion	Experimental	%	SMONE	%
Absent	173	96.1	184	97.4
Beginning	1	0.6	2	1.1
Smooth	3	1.7	2	1.1
<1/4	0	0.0	0	0.0
1/4 - ½	3	1.7	1	0.5
1/2 - ¾	0	0.0	0	0.0
>3/4	0	0.0	0	0.0
Grand Total	**180**	**100.0**	**189**	**100.0**

Appendix 1C: Ocean Condition Rating



Appendix 1C Figure 1: Ocean Condition rating scale, showing the optimal and suboptimal conditions for shellfish foraging (pers. comm De Vynck).

Appendix 1D: Foraging Permits

Appendix 1D.1: Research Permit (RES2021–85)

forestry, fisheries & the environment

Department:
Forestry, Fisheries and the Environment
REPUBLIC OF SOUTH AFRICA

Foretrust Building, Martin Hammerschlag Way, Foreshore, Cape Town, 8001

Reference: RES2021-85
Enquiry: Dr Kim Prochazka
Tel.: 021 402 3546
Fax:021 402 3639

E-mail : researchpermits@daff.gov.za

Mr Carl Louis Holmes
University of Witwatersrand
71 Main Road
Eastleigh, Edenvale
1609

Attention: Dear Mr Carl Louis Holmes

INTEGRATED ENVIRONMENT AND FISHERIES RESEARCH AND DEVELOPMENT PERMIT FOR THE PURPOSES OF A SCIENTIFIC INVESTIGATION OR PRACTICAL EXPERIMENT IN TERMS OF SECTION 83 OF THE MARINE LIVING RESOURCES ACT, 1998 (ACT NO. 18 OF 1998).

This is an integrated research permit issued jointly by two Chief Directorates from the Department of Forestry, Fisheries and the Environment, authorising a scientific investigation or practical experiment in terms of Section 83 of the Marine Living Resources Act of 1998 (Act No. 18 of 1998) ("the Act"), which experiment or investigation includes both environmental and fisheries components as part of the project.

I, the undersigned, Director: Resources Research, Branch: Fisheries Management, Department of Forestry, Fisheries and the Environment acting in pursuance of the delegated authority conferred by the Honourable Minister of Environment, Forestry and Fisheries as contemplated in terms of Section 79 of the Marine Living Resources Act of 1998 (Act No. 18 of 1998) ("the Act") hereby issue this permit, in terms of Section 83 of the Act, to the following person(s)/institution to engage in the scientific investigation or practical experiment referred to below:

I, the undersigned, Director: Biodiversity and Coastal Research, Branch Oceans and Coasts, Department of Forestry, Fisheries and the Environment acting in pursuance of the delegated authority conferred upon me by the Honourable Minister of Forestry, Fisheries and the Environment as contemplated in terms of Section 79 of the Marine Living Resources Act of 1998 (Act No. 18 of 1998) ("the Act") hereby permit, in terms of Section 83 of the Act, the following person(s)/institution to engage in the scientific investigation or practical experiment referred to below:

PERMIT REFERENCE NUMBER: RES2021-85
PERMIT PERSON(S): Mr Carl Louis Holmes
INSTITUTION: University of Witwatersrand
SCIENTIFIC INVESTIGATION OR PRACTICAL EXPERIMENT: Collection, possession and transportation of marine organisms for the purposes of research,

subject to the following conditions:

1. GENERAL CONDITIONS

1.1. This permit is issued subject to the provisions and regulations of the following laws:

Page 1 of 4

(a) The Marine Living Resources Act, 1998 (Act No. 18 of 1998) ("the Act"), and all regulations published in terms thereof;
(b) The National Environmental Management Act, 1998 (Act No. 107 of 1998) ("NEMA"), and in particular, the regulations that control vehicle use in the coastal zone (as amended);
(c) The National Environmental Management Biodiversity Act, 2004 (Act No. 10 of 2004);
(d) The National Environmental Management Protected Areas Act, 2003 (Act No. 57 of 2003);
(e) The Sea Birds and Seals Protection Act, 1973 (Act No. 46 of 1973); and
(f) Prevention of Pollution from Ships Act (Act No. 2 of 1986).
(g) National Environmental Management Integrated Coastal Management Act, 2008 (Act No. 24 of 2008)
(h) Any other relevant law
(i) All relevant COVIT 19 regulations, as published in the Government Gazette, should be adhered to during the period of the pandemic.
(j) All relevant COVIT 19 regulations by SAMSA, for the use of ships and boats should be adhered to during the period of the pandemic.

1.2. This permit is intended to facilitate *bona fide* research and should not be used for the purposes of financial gain by the Permit Holder.

1.3. If, in the opinion of the Chief Director or Director there are sound reasons for doing so, the Chief Director or Director may amend the relevant conditions of the permit.

1.4. Any reference to the Permit Holder in these permit conditions includes the entity or person, his/her or its employees (whether permanent, full-time or part-time), his/her or its contractors, agents or advisers, being cognisant of the course and scope of their contractual relationship.

1.5. A breach of the provisions of the Act, regulations or these permit conditions by the Permit Holder may result in the initiation of legal proceedings (civil or criminal). A breach includes:

(a) furnishing information to which the Department of Environmental Affairs, Forestry and Fisheries (the Department) is entitled, which is not true or complete;
(b) contravening or failing to comply with a permit condition or with the provisions of the relevant legislation in Section 1.1.

(c) being convicted of an offence in terms of the relevant legislation in Section 1.1.; or

1.6. The Permit Holder shall store at their registered place of business/residence the original permit issued. The Permit Holder shall at all times, have available a true certified copy of this permit which should be produced on demand by any law enforcement official.

1.7. This permit shall only be utilized by the individual/organisation whose name appears on the permit.

1.8. If the permit is in the name of an institution/company/close corporation the individual utilizing the permit shall in addition to a certified copy of this permit, be in possession of identification and/or letter which identifies the individual as an authorized person or employee of the permit holder.

1.9. Any individual utilizing this permit shall in addition to the above conditions have a certified copy of any other permit/exemption required in terms of other legislation including any permit or exemption in terms of the Marine Living Resources Act, 1998 (Act No. 18 of 1998).

1.10. An application for a future permit may be refused if the conditions of this permit are not adhered to.

1.11. In terms of the Marine Living Resources Act, the Permit Holder is obliged to report to the Minister any contravention of the provisions of the MLRA by any other person.

1.12. The Permit Holder must safely store all inorganic waste material, garbage and pollutants on board the vessel or at the site of research activities if on land. Should the Permit Holder discard any inorganic waste material, garbage or pollutants into the sea or coastal environment, the Department may institute legal proceedings (civil or criminal) which may include suspension of the permit for a period determined by the Department and the Permit Holder shall take those steps considered necessary in terms of relevant legislation to remedy any pollution caused.

1.13. This permit does not in any way absolve the Permit Holder from the obligations of and adhering to the remainder of the provisions and conditions of the MLRA, regulations or any other law.

1.14. Any installations must be removed on termination of the project(s).

1.15. Specimens collected in terms of this permit shall not be sold or offered for sale.

1.16. This permit may not be used in marketing materials of the Permit Holders, or in any way to contract business to the Permit Holder.

1.17. No harmful chemicals are to be used when collecting marine species. Limited use of fish anaesthetics (including rotenone) is permitted if no other suitable technique is available to collect fishes and should be kept to a minimum. Local authorities should be advised when rotenone is to be used to collect fish.

1.18. No vehicle may be used in the coastal zone in terms of this permit unless the permit holder is in possession of a valid permit to use a vehicle in the coastal zone in terms of the Regulations for the Control of Use of Vehicles in the Coastal Zone (GNR 1426 of 7 December 2004).

1.19. Reports as stipulated in the 'Specific Conditions' must be submitted to the Director: Resources Research, Department of Forestry, Fisheries and the Environment, Branch: Fisheries Management (Attention: Dr Kim Prochazka), Private Bag X2, Vlaeberg, 8018 Such reports must be submitted within at least one month of the expiration date of the permit, or earlier if required.

1.20. The report, as required under Condition 1.19, should provide details of the dates, locations, species and quantities collected on the template provided by the Department.

1.21. This permit may not be utilised within a marine protected area for collecting, monitoring or any other activity which is prohibited in terms of section 43 of the Act and regulations unless such activity is specifically authorised in the section 4 of this permit.

2. SPECIFIC CONDITIONS

2.1. This permit allows the collection, possession and transportation of marine organisms for *bona fide* research of Mr Carl Homes from the University of Witwatersrand.

2.2. A certified copy of this permit shall be carried by staff during collections and must be shown to a Fishery Control Officer or any other authorized person on demand. Staff undertaking collections shall identify themselves, if requested to do so, by means of an identification document issued by Stellenbosch University.

2.3. The following species be collected as highlighted in the table:

Species/ Group	Quantity	Area(s) of collection	Method(s) of collection
Turbo sarmaticus	150	Still Bay Area	by hand

2.4 The report, as required under Condition 1.19, should provide details of the dates locations, species and quantities collected. The report should further provide a summary of the major research findings and outcomes.

3. SPECIFIC CONDITIONS FOR BIODIVERSITY AND COASTAL RESEARCH

3.1. No mammals, turtles, marine birds or any protected marine species(TOPS) may be collected or disturbed.

3.2. No specimens should be used in any way in a bioprospecting context

4. CONDITIONS PERTAINING TO ACTIVITIES WITHIN MARINE PROTECTED AREAS

4.1. This permit does not allow collection within Marine Protected Areas.

5. PERMIT VALIDITY PERIOD

This permit is valid from **1 January 2021** until **31 December 2021.**

DR GERHARD CILLIERS
DIRECTOR: BIODIVERSITY AND COASTAL RESEARCH
BRANCH: OCEANS AND COASTS
DATE: 10/08/2021

DR KIM PROCHAZKA
DIRECTOR: RESOURCES RESEARCH
BRANCH: FISHERIES MANAGEMENT
DATE: 18/08/2021

Appendix 1D.2: Additional Fishing Permit (1052834)

www.postoffice.co.za
Customer Care Number 0860 111 502
Crime Buster HotLine 0800 033 554

TIONAL FISHING PERMIT

(S) [X] MONTHLY (0919M) [ ]

GRICULTURE, FORESTRY AND FISHERIES
BAAI 8012 (021) 402 3911 (021) 402 3362
www.daff.gov.za

This permit is issued to the permit holder whose name appears below, subject to the conditions hereunder and the restrictions in respect of areas, species, minimum sizes, bag limits and fees payable as determined in terms of the Marine Living Resources Act, 1998 (Act No. 18 of 1998), and / or the regulations and notices promulgated thereunder as amended from time to time.
Please Note: This permit is NOT applicable for Freshwater Recreational Fishing.

PERSONAL DETAILS (All fields must be fully completed)

| | | |